https://ntrs.nasa.gov/search.jsp?R=19910009855 2020-03-19T18:49:47+00:00Z

NASA Technical Memorandum 102768

COMPARATIVE MORPHOLOGY OF CONFIGURATIONS WITH REDUCED PART COUNT DERIVED FROM THE OCTAHEDRAL-TETRAHEDRAL TRUSS

Haresh Lalvani and Timothy J. Collins

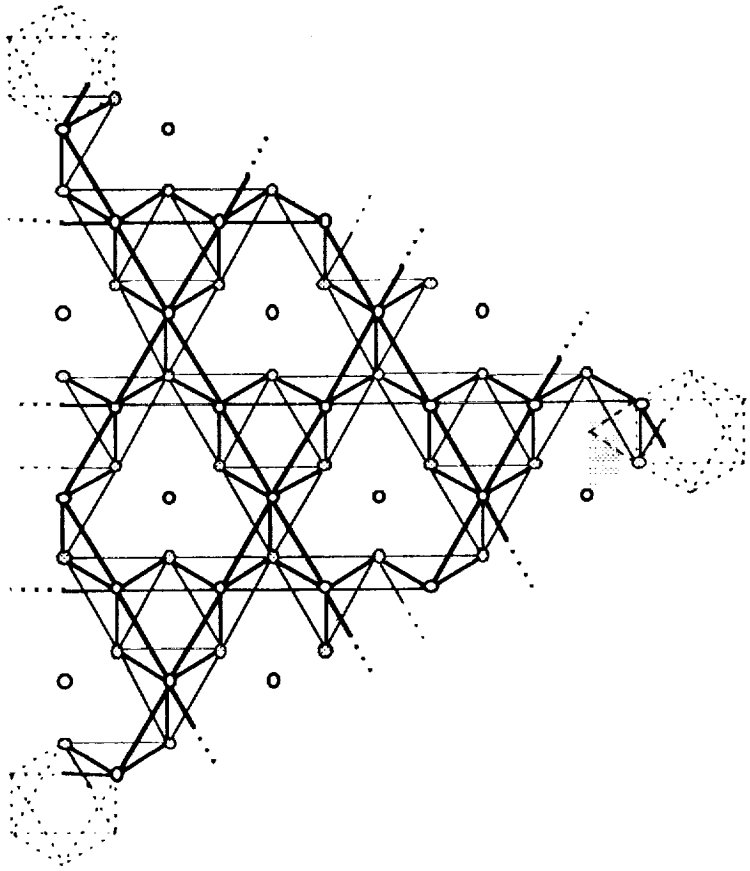

February 1991

National Aeronautics and
Space Administration

Langley Research Center
Hampton, Virginia 23665

(NASA-TM-102768) COMPARATIVE MORPHOLOGY OF CONFIGURATIONS WITH REDUCED PART COUNT DERIVED FROM THE OCTAHEDRAL-TETRAHEDRAL TRUSS (NASA) 132 p CSCL 22B

N91-19168

Unclas
G3/18 0002587

CONTENTS

NOMENCLATURE

E	number of edges (struts) in a structure
E_f	number of edges (struts) in the fundamental region of a periodic structure
E_m	number of edges (struts) in a non-redundant structure defined by the Maxwell equation
E_t	number of edges (struts) in the unit triangle
f	the number of divisions (fundamental regions) along the side of an array; also termed the 'frequency' of subdivision of the array
$f1$	the number of divisions (unit triangles) along the side of the fundamental region; this is the frequency of the fundamental region
r	number of redundant struts in the unit triangle
R	redundancy ; defined as the ratio of the redundant struts to the total number of struts; in infinite periodic configurations this is the same as the ratio of struts (or fractions of struts) to nodes (or fractions of nodes) within the fundamental region or the unit triangle
t	number of unit triangles in a fundamental region of any size
T_t	number of unit triangles in a periodic triangular or rhombic array
T_f	number of fundamental regions in a periodic triangular or array
V	number of vertices (nodes) in a structure
V_f	number of vertices (nodes) in the fundamental region of a periodic structure
V_t	number of vertices (nodes) in the unit triangle

LIST OF FIGURES

INTRODUCTION

Morphology, an interdisciplinary study which focuses on the grammar of form and structure, draws upon various interdependent aspects of geometry, symmetry, topology, structure and design. It thus provides a fundamental and integrative approach to the study of large space structures composed of many identical component parts. The modularity, the flexibility, and the lightness makes these structures attractive for covering large areas. Morphological techniques can be used for deriving a large number of space structures with novel geometries which can cover a fixed area with fewer component parts. This paper presents such techniques.

Reducing the number of component parts required for large space structures is advantageous for several reasons. Reduced weight (payload), reduced manufacturing cost, and reduced on-orbit assembly time are among the more attractive reasons to support the search for space structures constructed with fewer components. However, reducing the number of struts and nodes from a pin-jointed structure is not simple. Structures can become unstable when struts are removed from a stable configuration, and even if stability is retained there may be a substantial loss in "stiffness".

From the standpoint of geometry alone, uniformly periodic structures derived from known truss configurations by removing struts or nodes are not known. This paper addresses this issue, and presents techniques for systematically deriving new types of configurations from the octahedral-tetrahedral truss by removing struts. This truss is known as the "octet truss" [1] or the "tetrahedral truss" [2]. It has been commonly used in terrestrial architecture and has been proposed for several NASA projects. In this paper, the octet truss serves as a reference configuration for the morphology and analysis of a large number of configurations which are derived from it.

The paper is divided into four parts:

Part 1 deals with the morphology of the octet truss, and focuses on its geometry, symmetry and part count.

Part 2 describes structure-generation techniques which enable the derivation of new configurations from the octet truss by systematically removing struts and nodes.

PRECEDING PAGE BLANK NOT FILMED

PAGE VIII INTENTIONALLY BLANK

Part 3 describes nine examples of double-layer truss configurations obtained by applying the techniques described in Part 2. From the large number of geometric configurations possible, an assortment of structurally stable configurations are selected and described. These differ in their morphology and offer various architectural and structural advantages.

Part 4 briefly discusses the rationale including some practical and analytical considerations associated with the truss configurations presented in Part 3 and summarizes the results of the paper.

The techniques for generating structures described here are general and extend to a similar derivation of configurations from other trusses and space structures. Interesting candidates for such extension are the larger family of octahedral-tetrahedral configurations from the entire symmetry of the cube, and the wider range obtained from the symmetry of the icosahedron, a regular polyhedron with twenty equilateral triangular faces. Such configurations introduce several different angles and strut lengths, and expand the vocabulary of space architecture.

COMPARATIVE MORPHOLOGY OF CONFIGURATIONS WITH REDUCED PART COUNT DERIVED FROM THE OCTAHEDRAL-TETRAHEDRAL TRUSS

Haresh Lalvani[*]
Senior Research Scientist
Joint Institute for Advancement of Flight Sciences
George Washington University

and

Timothy J. Collins
Aerospace Engineer
NASA Langley Research Center

PART 1
MORPHOLOGY OF THE OCTAHEDRAL-TETRAHEDRAL CONFIGURATION (OCTET TRUSS)

1.1 Geometry

The octahedral-tetrahedral (octet) truss configuration used here is well-known. It is composed of a periodic array of "regular" octahedra and tetrahedra, each composed of equilateral triangular faces. The octahedron has eight faces and the tetrahedron has four faces. Since the face triangles in the two cases have equal sides and angles, these two polyhedra are termed regular. The array completely fills 3-dimensional space without gaps and is thus referred to as a "space-filling". The octet truss itself, as is commonly used, is a slice from the space-filling[1]. The design and structural characteristics of the octet truss are discussed in references [3-5] for both flat and curved trusses.

A portion of the octet configuration is shown in Figure 1 as a truss made up of nodes and struts. This truss can be decomposed into three layers: the top layer, the core, and the bottom layer which are shown separately in the figure. In its plan view (shown on the right side of Figure 1) the top and bottom layers are "tessellations" of equilateral triangles in shifted position; the word tessellation has a Latin origin and means a mosaic or tiling. The core, which consists of inclined members in a 3-dimensional zig-zag array, is a tessellation of regular hexagons in this view.

[*]Also: Professor, School of Architecture, Pratt Institute, Brooklyn, NY 11205 (Permanent Address); on sabatical from Pratt Institute at the time of this work during the Fall 1989 and Spring 1990 semesters.

Note that the octet array is actually composed of three polyhedra, and not two. In addition to the octahedron there are two types of tetrahedra. One is an "upright" tetrahedron sitting on its triangular base and having a vertex lying in the top truss layer as shown in Figure 2. The other is an "inverted" tetrahedron with its vertex lying in the bottom truss layer. The vertex of an upright tetrahedron corresponds to a top layer truss node and is represented by a white circle. The vertex of an inverted tetrahedron corresponds to a bottom layer truss node and is represented by a shaded circle. An octahedron has three top layer nodes and three bottom layer nodes at its vertices. The center of the octahedron is represented by a star as shown in Figure 2.

One possible triangular array of the octet configuration is shown in Figure 3a. The particular configuration shown has an inverted tetrahedron (shown in dotted lines) at the apex marked *O*, and will be referred to as OCTET1 throughout the paper. In addition, the other two corners of the array are also inverted tetrahedra. A portion of the OCTET1 geometry in an infinite array is shown in Figure 3b. An alternative triangular array (and corresponding infinite portion) of the octet configuration is shown in Figures 4a and 4b. The triangular array has an octahedron at each of its three corners. This configuration of the octet truss will be referred to as OCTET2 in this paper. The practice of showing both triangular and infinite portions of truss arrays will be carried throughout this paper. Thus Figures 3b and 4b are presented even though it is obvious that the infinite configurations of OCTET1 and OCTET2 are identical. The usefulness of these two configurations will become apparent when techniques for generating reduced-part-count geometries are discussed later in the paper. A third type of triangular array is also possible. This arrangement has three different polyhedra at its corners, and can be obtained from OCTET1 or OCTET2 by keeping the apex *O* fixed and making the array smaller or larger such that the other two corners have different polyhedra.

1.2 Symmetry

The octet truss, like all periodic configurations, can be characterized by its symmetry. An understanding of its symmetry provides a basis for generating new structures related to the octet configuration; such new structures will be described in Part 2. Symmetry also provides an expedient way to determine the part count, or the number of component parts, in a particular truss configuration.

1.2.1 Unit Triangle (Kaleidoscope)

The symmetry of the octet configuration[2] can be understood by identifying its symmetry elements and the "unit" polygon or polyhedron. The unit polyhedron of the octet configuration is a triangular prism. The plan view of this prism is an equilateral triangle. This triangle is the unit polygon of the octet truss as shown in Figures 3 and 4, and is the spatial unit which generates the entire octet configuration by using many replicas of the same unit. It will be referred to as the "unit triangle" throughout this paper. Since all configurations in this paper will be shown in their plan view, it will be convenient to describe the octet configuration, and all the derived configurations described in Parts 2 and 3, in terms of this unit triangle. The unit triangle of the octet configuration is shown in Figure 5. It is bounded by six symmetry elements, namely, three different axes of rotation and three different mirror planes (see right side of Figure 5).

The three different axes of rotation are 3-fold axes of symmetry determined by the vertical axes of symmetry passing through each of the three polyhedra shown in Figure 2. A 3-fold axis of rotation divides space into three identical regions, where each region can be superimposed over the other by a rotation of 120^{o} (or $\pi/3$) about this axis. In Figure 5, these three axes are denoted as follows : the white triangle for the vertical axis through the upright tetrahedron, the shaded triangle for the axis through the inverted tetrahedron, and the star with the black triangle for the axis through the octahedron. The three mirror planes are shown in heavy lines and join two adjacent axes. Note that the symbols for the rotation axes shown in Figure 5 specifically denote rotation axes that have an associated (adjacent) mirror plane. This is in contrast to 3-fold rotation axes which will become relevant later that do not have an associated mirror plane. Note that the mirror planes are vertical and perpendicular to the plane of the octet truss. The three mirror planes thus define a 3-dimensional region shaped as a triangular prism; this is the unit polyhedron mentioned earlier. This region, bound by mirrors, acts like a 3-dimensional kaleidoscope. The portion of the octet truss within this kaleidoscope multiplies by reflections about the mirror planes to generate an infinite octet configuration.

The unit triangle contains fractions of truss struts and nodes (shown on the left in Figure 5). The top, core and bottom layers have "half-struts" within the unit triangle which become full struts after reflection. These three layers are shown separated in Figure 6. While the portions of top and bottom struts within the unit triangle struts are half as long as the full strut, the core strut is halved lengthwise. The top and bottom nodes are each 1/6th

portions of a full node determined by the 60^{o} angle of the unit triangle. From these fractional parts within the kaleidoscope, the entire octet truss is generated by reflections. Before this process is described, it is important to point out that the unit triangle can be further decomposed into a smaller region called the "fundamental region" [6]. This is described next.

1.2.2 Fundamental Region

The unit triangle of the octet truss has a subtle symmetry within it. It can be halved into two smaller right-angled triangular regions by a vertical plane passing through the octahedron (Figure 7, top). The right-angled triangle is the minimum unit which is necessary to generate the entire structure by "symmetry operations" and is termed the "fundamental region" (Figure 7, bottom). The vertical plane is indicated by a dashed line and is referred to as a plane of "inversion". In addition to this plane, the fundamental region of the octet truss is bound by two mirror planes, and two 3-fold axes of symmetry lying on two of its vertices. One vertex is determined by an octahedron and the other by a tetrahedron.

By inversion about the vertical plane, everything lying on the bottom right of the plane and facing up is converted to top-left and facing down. In Figure 7, this is illustrated by shading the two halves of the unit triangle in two different shades. The darker shade represents the bottom right-half of the octet truss and includes the bottom 1/6 node, the bottom half-strut and half of the core strut lying below the "mid-plane" of the truss; the mid-plane is an imaginary horizontal plane lying midway between the top and bottom truss layers and which divides the truss into upper and lower halves. By inversion, the darker shade becomes the lighter shade, which represents the top left-half of the truss and includes the top 1/6 node, the top half-strut and the top half of the core strut. Inversion around a plane, as described here, is also a 2-fold rotation around a horizontal axis lying on the mid-plane and passing through the center of the octahedron and the center of the core strut. Inversion flips an upright tetrahedron into an inverted tetrahedron.

1.2.3 Periodic Arrays of Unit Triangles

Many replicas of the unit triangle, each containing two fundamental regions, can be used to fill the plane and thus generate a periodic truss array. There are several different plane-

filling procedures. In each procedure, the fraction of the octet truss within each unit triangle (and hence fundamental region), repeats correspondingly to generate the full octet truss. One procedure which uses increasingly larger "triangular arrays" is shown in Figure 8. It uses the unit triangle as a repeating unit. The single unit triangle in (a) grows to an arrangement of four unit triangles in (b) by local reflections across the mirror planes, and further to nine unit triangles in (c) by additional local reflections. The process can be continued to get increasingly larger arrays of the unit triangle[3]. An array of 36 unit triangles is shown in (d).

The extent of plane-filling can be described in terms of the size of the triangular array. This size is specified by the number of divisions f along the outer edge of the triangular array, where f denotes the "frequency" of subdivision of the array [see Reference 1]. The four stages shown in Figure 8 thus are f=1, 2, 3, and 6 respectively.

The corresponding portions of the octet truss for each of the four stages in Figure 8 are shown in Figure 9. The rotation axes of the octahedra and tetrahedra shown in Figure 8 correspond exactly to the top nodes, bottom nodes, and the centers of octahedra shown in Figure 9. The top, core and bottom layers corresponding to these four stages are shown separated in Figure 10.

The number of unit triangles T_t in a triangular octet array can be described in terms of f:

$$T_t = f^2 \qquad \text{..... (1)}$$

Besides a triangular array, other useful periodic arrays of unit triangles are rhombic and hexagonal arrays. These will be discussed in more detail later. The number of unit triangles in a rhombic array is $2xT_t$, since a rhombus is composed of two triangles. In a hexagonal array, the number of unit triangles is $6xT_t$ since a hexagon is composed of six triangles. For the purpose of formulating analytical models of various truss configurations, hexagonal arrays were used. These were obtained by rotating triangular arrays, such as those in Figures 3 and 4, around the apex marked *O* in 60^o increments.

For the purposes of this study, a triangular array with f=12 was chosen as a baseline configuration. This array is composed of 144 unit triangles and corresponds exactly to configurations OCTET1 or OCTET2 shown earlier in Figures 3a and 4a. For a 2 meter strut length, f=12 produces a 24 meter wide (edge to edge) hexagonal array. The

size and shape of such a hexagonal truss array were considered practical for several future NASA applications currently under consideration.

1.3 Part Count

The number of component parts or "part count" of a space structure is an important consideration in the design, manufacturing, and assembly of space structures. The fundamental region and the unit polygon/polyhedron provide an expedient way to determine the part count in periodic space structures. Such a part count is here termed the "fractional part count". The fundamental region has been used to derive the part count in polyhedral structures in reference [7]. The part count within the fundamental region is given by V_f and E_f, where V_f is the number of nodes (or vertices) and E_f the number of struts (or edges) within the fundamental region. The part count within a unit triangle given by V_t and E_t, where V_t is the number of nodes and E_t the number of struts in the unit triangle. Either V_f and E_f, or V_t and E_t, can be used to derive the total part count in a periodic structure. However, V_t and E_t will be used in Part 3 as a basis for comparing the part counts of different configurations derived from the octet truss.

1.3.1 Part Count for the Infinite Octet Truss

In the case of the octet configurations OCTET1 and OCTET2, the unit triangle is the smallest region which has component parts from the top, core and bottom layers. Thus V_t and E_t and are derived first and can be halved to obtain V_f and E_f since there are two fundamental regions in the unit triangle. The portion of the truss that lies within the unit triangle was already shown in Figure 5. The top and bottom struts are each halved in the region, the core member lies on the mirror plane and is therefore also halved since it is shared with a neighboring unit triangle. That is,

$$E_t(\text{top}) = E_t(\text{bottom}) = E_t(\text{core}) = 1/2 \qquad \ldots\ldots\ldots\ldots\ (2)$$

Since each of the three layers of the truss have a half-strut within the unit triangle, it follows that the number of struts in each layer equals 1/3rd the total number of struts, a result reported in reference [2]. Further, the total number of struts E_t in the unit triangle, obtained by adding the struts in each of the three layers, equals 3/2, i.e.

$$E_t = 3/2 \qquad \text{..... (3)}$$

In Figure 5, we also see that the unit triangle contains 2 fractional nodes where each fraction is 1/6th of a full node. Each node is shared by six regions meeting at a 3-fold axis of rotation and is thus divided into six equal fractions. The total number of nodes V_t within the unit triangle equals 2 times 1/6 or 1/3, i.e.

$$V_t = 1/3 \qquad \text{..... (4)}$$

From relations (3) and (4),

$$E_t = (9/2)V_t \qquad \text{..... (5)}$$

This relation, based on the unit triangle, also gives the proportion of the total number of struts E to the total number of nodes V in the infinite octet truss since V_t and E_t are both multiplied the same number of times in a periodic array. Relation (5) can also be described in terms of V_f and E_f by replacing E_t by E_f, and V_t by V_f, respectively.

1.3.2 Redundancy in Infinite Configurations

For any particular truss, those struts which are not necessary to provide a rigid (stable) structure are generally termed redundant. The redundancy in an infinite periodic configuration can be defined as the ratio of struts to nodes in the fundamental region or alternatively in the unit polygon/polyhedron. Since the unit polygon/polyhedron will be used for comparative part count studies in Part 3, the redundancy here is described in terms of the unit triangle. From the Maxwell equation [8], the number of struts E_m in the unit triangle of a non-redundant infinite truss configuration with V_t nodes can be expressed as :

$$E_m = 2V_t \quad \text{(2-dimensional case)} \qquad \text{..... (6)}$$

and

$$E_m = 3V_t \quad \text{(3-dimensional case)} \qquad \text{.....(7)}$$

The number of redundant struts r in the unit triangle equals E_t-E_m, i.e.

$$r = E_t - E_m \qquad \text{.....(8)}$$

The redundancy R is defined here as the ratio of the number of redundant members r to the number of members E_t. That is,

$$R = r / E_t = (E_t - E_m)/ E_t = 1 - (E_m/ E_t) \qquad \text{..... (9)}$$

Substituting for E_m from (6) and (7) respectively in (9),

$$R = 1 - (2V_t / E_t) \quad \text{(2-dimensional case)} \qquad \text{..... (10)}$$

$$R = 1 - (3V_t / E_t) \quad \text{(3-dimensional case)} \qquad \text{..... (11)}$$

For the infinite octet configuration, the redundancy R can be obtained by substituting the values of V_t (=1/3) and E_t (=3/2) from (3) and (4) in relation (11). This gives:

$$R = 1/3 \ \text{(or 33.33\%)} \quad \text{(double-layered case)} \qquad \text{..... (12)}$$

That is, the octet truss has a redundancy of 1/3 (33.33%) within the unit triangle. It follows that the entire infinite truss also has 1/3rd redundant members. Alternatively, the redundancy from the fundamental region can be obtained by substituting V_t and E_t by V_f (=1/6) and E_f (=3/4) respectively in relation (11).

The redundancy of 33.33% defines the upper limit for infinite truss configurations derived from the octet truss. All derivatives obtained by removing struts will have fewer members than the octet configuration and they will thus have $R \leq 33.33\%$. The redundancy of the top and bottom layers can be similarly derived using relation (10). From Fig.6, both top and bottom single layers have V_t=1/6 and E_t=1/2. Substituting these values in relation (10) gives

$$R = 1/3 \ \text{(or 33.33\%)} \quad \text{(single-layered case)} \qquad \text{..... (13)}$$

In the various examples described in Part 3, this limit will provide a reference for the single layers of derivative configurations.

1.3.3 Part Count in a Periodic Array

The total part count in a periodic array can be determined by multiplying the number of parts within a unit polygon by the number of unit polygons in the array. Considering triangular arrays of the octet configuration, the part count within the unit triangle is given by relations (3) and (4), and the number of unit triangles in a triangular array is given by relation (1). Multiplying both (3) and (4) by (1),

$$E = T_t \times E_t = f^2 \times E_t \qquad \text{..... (14)}$$

$$V = T_t \times V_t = f^2 \times V_t \qquad \text{..... (15)}$$

where E and V are the number of struts and nodes respectively in a triangular array of the octet configuration. Alternatively, E and V can be determined by multiplying E_f and V_f, respectively, with the number of fundamental regions T_f in a triangular array. The number in a rhombic array is twice, and in a hexagonal array six times the number in a triangular array. Examples of determining part count will be discussed in Part 2 of the paper.

PART 2
STRUCTURE-GENERATION TECHNIQUES

From the octet truss configuration an extremely large number of structures can be derived by removing struts and/or nodes. Systematic structure-generation of a variety of space structures by combinatorial addition or removal of edges within a fundamental region has been described in [7]. This includes a large class of polyhedra and some examples of space-filling polyhedral structures. Extension of this method to the generation of complex 2-dimensional periodic patterns has been described in [9]. The techniques presented in this paper are an extension of the prior work to double-layered space structures and are restricted to configurations derived from the octet truss. In all examples of configurations described in this paper, the node positions of the octet truss (OCTET1 or OCTET2) and the derived configuration are the same. The derived configurations vary in their geometry, type of symmetry, the number of struts and nodes, and structural performance.

Since the double-layered configurations are complex in their geometry and symmetry, they are decomposed into separate top, core and bottom layers. These are then superimposed to form a complete structure. Of the three layers, the top and bottom layers were found to be more important in generating new configurations by removing struts and nodes from the octet configuration. The specific geometry of examples of the derivative double-layered configurations will be described in Part 3. The core geometry of the source octet configuration (OCTET1 or OCTET2) was left unchanged in two-thirds of the examples. In the remaining one-third cases, some core struts were removed because their associated nodes in the top or bottom layers had been removed. In these cases, the core geometry was thus dependent on the geometry of the top and bottom layers.

The separated top and bottom layers act like "single-layer configurations". The types of permissible symmetries of single-layer configurations are described first in this section. The concept of extending the fundamental region to a larger size is described next, and is followed by a description of plane-filling procedures. The method of removal of struts and nodes to generate two different classes of single-layer configurations with a reduced part count is described next. In some cases, top and bottom layers having an identical geometry and symmetry are superimposed after a rotation or a reflection of one of the layers. In other cases, two different geometries and symmetries are superimposed to obtain a double-layered configuration.

2.1 Permissible Symmetries

When some nodes and struts are removed, the derived configuration may have a different symmetry than the original octet truss. For the top and the bottom single layers, each taken separately, there are only three permissible symmetries[5] that are compatable with the octet truss geometry [10]. These three symmetries use only 3-fold axes of symmetry. Although 6-fold symmetry is possible at a node of a single-layer configuration, for double-layer configurations, such 6-fold symmetry becomes 3-fold. When top and bottom single layers are superimposed, as in the octet truss, the double-layered configurations obtained this way have more complex symmetries. The permissible symmetries for double-layered configurations derived from the octet truss are eight[4] in number. Such symmetries are described in reference [11]. The three permissible symmetries for the top and bottom layers of the octet truss with struts and/or nodes removed will be referred to as Symmetry Types A, B and C, and are shown in Figure 11. As will be described next, the fundamental regions of these three types of symmetry are different. Each fundamental region has a different shape and is bound by different symmetry elements. It is noted that because the fundamental regions discussed throughout the remainder of the paper are for single-layer configurations (all struts lie in a plane), these fundamental regions differ from the double-layer fundamental region shown for the octet truss in Figure 7. Recall that a fundamental region is the minimum truss unit necessary to generate an entire truss array by symmetry operations.

2.2 Fundamental Regions of the Permissible Symmetries

The fundamental region of **Symmetry Type A** is a kaleidoscopic equilateral triangle. It is bound by three mirror planes on the sides of the triangle, and three different 3-fold axes of rotation at the vertices. The three different axes shown in the figure correspond to axes through the two different tetrahedra and the octahedron. Alternatively, the axis could pass through three tetrahedra or three octahedra. This is the type of symmetry characteristic of the top or bottom layer of the octet truss configuration.

The fundamental region of **Symmetry Type B** is an isosceles triangle, with an obtuse angle of 120^{o}. The two acute vertices have the same 3-fold axis of rotation and the side joining these two is a mirror plane. The other two sides (shown as dashed lines) define the edges of the fundamental region only and are not mirror planes. The obtuse vertex is a different type of 3-fold axis of rotation. There are no mirror planes passing

through this axis of rotation. The notation is modified to show the pinwheel (or rotary) nature of the axis by extending the sides of the small triangle in a clockwise or counter-clockwise manner. In the figure, the three axes shown in the fundamental region pass through three upright tetrahedra. Alternatively, the three axes could pass through three inverted tetrahedra or three octahedra. Three such regions, obtained by a 3-fold rotation around the obtuse vertex (pinwheel), make a larger kaleidoscopic equilateral triangle.

The fundamental region of **Symmetry Type C** is a rhombus with acute angles of 60^{o}. It has three 3-fold axes of rotation which are different and a fourth 3-fold axis which is identical to any one of these three. There is no mirror plane in this region and hence all the 3-fold axes of rotation act like pinwheels. The notation of the axes is modified accordingly as in the last example. In the figure, the three different axes pass through the inverted tetrahedron, the upright tetrahedron and the octahedron. The fourth axis is shown through an upright tetrahedron.

2.3 Fundamental Regions of Increasing Size

Several unit triangles of the octet truss can be fused together to generate fundamental regions of increasing size for each of the three types of symmetries shown in Figure 11. In each case the unit triangles, which are smaller, "subdivide" the interior of the larger fundamental region. Such subdivision permits the possibility of defining fundamental regions of any size containing any number of struts and nodes. It will be shown that larger fundamental regions allow for a larger number of strut and node combinations which can be removed to derive reduced-part-count structures. Details of this concept will now be described for each symmetry type. Alternative subdivisions of the fundamental region have been addressed in [9].

Symmetry Type A: A sequence of increasingly larger fundamental regions for Symmetry Type A is shown in Figure 12a. The size of the fundamental regions is specified by the frequency f1 which equals the number of unit divisions (or unit triangles) along an edge of the region. In Symmetry Type A, this division is along the edge of the region as shown. The first stage, f1=1, is the smallest possible fundamental region for this symmetry type and has the same size as the unit triangle of the octet configuration. The second stage, f1=2 fundamental region, is composed of four unit triangles (shown in

dotted lines). The f1=3 fundamental region has 9 unit triangles (also shown in dotted lines), the f1=4 fundamental region has 16 unit triangles, and so on.

For each fundamental region shown in Figure 12a, the outer three sides are mirror planes as required by Symmetry Type A, and the three vertices on the outer corners are three different axes of symmetry. In the figure, the vertex marked *O* is kept fixed and corresponds to an axis through an inverted tetrahedron in the example shown. As f1 increases, the other two axes change and are specified by the sequence of the three different polyhedra in the octet array (compare with Figure 8 or 9).

The number of unit triangles t in a fundamental region of frequency f1 and Symmetry Type A can be described as follows :

$$t = (f1)^2 \qquad \text{..... (16)}$$

and is similar to equation (1) which gave the number of unit triangles in an octet truss array.

Symmetry Type B: A sequence of two increasingly larger fundamental regions for Symmetry Type B is shown in Figure 12b. Note that the subdivisions of the fundamental region for this symmetry are along the longer side of the fundamental region and are restricted to values of f1 which are multiples of 3. This is due to the nature of the 3-fold axis of rotation at the obtuse vertex of the fundamental region which requires a rotation of 120^{o} at this vertex. By this rotation, a 3-fold axis lying at one acute vertex of the fundamental region is rotated to the other acute vertex. Thus the two acute vertices of the fundamental region must be the same. This occurs only when f1 equals 3, 6, 9, 12 .... and so on. In the figure, each 3-fold axis is through an inverted tetrahedron as indicated by the shaded triangles. Alternatively, the 3-fold axes could be through upright tetrahedra or octahedra only, but here too the values of f1 are restricted to multiples of 3.

The number of unit triangles t in a fundamental region of frequency f1 and Symmetry Type B can be described as follows :

$$t = 1/3 \times (f1)^2 \qquad \text{..... (17)}$$

Symmetry Type C : In Symmetry Type C there are two different ways[6] to obtain larger rhombic fundamental regions which are subdivided into unit triangles. Alternative 1 is shown in Figure 12c, and is based on "doubling" the fundamental regions of Type A shown in Figure 12a. The number of unit triangles t is also doubled in Alternative 1, and is given by :

$$t = 2 \times (f1)^2 \qquad \text{..... (18)}$$

where f1 is any integer. Here the frequency f1 is given by the number of divisions along the shorter diagonal of the rhombic fundamental region.

Similarly, Alternative 2 (Figure 12d) is obtained by "doubling" the fundamental regions of Type B shown earlier in Figure 12b. Again, f1 is restricted to multiples of 3 as in Type B, and is given by the number of divisions along the longer diagonal of the rhombic fundamental region. The number of unit triangles t is double that in Type B and can be expressed as :

$$t = 2/3 \times (f1)^2 \qquad \text{..... (19)}$$

2.4 Plane-filling Procedure

Once a fundamental region with a specific value of f1 is determined, many replicas of this region can be used to fill the plane. In other words, periodic truss arrays are generated which contain many replicas of the fundamental region each of which is composed of one or more unit triangles. The procedure for plane-filling is slightly different for the three types of symmetries.

Symmetry Type A:

In Symmetry Type A, the procedure of plane-filling is the same as described earlier in Section 1.2.3 to obtain a triangular array of unit triangles whereby the equilateral triangle fundamental region is repeated by local reflections about the mirror planes. An array using f1=1 fundamental regions (same as unit triangles) is shown in Figure 13. The extent of plane-filling is specified by f as before. In the figure shown, f=6. In Figure 14, a fundamental region with f1=2 is used to generate an array with f=3. The number of

fundamental regions T_f in a triangular array of frequency f and having Symmetry Type A is given by the following relation which is similar to relation (1):

$$T_f = (f)^2 \qquad \text{(Type A)} \qquad \ldots\ldots\ldots\ldots (20)$$

The number of unit triangles is the same in Figures 13 and 14. In Figure 14, the f1=2 fundamental region with t=4 is four times as large as the f1=1 fundamental region in Figure 13 which has t=1. The f1=2 region fills a triangular array of the same area with one-fourth as many units. For a fixed area, f decreases as f1 increases. The number of unit triangles T_t in a triangular array of frequency f and composed of fundamental regions of frequency f1 is obtained by multiplying the number of unit triangles in a fundamental region by the number of fundamental regions.

$$T_t = t \times T_f$$
$$Tt = (f \times f1)^2 \qquad \ldots\ldots\ldots\ldots (21)$$

Relation (21) is similar to relation (1) but is more general, and it holds for all three Symmetry Types. Each single layer of the octet truss is a special case of symmetry type A with each fundamental region having one unit triangle along the side of a fundamental region, i.e., f1=1 and $Tt = f^2$ as in relation (1).

Symmetry Type B:

In Symmetry Type B, the values of f1 are restricted to multiples of 3. The minimum case has f1=3 and is shown in Figure 15. By rotation about the pinwheel axis, three fundamental regions form a large equilateral triangle which is then repeated by reflections (as in Sec.1.2.3) to generate a triangular array. In the example shown, f=2 and the number of unit triangles equals 36 as in the previous two cases. Relation (21) holds for the number of unit triangles, and relation (20) for the number of fundamental regions T_f is modified as follows:

$$T_f = 3(f)^2 \qquad \text{(Type B)} \qquad \ldots\ldots\ldots\ldots (22)$$

Symmetry Type C:

In Symmetry Type C, a different plane-filling procedure is used to generate periodic arrays rhombic fundamental regions. Instead of repeated reflections, 3-fold rotations are used to generate a rhombic array as shown in Figure 16[7]. The rhombic array

is twice the size of the triangular array, and can be described in terms of f and f1 as in the other two cases. Here f1 can be any number. For rhombic configurations, the number of unit triangles T_t in the fundamental region and the number of fundamental regions a periodic T_f array are given by:

$$T_t = 2(f \times f1^2) \qquad T_f = (f)^2 \qquad \text{(Type C, Alternative 1)} \qquad \ldots\ldots\ldots\ldots (23)$$

$$T_t = 2(f \times f1^2) \qquad T_f = 3(f)^2 \qquad \text{(Type C, Alternative 2)} \qquad \ldots\ldots\ldots\ldots (24)$$

2.5 Removal of Struts and Nodes

Once a larger fundamental region with frequency f1 and containing truss struts and nodes is obtained, an extremely large number of truss configurations can be derived by removing struts and nodes from this region[8]. The larger fundamental region contains a larger portion of the octet configuration. This is shown in Figure 17 with fundamental regions of increasing size derived from the top layer of OCTET1[9]. The stages f1=1,2,3,4 and 6 correspond to the symmetry representations shown in Figure 12a and the number of component parts in the fundamental region increases as f1 increases. This permits more combinations for strut or node removal enabling the generation of an increasingly larger number of derived structures. When the fundamental region with removed parts is repeated to fill space, configurations with reduced part count are obtained. The new structure has a different geometry, and its symmetry may or may not be the same as the structure from which it is derived.

Two useful classes of single-layer configurations with a reduced part count are identified in this section. The first class includes configurations from which only struts are removed and all nodes are retained. The second class of structures includes examples where single nodes, or a group of nodes are removed along with associated struts. One example of each type of configuration is described here to illustrate the technique, and others will be shown in Part 3.

The first example (Figure 18) shows the generation of a single-layer configuration by removing struts only. It has a Symmetry Type A, the fundamental region has f1=2, and the triangular array has f=6 (illustration on right). The "source" fundamental region, corresponding to the equivalent region of OCTET1 from which the struts are removed (compare with f1=2 region in Figure 17), is shown on left (top) and contains one full strut and two half-struts. From this many combinations of struts can be removed. In the

example shown, one half-strut is removed from the source fundamental region to obtain a "derived" fundamental region shown above it (bottom left). When this new fundamental region is repeated to fill the plane by reflections, a new single-layer configuration is obtained. This new configuration has struts removed from it in a periodic manner as shown in the illustration[10].

Larger fundamental regions also permit the removal of more combinations of struts and nodes for the purpose of deriving new configurations. One example is shown for Symmetry Type B with f1=6 in Figure 19. The source fundamental region is again shown at top left, the derived one at bottom left, and the triangular array on the right. The source fundamental region has 5 full struts and 2 half-struts from which 2 full and 1 half-strut are removed. In addition, the source has 1 full and 2 half-nodes from which 1 half-node is removed. Note that the removed half-node is still shown in the figure for visualization purposes. However it is clear in the truss array that this node has been removed because no struts are attached to it. When repeated to fill the plane, the triangular array shows the larger open spaces that are generated within the single layer. When the triangular array itself is repeated, e.g. to generate a hexagonal truss array, the open spaces become closed open areas in the shape of a non-regular hexagon (see for example, the top layer of Fig.29d).

2.6 Superimposition of Layers

From the large number of single-layer configurations which can be generated by the techniques just described, a still larger number of double-layer configurations can be obtained by superimposing any top over over any bottom layer and adding core members. The size of the array fixes f for both layers. The matching of the two layers is guaranteed as long as f1 is kept the same in both. Superposition of two layers with different values of f1 is possible, and symmetry is retained as long as one value of f1 is a simple multiple of the other. Although this paper presents examples where top and bottom layers have the same symmetry, it is possible for the two layers to have different symmery types.

A variety of examples will be described in Part 3. Some of the most useful cases are configurations where the two layers are identical in their geometry and symmetry. This guarantees the same part count and same assembly procedure for the two layers. Several examples of this type will be shown.

2.7 Summary of Structure-Generation Procedure

From the preceding sections, the procedure for generating a periodic double-layered configuration with a reduced part count can be summarized as follows :

1. Separate the double layer of the source octet configuration (OCTET1 or OCTET2) into top and bottom layers.

2. Apply the following structure-generation techniques to the separate layers :

    i) Select the type of fundamental region by selecting the Symmetry Types A, B or C.

    ii) Specify f1, the frequency of the fundamental region.

    iii) Remove struts or nodes from the fundamental region.

    iv) Apply an appropriate plane-filling procedure using reflections, rotations or translations, to the fundamental region which has struts and nodes removed (this specifies f).

3. Superimpose the top and bottom layers.

4. Insert the core, i.e. connect the top and bottom nodes with appropriate core struts.

Note that the same procedure of removing struts and nodes can be applied to the core. However, in the examples described in Part 3, the core was either kept intact or its geometry was determined by the top and bottom layers. The dependent nature of the geometry of the core will become clear with specific examples.

2.8 Part Count and Redundancy of Derived Configurations

For any derived periodic array, a general procedure for determining the part count and the redundancy is as follows :

1) Determine f and f1; f is the frequency of the fundamental regions within the array and f1 is the frequency of the unit triangles within the fundamental region.

2) Determine E_f and V_f, the number of struts and nodes within the fundamental region (after struts and nodes are removed); this can be done by determining the fundamental region of the configuration and counting the parts within it. Note fractional parts as appropriate.

3) Determine t, the number of unit triangles within the fundamental region; this can be derived from relations (16-19).

4) Determine Tf, the number of fundamental regions in the periodic array[11]. This is different for each Symmetry Type and is given by from relations (20) and (22-24).

5) Determine E_t and V_t, the number of struts and nodes within the unit triangle; this can be obtained by dividing the result of Step 1 by Step 2, i.e.

$$E_t = E_f / t \qquad \cdots\cdots\cdots\cdots (25)$$

and

$$V_t = V_f / t \qquad \cdots\cdots\cdots\cdots (26)$$

6) Determine R, the redundancy of the configuration; this is derived from relation (10) for a single-layer configuration.

7) Determine T_t, the number of unit triangles in the periodic array with fundamental regions of frequency f.

8) Derive E and V, the total number of struts and nodes in the periodic array.These can be obtained in two different ways :

   i) from the fundamental region by multiplying the results of steps 2 and 3, i.e.

$$E = E_f \times T_f \qquad \cdots\cdots\cdots\cdots (27)$$

and

$$V = V_f \times T_f \qquad \cdots\cdots\cdots\cdots (28)$$

or

   ii) from the unit triangle by multiplying the results of steps 3 and 5, i.e.

$$E = E_t \times T_t \qquad \cdots\cdots\cdots\cdots (29)$$

and

$$V = V_t \times T_t \qquad \cdots\cdots\cdots\cdots (30)$$

All of the relations described so far are summarized in Table 1.

	Symmetry Type A (Triangular Array)	Symmetry Type B (Triangular Array)	Symmetry Type C (Rhombic Array)	
			Alternate 1	Alternate 2
Unit Triangles in Fundamental Region (t)	$f1^2$	$\frac{f1^2}{3}$	$2f1^2$	$\frac{2}{3}f1^2$
Fundamental Regions in Array (T_f)	f^2	$3f^2$	f^2	$3f^2$
Unit Triangles in Array (T_t)	$(f \times f1)^2$	$(f \times f1)^2$	$2(f \times f1)^2$	$2(f \times f1)^2$
Number of Struts in Unit Triangle (E_t) $E_t = \frac{E_f}{t}$	$\frac{E_f}{f1^2}$	$\frac{3E_f}{f1^2}$	$\frac{E_f}{2f1^2}$	$\frac{3E_f}{2f1^2}$
Number of Nodes in Unit Triangle (V_t) $V_t = \frac{V_f}{t}$	$\frac{V_f}{f1^2}$	$\frac{3V_f}{f1^2}$	$\frac{V_f}{2f1^2}$	$\frac{3V_f}{2f1^2}$
Struts in Array (E) $E = E_f T_f$ or $E = E_t T_t$	$E_f f^2$ or $E_t(f \times f1)^2$	$3E_f f^2$ or $E_t(f \times f1)^2$	$E_f f^2$ or $2E_t(f \times f1)^2$	$3E_f f^2$ or $2E_t(f \times f1)^2$
Nodes in Array (V) $V = V_f T_f$ or $V = V_t T_t$	$V_f f^2$ or $V_t(f \times f1)^2$	$3V_f f^2$ or $V_t(f \times f1)^2$	$V_f f^2$ or $2V_t(f \times f1)^2$	$3V_f f^2$ or $2V_t(f \times f1)^2$

Table 1.

Summary of Equations for Single-Layer Truss Arrays of the Three Symmetry Types.

Examples

I. As an example, the derivation of the part count and redundancy of the single-layer truss configuration of Symmetry Type A derived by removing struts from the top layer of OCTET1, shown in Figure 18, is described.

1) The source fundamental region (on top left) has a frequency 2, i.e. **f1=2**. This region has 1 full strut and 2 half-struts, making a total of 2 struts, i.e. E_f=2. It also has a 1/6th node at a vertex and a 1/2 node at the opposite edge of the triangular region, making a total of 2/3rd nodes, i.e V_f=2/3. The derived periodic array has 6 fundamental regions along a side, i.e. **f=6**.

2) In the derived fundamental region (shown below on left), one half-strut is removed while the nodes remain unchanged, i.e. **E_f=3/2** and **V_f=2/3**.

3) The number of unit triangles in the fundamental region, given by relation (16), equals 4, i.e.**t=4**.

4) The triangular array on the right is obtained by using the plane-filling procedure for Symmetry Type A, i.e. repeated reflections of the fundamental region, and has a frequency f=6. The number of fundamental regions T_f in the triangular array of f=6 as shown is determined by relation (20) and gives **T_f=36**.

5) Since the fundamental region has 4 unit triangles, **E_t=3/8** (from relation (25)), and **V_t=1/6** (from relation (26)).

6) The redundancy R, obtained by substituting E_t and V_t into relation (10), is **R = 1/9** or 11.11%.

7) The number of unit triangles T_t is obtained by substituting for f and f1 in relation (21) and gives **T_t=144**.

8) The total number of struts E, obtained by substituting for E_f and T_f in relation (27) or substituting E_t and T_t in relation (29), gives **E=54**. Similarly, the total number of nodes V, obtained by substituting for V_f and T_f in relation (28) or V_t and E_t in relation (30), is **V=24**.

II. The part count and redundancy for the example array having Symmetry Type B and shown in Figure 19, derived from the top layer of OCTET1 by removing nodes and struts, is similarly derived as outlined below and as shown in the figure.

1) f1=6 , f=2
2) E_f=7/2 and V_f=3/2
3) t=12
4) T_f=12
5) E_t=7/24 , V_t=1/8

6) R=1/7
7) T_t=144
8) E=42 , V=18

III. Finally, another example of structure generation and of determining part count and redundancy for a single-layer truss configuration with struts only removed will be given for a rhombic array. Figure 20 shows a single-layer configuration of symmetry type C (alternate 2) obtained by removing struts from the top layer of OCTET2. Derivation of the part count and redundancy for this array is outlined as follows:

1) f1=3 , f=4
2) E_f=2 and V_f=1
3) t=6
4) T_f=288
5) E_t=1/3 , V_t=1/6
6) R=0 (no redundant struts in this single-layer configuration)
7) T_t=288
8) E=96 , V=48

Note that for all of the examples given the values obtained for E and V can be verified by directly counting the number of struts and nodes in Figures 18, 19, and 20. When doing this, all struts and nodes lying on the edges of the derived array must be assigned their appropriate fractional count. For example, the outer edge of the array in Figure 20 contains 16 half nodes.

This procedure will be used throughout Part 3 for configurations derived from the octet truss, but will focus on fractional part count and redundancy which are necessary for a comparative study of the different configurations. In double-layered truss structures, the part count for each layer, the top, bottom and core, is derived separately. The number of struts are obtained by adding the strut count for each layer, and the number of nodes is obtained by adding the node count in the top and bottom layers. Since the top, core and bottom layers may have a different symmetry or fundamental regions of different size, the fractional part count can be obtained by adding E_t and V_t for the separate layers.

Note that the above procedure applies to both 2-dimensional and 3-dimensional configurations, but in the case of the latter the fundamental regions are 3-dimensional and

hence more complex. Although beyond the scope of this paper, it is possible to generalize this procedure for application to all other double-layered and multi-layered symmetries by using 3-dimensional fundamental regions, and by replacing the unit triangle with the more general concept of a "unit polygon" or a "unit polyhedron".

PART 3
CONFIGURATIONS WITH REDUCED PART COUNT

In this part, the structure-generation techniques described in Part 2 are applied to derive a variety of double-layered structures. The motivation for the examples shown here will be explained later in Section 3.3. No attempt has been made to be exhaustive. The selection shown here is representative and includes configurations with interesting geometries and structural properties. This selection excludes several configurations which were considered but were found to be unstable or to have a substantially reduced structural performance (see section 4.1). Some of the configurations lend themselves towards an integration of architectural and functional requirements with the structure. The notable examples are structures with open spaces which permit insertion of modules or other structures.

This part is separated according to the two classes of structures discussed in Part 2, namely, configurations with only struts removed, and those with both struts and nodes removed. In each class, structures are derived from the source octet configurations, OCTET1 and OCTET2. These two configurations were described in Part 1 (see Figures 3 and 4), and provide the starting point for generating new structures. The top and bottom layers of the two source configurations are shown in Figures 21 and 22 respectively. As described earlier, the fundamental region (shown on left in each figure) has f1=1 and the array has f=12. Since the fundamental region and the unit triangle are the same in each layer, the number of unit triangles in the fundamental region is t=1 for the top and bottom layers. The part count in the fundamental region and the unit triangle is also the same. The number of fractional struts in each layer equals 1/2, i.e. $E_f = E_t = 1/2$. The number of fractional nodes in the top and bottom layers equals 1/6, i.e. $V_f = V_t = 1/6$.

The top and bottom layers of OCTET1 and OCTET2 layers act as master templates from which the top and bottom layers of the derivative configurations are obtained. The same procedure is used for the core. The derived top, bottom and core layers are then superimposed to obtain a new double-layered configuration. The positions of the nodes in the top and bottom layers of the new configurations remains the same as the source configuration in all cases. The size of the unit triangle also remains the same in the source and all derived configurations. Keeping the unit triangle fixed is an important constraint and provides a fixed unit measure for all configurations.

A total of nine different derivative double-layered configurations are described here. Of these, four are obtained from the octet configurations by removing struts only and the remaining five have both nodes and struts removed. The latter includes one example of a configuration where nodes are removed from one layer layer only, while the other four have nodes removed from top and bottom layers. The derived configurations vary significantly from one another in their geometry, symmetry and the distribution of struts and struts in the fundamental region. Each configuration is identified by a name. These examples are only a small part of an infinite number of configurations with a reduced part count which can be derived by the structure-generation techniques used here. Clearly many more examples can be derived by mixing-and-matching different top and bottom layers. An infinite number of double-layer configurations can be generated in this way. The number of possible double-layer configurations increases with f1, as in the case of the top or bottom layer alone, and is greater than the number of configurations possible from each separate layer.

For comparative purposes, all examples are shown as triangular arrays and correspond exactly to the size of the source octet arrays shown earlier in Figs.3a and 4a. In each case, triangular arrays of the top layer are shown in heavy lines and the bottom layer are shown with lighter lines. The separate single layers are shown first and are followed by the superimposed double layers. In examples where nodes are removed, the core configuration is also shown. The fundamental region and the source region of the source octet configuration are shown separately alongside. Within the array itself, the fundamental region at the apex *O* is shaded and is subdivided into unit triangles. This subdivision into unit triangles defines f1 which gives a measure of the size in unit triangles of the fundamental region. The number of unit triangles t in the fundamental region is derived from relations (16-19).

3.1 Configurations with Only Struts Removed

Four examples of double-layered configurations derived by removing struts only are described here. Of these, two are derived from OCTET1 and two from OCTET2, Three examples have the same geometry (and hence same symmetry) for the top and bottom layers. Such configurations may be candidates for easier assembly since the procedure described for one layer applies to the other. The fourth example combines two layers of different geometry and symmetry, and in addition each layer has a different value

for f1. In all four examples described here, the "full" core is inserted and joins the two layers; the term full is used when no struts are removed.

3.1.1 Configuration TOROID1 (#1)

Top layer

The triangular array of the top layer of the configuration named TOROID1 (Figure 23a) is an interesting array of alternating large triangles, half of which are "empty" and the other half are triangulated, making the entire configuration rigid in the plane. The empty triangles permit large open areas without removing any nodes.

This top layer is an array with Symmetry Type A. Its fundamental region, is shown shaded. Within the array, the fundamental region is subdivided into 4 unit triangles (shown in dashed lines). Thus t=4. Its outer edge is thereby divided twice and thus f1=2. The array of fundamental regions, also shown in dashed lines throughout the configuration, has f=6. The fundamental region containing a portion of the top layer, is shown separately on the left side (bottom). As before, the source region from the top layer of OCTET1 (no struts removed), also with f1=2, is shown above it. This region has no nodes or struts removed.

Referring to the source region of OCTET1, it has 1 full strut and 2 half-struts, making a total of 2 struts. It also has 1 half-node, lying at the middle of the edge on the lower side, and a 1/6th node lying at the top vertex of this region and thus. In the derived configuration 1 half-strut is removed and the number of nodes is unchanged. Thus, for the derived fundamental region $E_f = 3/2$ and $V_f = 2/3$. Since t=4, $E_t = 3/8$ and $V_t = 1/6$ (from relations (25) and (26)). Substituting for E_t and V_t in relation (10), or E_f and V_f in their place, the redundancy is $R = 1 - 2 \times 1/6 \times 8/3 = 1/9$ (or 11.1%).

Bottom Layer

The bottom layer of TOROID1 (Figure 23b) has the same geometry and symmetry as the top layer, but here it has a node lying at the apex *O* (compare with Figure 23a). The fractional part count and the redundancy is the same as the top layer.

Core

The core is the same as a full core since no struts are removed. E_t, the number of struts in the unit triangle of the core, is the same as OCTET1 (see Figure 5). Thus $E_t = 1/2$ (from relation (2)). Node that since all nodes are considered to be part of either the top or bottom truss layers, the core will never contain any nodes.

Superimposed Layers

The double-layer configuration TOROID1 (Figure 23c, shown magnified) is obtained by superimposing the top and bottom layers just described and inserting the full core. A portion of the infinite configuration is shown in Figure 23d. This superimposition produces an interesting configuration composed of interlocking "rings" of octahedra and tetrahedra and a periodic array of "holes" (hence the name "Toroid"). The holes may be useful for inserting various modules, e.g those used for experiments, habitation, etc. or other parts of a spacecraft. Even though struts are removed from the top and bottom layers, triangulation is maintained on the top and bottom surface.

The values of E_t and V_t for the superimposed layers equals the sum of E_t and V_t for the three separate layers. Thus $E_t = 3/8 + 3/8 + 1/2 = 5/4$. Similarly, V_t equals the sum of fractional nodes in the top and bottom layers, i.e. $V_t = 1/6 + 1/6 = 1/3$. From relation (11), $R = 1 - 3 \times 1/3 \times 4/5 = 1/5$ or 20%. The configuration TOROID1 thus has a redundancy of 20%. This is 13.3% less than the redundancy of OCTET1 from which it is derived (R=33.3%).

3.1.2 Configuration REDUCED1 (#2)

Top Layer

The top layer of REDUCED1 (Figure 24a) also has large size "empty" triangles, but here these are arranged in a pin-wheel manner around a central smaller triangle. It has Symmetry Type B, and the shaded fundamental region is an obtuse triangle. The region at apex *O* is subdivided into 3 unit triangles (1 full and 4 half unit triangles) which divide the outer edge of the region three times. Thus t=3 and f1=3. Three such regions make a larger equilateral triangle which, along with its three fundamental regions, is repeated in an array of f=4.

The source region from the full top layer of OCTET1, also with f1=3, has 1 full and 1 half-strut, and 1 half-node. In the derived configuration, 1 half-strut is removed making $E_f = 1$. Also, in the derived configuration the half-node is retained, making $V_f = 1/2$. Substituting for t and E_f in relation (25), $E_t = 1/3$. Similarly, substituting for t and V_f in relation (26), $V_t = 1/6$. Substituting for E_t and V_t in relation (10), the redundancy R=0 (or 0%). This layer is thus a non-redundant single-layer configuration. Of course, by itself this configuration is not a stable structure.

Bottom Layer

The bottom layer of REDUCED1 (Figure 24b) also has empty triangles but the geometry is different from the top layer. The empty triangles are similar in arrangement as the top layer of TOROID1, but the filled triangles are not fully triangulated as in the earlier example and they have one less strut. It has Symmetry Type B and the fundamental region has f1=6 and the array has f=2. The number of unit triangles in the fundamental region is t=12 (from relation 15). It has the largest fundamental region of all the examples described in this paper.

The source region of OCTET1 with f1=6 has 5 full and 2 half-struts making a total of 6 struts. Note that the two struts on the left edge of the fundamental region are not included here. Recall that for Symmetry Type B the fundamental region is rotated 3 times to create an equilateral triangle which is then repeated to complete an array. The two "missing" struts will be "filled in" as a result of the 3-fold rotation. From this, 1 full and both half-struts are removed, i.e. for the derived array E_f=4. From relation (25), $E_t = 4/12 = 1/3$. The source region also has a one-third node, 2 one-twelveth nodes (only the fractional portions of the nodes strictly inside the fundamental regions are counted and only nodes that will be connected by struts after the 3-fold rotation are included) , and 3 half-nodes, making a total of 2 nodes. In the derived fundamental region no nodes are removed, thus $V_f = 2$. From relation (26), $V_t = 2/12 = 1/6$. Substituting for E_t and V_t in relation (10), the redundancy R = 0 (or 0%). This configuration thus has 33.3% fewer struts than the bottom layer of OCTET1 and is also an example of a non-redundant single-layer configuration.

Core

The core is the same as a full core of OCTET1 since no struts are removed. Thus $E_t = 1/2$.

Superimposed Layers

The double-layer configuration REDUCED1 (Figure 24c, also shown magnified) is obtained by superimposing the derived top and bottom layers. A portion of the infinite configuration is shown in Figure 24d. In REDUCED1, the top layer, taken independently, has a f1=3, and the bottom layer has f1=6. This is the only example described here which has different values of f1 in the two layers. The matching is assured since the f1 values of the two layers are a simple multiple of one another. Note that although the symmetry of the top and bottom layers is the same, their geometries are quite different. This provides an example of "mix-and-match" where configurations with two completely different geometries are overlaid with the restriction that the two values of f1 are simple multiples of one another. It is easy to see from this example how an extremely large number of structures can be generated by mixing-and-matching top and bottom layers independently of their geometry. The number of possibilities increase when two different symmetries are overlaid. Double-layer configurations with different top and bottom layers permit different functional possibilities for the top and bottom surfaces.

The values of E_t for the superimposed layers equals the sum of E_t for the three layers. Thus $E_t = 1/3 + 1/3 + 1/2 = 7/6$. Similarly, V_t equals the sum of fractional nodes in the top and bottom layers, i.e. $V_t = 1/6 + 1/6 = 1/3$. From relation (11), R = 1/7 or 14.3% as compared to the value of R=33.3% for OCTET1 from which this structure was derived.

3.1.3 Configuration REDUCED2 (#3)

Top Layer

The top layer of REDUCED2 (Figure 25a) has a Symmetry Type C (alternate 1, see Figure 12c) and is composed of triangles and rhombi. It is characterized by an absence of mirror planes and is shown as a rhombic array which is twice the size of the source triangular array. It is composed of alternating triangles and hexagons, but the hexagons are subdivided into three rhombi. The fundamental region is also a rhombus which is subdivided into unit triangles. The fundamental region has f1=2 and is composed of 8 unit triangles, i.e. t=8. The array has f=6.

The source rhombic region of OCTET1 with f1=2 has 3 full and 2 half-struts making a total of 4 struts from which 1 full strut is removed in the derived fundamental

region. Thus $E_f = 3$, and from relation (25), $E_t = 3/8$. The full fundamental region also has 2 half-nodes lying at two edges and a 1/3rd node at the vertex of the rhombus. In the derived fundamental region, no node is removed. Thus $V_f = 4/3$, and $V_t = 1/6$. From relation (10), the redundancy R = 1/9 (or 11.1%).

Bottom Layer

The bottom layer (Figure 25b) has the same geometry and symmetry as the top layer just shown. In is in a shifted position, and is also a reflection of the top layer. This can seen by noting that the orientation of the rhombi within each hexagon of the bottom layer is a reflection of the rhombi within each hexagon of the top layer. The fundamental region is similar in the top and bottom layers, and the fractional part count and redundancy remain unchanged, i.e. R=1/9. An alternative bottom layer can have the rhombi within each hexagon oriented the same way as the top layer.

Core

The core is the same as the full core of OCTET1 since no struts are removed. Thus $E_t = 1/2$.

Superimposed Layers

The double-layered configuration REDUCED2 (Figure 25c, shown magnified), like TOROID1, has the same geometry for the top and bottom layers. A portion of the infinite configuration is shown in Figure 25d. Each layer has Symmetry Type C. Looking at the top surface, the tetrahedra and the octahedra lying below the rhombi are "incomplete", while those lying below the triangles are full. The full octahedra share a top vertex with the full inverted tetrahedra. This configuration has no mirror symmetry anywhere. The 3-fold rotational symmetry can be seen by the pin-wheel arrangement around the full octahedra, the full inverted tetrahedra and the full tetrahedra.

The values of E_t for the superimposed layers equals the sum of E_t for the three layers. Thus $E_t = 5/4$. Similarly, V_t equals the sum of fractional nodes in the top and bottom layers, i.e. $V_t = 1/3$. From relation (11), R = 1/5 or 20%. The configuration REDUCED2, like TOROID1, has a redundancy of 20% as compared to 33.3% for OCTET1 from which it is derived.

3.1.4 Configuration REDUCED3 (#4)

Top Layer

The top layer of REDUCED3 (Figure 26a) has the same geometry (appearing inverted) as that of the top layer of REDUCED1 (see Figure 24a). However, in this case the symmetry is different and corresponds to Symmetry Type C, (alternate 2, see Figure 12d). The rhombic array has no mirror-symmetry and cannot be bisected into two halves by a mirror plane. Compared with REDUCED1, the fundamental region is a rhombus and is reduced the size of the fundamental region in the earlier example. The fundamental region has f1=3. The number of unit triangles in the fundamental region, given by relation (19), is t=6. The array is also a rhombus with f=4.

The source region of the full OCTET2 has 1 full node and 3 full struts. In the derivative, 1 strut is removed. Thus $E_f = 2$. From relation (25), $E_t=1/3$. Also, in the derivative the node is retained. Thus $V_f = 1$, and $V_t = 1/6$ (from relation (26)). The redundancy is R = 0 (or 0%). The top layer of REDUCED3 is another example of a non-redundant 2-dimensional structure.

Bottom Layer

The bottom layer (Figure 26b) has the same geometry and symmetry as the top layer. The only difference is that here the large triangles are pointing down, whereas in the top layer the same triangles were pointing up. The fractional part count and the redundancy are the same as for the top layer.

Core

The core is the same as the full core of OCTET2 since no struts are removed. Thus again $E_t = 1/2$.

Superimposed Layers

The double-layered configuration REDUCED3 (Figure 26c, shown same size as the top and bottom layers) is obtained by superimposing the top layer and the bottom layer as shown and inserting the full core. A portion of the infinite configuration is shown in Figure 26d. The small triangles of one layer are placed directly over the large triangles of the other layer. Since the two point the same way this produces concavities in the shape of frustums of larger tetrahedra which are separated by smaller full octahedra. Looking at it from above, each full octahedron is surrounded by three frustums which are facing up

alternated by three which are facing down. This makes the configuration look like an undulating surface around the octahedron.

The values of E_t for the superimposed layers equals the sum of E_t for the three layers. That is, $E_t = 7/6$. Similarly, V_t equals the sum of fractional nodes in the top and bottom layers, i.e. $V_t = 1/3$. From relation (11), R = 1/7 or 14.3% (which is the same as for configuration REDUCED1) as compared to R=33.3% for OCTET2 from which it is derived.

3.2 Configurations with Nodes and Struts Removed

This class of configurations consists of structures in which nodes are removed periodically over the entire structure. Struts attached to these nodes are removed in the process. This is achieved by removing nodes and struts from the fundamental region. Struts attached to this node are also removed in the process. Configurations of this type have larger open areas within a structure, making it lighter and providing the possibility for efficient attachment of larger spacecraft components. The open areas are not restricted in size in many examples.

The removal of nodes can be thought of as removing entire portions of the octet configuration. This removal leaves behind empty spaces in the shape of large sized polyhedra or portions of such polyhedra. In cases where the empty spaces are "holes", a special class of structures termed "toroidal" configurations are obtained. One example of a toroidal structure with small holes (TOROID1) , has already been discussed.

Five double-layered configurations with nodes and struts removed are presented. Two examples of these are derived from OCTET1, and three from OCTET2. These five include three examples of double-layered toroidal structures.

3.2.1 Configuration SKEW1 (#5)

Top Layer

The top layer of SKEW1 (Figure 27a) is a well-known semi-regular tessellation composed of hexagons and triangles, where the hexagons can be seen as "islands"

surrounded by "rings" of triangles. Each ring can be thought of as a flat torus. This configuration can be left-handed or right-handed, and is the only example in this paper where the centers of symmetry, when joined, produce a skewed triangular grid. Skewed triangular grids have a Symmetry Type C. The fundamental region is a rhombus which is embedded in the skewed grid. The fundamental region has Symmetry Type C but because it is also skewed, it is different than either alternate 1 or alternate 2 as shown in Figure 12. The unit triangles within the shaded fundamental region at *O* are skewed with respect to the rhombus. Skewed grids cannot be described in terms of a single division like f1 since a second parameter f2 is necessary; details are described in [12]. The number of unit triangles in the fundamental region equals 14, i.e t=14.

The source full region of OCTET1 has 7 full struts in its fundamental region from which 2 struts are removed. Thus $E_f = 5$. From relation (25), $E_t = 5/14$. The full region also has 2 full nodes in the interior of the rhombus and a 1/3rd node which is removed. Thus $V_f = 2$. From relation (26), $V_t = 1/7$. From relation (10), the redundancy R = 1/5 or 20%. In the figure, the removed node is shown in the fundamental region and the array, but is clearly disconnected from the rest of the structure.

Bottom Layer

The bottom layer (Figure 27b) has the same symmetry and geometry as the top layer. It is in a shifted position with the apex *O* lying at the center of a hexagon of the tessellation. By comparison, the top layer has the apex *O* at the center of a triangle. Within the fundamental region (and hence the unit triangle), the part count and the redundancy is the same in each layer though the distribution of the nodes and struts is different. For example, in the case of nodes, the bottom layer has two 1/6th nodes while the top has one 1/3rd node.

Core

The core (Figure 27c) has an interesting geometry consisting of hexagons surrounded by 12-sided non-convex polygons in a trefoil shape. The core struts are removed along with the nodes on the top and bottom layers. The core thus has a dependent geometry.

The full region of OCTET1 has 7 struts from which 2 struts are removed. Thus $E_f = 5$. From relation (25), $E_t = 5/14$.

Superimposed Layers

The double-layered configuration SKEW1 is obtained by superimposing the top layer and the bottom layer and inserting the core. A rhombic array is shown in Figure 27d and a portion of the infinite configuration is shown in Figure 27e. In the superimposed position, the polygons of one layer are juxtaposed over different parts of the other layer. The triangles overlaid on the hexagons, and the hexagons overlaid on the triangles, define an undulating triangulated surface. Some triangles of the top layer are overlaid on inverted triangles of the bottom layer and make full octahedra. Other triangles of the top layer are overlaid on nodes of the bottom layer and make full inverted tetrahedra. Three inverted tetrahedra surround the full octahedra to make a composite module which is repeated at specific locations. SKEW1 is an interesting example of an all triangulated structure derived from the octet configuration.

As before, the value of E_t for the superimposed layers equals the sum of E_t for the three layers. That is, $E_t = 5/14 + 5/14 + 5/14 = 15/14$. Similarly, V_t equals the sum of fractional nodes in the top and bottom layers, i.e. $V_t = 1/7 + 1/7 = 2/7$. From relation (11), $R = 1 - 3 \times 2/7 \times 14/15 = 1/5$ or 20%. The configuration SKEW1 has a redundancy of 20% compared with 33.3% for OCTET1 from which it is derived.

3.2.2 Configuration MINIMUM1 (#6)

Top Layer

The top layer of MINIMUM1 (Figure 28a) is a semi-regular tessellation composed of alternating triangles and hexagons. The hexagons, six times the area of the triangle, are obtained by removing the node lying in the center of each hexagon. This configuration has Symmetry Type A, the fundamental region has f1=2, and the array has f=6. The fundamental region has 4 unit triangles, i.e. t=4.

The source region of the octet layer has 1 full and 2 half-struts making a total of 2 struts from which 1 full strut is removed. Thus $E_f = 1$, and from relation (25), $E_t = 1/4$. In addition, the full configuration has a half-node lying on the mid-edge of the region and a 1/6th node at the vertex from which the 1/6th node is removed. Thus $V_f = 1/2$. from relation (26), $V_t = 1/8$. The redundancy is $R = 0$ (or 0%). This is another example of a non-redundant 2-dimensional configuration. As before, the removed node is shown for visualization purposes although it is disconnected from the rest of the configuration.

Bottom Layer

The bottom layer (Figure 28b) is already a familiar one from earlier examples and is identical to the top layer of TOROID1 (see Figure 23a and earlier description). Note that this layer has only struts removed. The part count and the redundancy is the same as the top layer of TOROID1, i.e. $E_t = 3/8$, $V_t = 1/6$ and R = 1/9 (or 11.1%).

Core

The core (Figure 28c), in the plan view shown, is composed of hexagons surrounded by the non-convex 12-sided polygons as seen earlier in the core of SKEW1 (Figure 27c). The full core has 1 full and 2 half-struts making a total of 2 struts; the half-struts lie on the edges of the region. In the derived core, 1 half-strut is removed. Thus $E_f = 3/2$. Here also t=4. Thus $E_t = 3/8$ (from relation (25)).

Superimposed Layers

The double-layered configuration MINIMUM1 (Figure 28d, shown magnified), obtained by superimposing the top, bottom and core layers, is an interesting example of a hybrid configuration where the top and bottom layers are of different classes. The top has nodes and struts removed while the bottom layer has only struts removed. After superposition, the configuration obtained is composed of full octahedra and full tetrahedra only. In this sense, MINIMUM1 is also an "octet" configuration though with many components removed. A portion of the infinite configuration is shown in Figure 28e.

Each octahedron is surrounded by 3 upright tetrahedra. This arrangement acts like a composite module which is repeated throughout the array, as in SKEW1. Three such modules are connected by an inverted tetrahedron. The three inclined faces of the inverted tetrahedra lie on three inclined 2-dimensional trusses which are continuous. The entire configuration has three parallel sets of inclined trusses intersecting at 120^o.

The sum of fractional struts from each layer makes Et = 1. The sum of fractional nodes of the top and bottom layers makes Vt = 7/24. The redundancy R = 1/8 (or 12.5%), from relation (11). Of all examples discussed in this paper, MINIMUM1 has the lowest redundancy (hence the name MINIMUM1).

3.2.3 Toroidal Configurations

Three examples of toroidal configurations are presented. The formal aspects are first described and are followed by specific examples of the configurations TOROID2, TOROID3 and TOROID4 (see Figures 29d, 30d and 31d).

Periodic toroidal configurations are composed of doughnut-shaped modules in 2- or 3-dimensional arrays where individual doughnuts (tori) are fused together to make a continuous structure. In the examples described here, the torus is composed of linear tubular segments. Each tubular segment is composed of linear arrays of tetrahedra and octahedra. The axes of these segments, and hence of the tori, define a network. These networks can have different topologies and sizes, and they correspond to plane tessellations (though in some cases only in their plan view).

Since the source structure for deriving these configurations is the octet configuration, only double-layered toroidal configurations are described here. The double-layered examples are a part of a large class of 3-dimensional toroidal configurations derived from 3-dimensional networks. Note that in the examples described here the interior space of the tubular segments is not "hollow". The exterior surfaces of these configurations define a continuous "toroidal surface". as required by the strict definition of a torus. The cross members in the interior are required for stability purposes in pin-jointed structures. When the tubular segments have a triangular cross-section, the configurations are pure toroidal surfaces since no interior struts are needed.

Toroidal configurations have an interesting property of recursion. The toroidal structures described here can be derived from simple tessellations by converting each single strut (edge) of the tessellation into tubular segments composed of an array of struts "wrapped" around a tube. Each strut (edge) of this wrapped array can again be converted into a tubular segment as in the previous step, and so on. This process of recursion provides a morphological device which enables us to cover larger areas with struts of the same size.

3.2.3.1 Configuration TOROID2 (#7)

Top Layer

The top layer of TOROID2 (Figure 29a) is a plane toroidal tessellation. It is composed of flat tori which enclose large open areas enclosed by triangulated strips. It is related to the skew tessellation of Figure 27a. Here the open areas are non-regular hexagons with alternating sides of two different lengths. In the illustration, the open areas are halved since the size of the array shown is relatively small. A larger-sized array than the one shown in the illustration would show the toroidal nature of this tessellation more clearly. The configuration shown has a Symmetry Type B, the fundamental region has f1=6, and the array has f=2. From relation (17), t=12.

The source region of the source octet layer has 5 full struts and 2 half-struts making a total of 6 struts. In the derived fundamental region, 2 full and 1 half-strut is removed . Thus $E_f = 7/2$, and $E_t = 7/24$. The octet configuration also has 1 full node in the interior of the region and 2 half-nodes on the edges from which 1 half-node is removed. Thus $V_f = 3/2$, and $V_t = 1/8$. The redundancy R = 1/7 (or 14.3%).

Bottom Layer

The bottom layer (Figure 29b) is a slightly different toroidal tessellation. Here the open areas (also shown halved) are large triangles. The edges of the large open triangles are three strut lengths long. This configuration also has Symmetry Type B, the fundamental region has f1=6, the array has f=2, and t=12 as in the top layer.

The source region of the octet layer with f1=6 has 5 full struts and 2 half-struts from which 1 full and 1 half-strut is removed in the derivative configuration (see the comments regarding strut and node count for this type of region in the discussion for the bottom layer of configuration REDUCED1). Thus $E_f = 9/2$, and $E_t = 3/8$. In addition, the full octet layer has a 1/3rd node at the obtuse vertex, two 1/12th nodes at the acute nodes and 3 half-nodes at the three edges of the region, making a total of 2 full nodes. From this the two 1/12th nodes are removed. Thus, $V_f = 11/6$, and $V_t = 11/6 \times 1/12 = 11/72$ (from relation (26)). Substituting for E_t and V_t in relation (10), the redundancy $R = 1 - 2 \times 11/72 \times 8/3 = 5/27$ (or 18.52%).

Core

The core (Figure 29c) has a dependent geometry composed of rows of hexagons (in the plan view). It has 5 full struts and 2 half-struts (half struts lie on the edge of the fundamental region) making a total of 6 struts. In the derived core, 1 full and 1 half-strut is removed. Thus $E_f = 9/2$. Since the core also has t=12, $E_t = 3/8$.

Superimposed Layers

The double-layered configuration TOROID2 (Figure 29d, shown magnified) is obtained by superimposing the three layers. A portion of the infinite configuration is shown in Figure 29e. The triangulated strips on the top and bottom, with the rows of hexagons in the core, make up the tubular segments of each torus. Three tubular segments meet around an inverted tetrahedron in a pinwheel manner. The vertical axis through each inverted tetrahedron is a 3-fold axis of rotation. Alternative toroidal structures can be obtained when the 3-fold axes pass through the upright tetrahedra, the octahedra, or a combination of these polyhedra. The empty spaces in the structure (shown halved) have a non-regular hexagon superimposed over a large equilateral triangle.

The sum of fractional struts from the three layer makes $E_t = 25/24$. The sum of fractional nodes of the top and bottom layers makes $V_t = 5/18$. From relation (11), the redundancy R = 1/5 (or 20%). Again, this should be compared with the value of R=33.3% for OCTET1 from which this configuration is derived.

3.2.3.2 Configuration TOROID3 (#8)

Top Layer

The top layer of TOROID3 (Figure 30a) has the same geometry and symmetry as the top layer of TOROID2 (see Figure 29a and the earlier description). It can be obtained from the earlier example by a reflection around the horizontal line passing through the apex *O*. The part count and redundancy are the same as the top layer of TOROID2, i.e. $E_t = 7/24$, $V_t = 1/8$, and R = 1/7 (or 14.3%). Also, t=12, as in the earlier example.

Bottom Layer

The bottom layer (Figure 30b) has the same geometry and symmetry as the top layer. It can be obtained from the top layer by a reflection around the horizontal line passing through the apex O. It is identical to the top layer of TOROID2 (Figure 29a). Again $E_t = 7/24$, $V_t = 1/8$, and R = 1/7.

Core

The core (Figure 30c) here is also composed of rows of hexagons in the plan view. The geometry, obtained by removing struts associated with the removed nodes, is also dependent as in the earlier examples. The full configuration has 5 full struts and 2 half-struts making a total of 6 struts from which 1 full and 2 half-struts are removed. Thus $E_f = 4$, and since t=12 as in the top and bottom layers, $E_t = 1/3$.

Superimposed Layers

The double-layered configuration TOROID3 (Figure 30d, shown magnified) is related to TOROID2 and is obtained by superimposing the layers as before. Here the three tubular segments meet around an octahedron. A portion of the infinite configuration is shown in Figure 30e. The empty spaces are composed of two identical non-regular hexagons overlaid over one another, but one is rotated at 60^o with respect to the other.

The fractional struts in the unit triangle $E_t = 11/12$, is obtained by adding the values of E_t for each of the three layers as before. Similarly, $V_t = 1/4$. Finally the redundancy is R = 2/11 (or 18.2%) as compared with 33.3% for OCTET2.

3.2.3.3 Configuration TOROID4 (#9)

Top Layer

The top layer of TOROID4 (Figure 31a) is a toroidal tessellation based on a different network. Here, the center-lines of the triangulated strips make a regular triangular grid, showing a self-similarity with the source triangular grid from which the configuration is derived. This self-similar recursion could be continued to the next stage where each individual strut within a triangulated strip could itself be a triangulated strip, and so on. The configuration shown has f1=4, f=3, and Symmetry Type A. The number of unit triangles in the fundamental region is t=16.

The source region of the octet layer has 6 full struts and 4 half-struts from which 1 full and 2 half-struts are removed in the derived fundamental region. Thus Ef = 6, and Et = 3/8. The full region also has 1 full node, 3 half-nodes and a 1/6th node from which the 1/6th node is removed. Thus Vf = 5/2 and Vt = 5/32. From relation (10), the redundancy is R = 1/6 (or 16.7%).

Bottom Layer

The bottom layer (Figure 31b) has the same geometry and symmetry as the top layer. One can be obtained from the other by a reflection around the horizontal line passing through the apex *O*. The part count and redundancy is the same as the top layer.

Core

The core (Figure 31c) is composed of rows of hexagons in a triangular arrangement determined by the network. The full region has 6 full struts and 4 half-struts making a total of 8 struts. In the derived core fundamental region, 2 half-struts are removed. Thus $E_f = 7$ and $E_t = 7/16$.

Superimposed Layers

The double-layered configuration TOROID4 (Figure 31d and 31e) is obtained by superimposing the top, bottom and core just described. This example, like TOROID2 and TOROID3, is also composed of tubular segments. Six such segments meet at the octahedron in the center of the array shown in the figure. The empty spaces are triangular holes composed of a smaller triangle superimposed over a larger triangle.

Taken together, $E_t = 19/16$ for all three layers. Similarly, $V_t = 5/16$. From relation (11), the redundancy for TOROID4 is given by $R = 4/19$ (or 21.1%) compared to 33.3% for OCTET2 from which it is derived.

PART 4
REMARKS AND SUMMARY OF RESULTS

4.1 Rationale and Analytical Considerations for the Truss Configurations Presented

It is possible to generate many different truss configurations using the structure-generation techniques presented in Part 2. Although approximately twenty-five configurations derived from the Octet truss were investigated in the work leading to this paper, only nine have been presented. It is noted that prior work for deriving and analyzing a special class of "statically determinate" reduced-part-count structures is presented in reference [13].

The selection of these nine configurations presented here was based on both practical and analytical considerations. For each reduced-part-count truss configuration, analytical (finite-element) models were formulated. Models were also constructed for the two configurations with full part count, OCTET1 and OCTET2. The analytical models were formulated by "cutting" a finite portion from the infinite configurations shown in Part 3.

The finite truss models were constructed to be hexagonal in shape. This shape is typical for many large space applications. Each model utilized strut and joint properties assumed to be typical for large precision truss applications. Descriptions of these properties can be found in reference [5]. A detailed presentation of analytical results is beyond the scope of this paper which focuses on the morphological aspects of each configuration. More details concerning the analytical results for the structures presented here are contained in reference [14]. The practical design and structural performance of the truss configurations are the subjects of current and future work. However, a few comments are appropriate here.

Each of the nine truss configurations presented is structurally stable (not a mechanism). Stability is not guarantied from the generation techniques presented in Part 2. Furthermore, visual inspection of a particular truss configuration is not in general a reliable means of detecting an unstable structure. Thus, the primary purpose of the analytical models was to insure stability.

The fact that a particular configuration is stable is not sufficient to make it useful. Several reduced part count configurations were examined that although stable, showed a significant decline in structural performance when compared to the original octet configurations. The gauge for structural performance in selecting the nine configurations presented here was free-free natural vibration frequency. Free-free vibration frequency provides a useful measure of structural stiffness. The natural frequencies of the truss models examined ranged from 16 Hz for configuration REDUCED3, to 21.7 Hz for both configurations OCTET1 and OCTET2. The reduction in frequency for the reduced part count configurations ranged from 15% for TOROID2 to 26% for REDUCED3. A more complete structural analysis of the various configurations and an in depth comparative study are underway at the time of this writing.

A primary motivation for finding reduced-part-count structures is to reduce complexity and on-orbit assembly time. The results of the finite element analyses indicate that it is possible to generate structures with significantly reduced part count and only a moderate decrease in structural performance. Reference [14] discusses some alternatives for overcoming reductions in structural performance white retaining reduced part count.

4.2 Summary of Results

The part count and the redundancy for the nine truss configurations are summarized in Table 2. The fractional part count, given by the number of struts E_t and nodes V_t within a unit triangle, is given for each truss. A comparison of part count is possible since the unit triangle is kept the same size throughout all the examples of derived configurations. The number of redundant struts (relations 7 and 8) is given in the third column. The ratio of redundant struts to the total number of struts, R, is given in the fourth column. The octet configurations OCTET1 and OCTET2 are given at the bottom to provide a reference.

No.	Configuration and Single-Layer Symmetry Types ( )	Struts in Unit Triangle (E_t)	Nodes in Unit Triangle (V_t)	Redundant Struts (r)	Redundancy (R)	
#1	TOROID1 (A)	5/4	1/3	1/4	1/5	(20%)
#2	REDUCED1 (B)	7/6	1/3	1/6	1/7	(14.3%)
#3	REDUCED2 (C)	5/4	1/3	1/4	1/5	(20%)
#4	REDUCED3 (C)	7/6	1/3	1/6	1/7	(14.3%)
#5	SKEW1 (C)	15/14	2/7	3/14	1/5	(20%)
#6	MINIMUM1 (A)	1	7/24	1/8	1/8	(12.5%)
#7	TOROID2 (B)	25/24	5/18	5/24	1/5	(20%)
#8	TOROID3 (B)	11/12	1/4	1/6	2/11	(18.2%)
#9	TOROID4 (A)	19/16	5/16	1/4	4/19	(21.1%)
#10	OCTET1 (A)	3/2	1/3	1/2	1/3	(33.3%)
#11	OCTET2 (A)	3/2	1/3	1/2	1/3	(33.3%)

Table 2. Comparative Fractional Part Count and Redundancy of the Octet Truss and Nine derived Configurations.

The reference octet trusses have R=33.3%. Among the derived configurations, the redundancy varies from a high of 21.1% for TOROID4 to the low of 12.5% for MINIMUM1.

A useful comparative measure for the relative part count of configurations can be given by the ratio of the number of struts to nodes. For infinite configurations, like the ones being discussed here, this ratio is given by Et/Vt. Table 3 lists this ratio for the nine configurations. The ratio is also equivalent to the number of struts per node in an infinite configuration with the same geometry. Thus the reference trusses, OCTET1 and OCTET2, have 4.5 struts for every node. The minimum value for this ratio is 3.0, which would occur for a non-redundant structure. All derivative configurations range between the two extreme values of 3.0 and 4.5. More specifically, the lowest ratio is 3.43 struts per node.

No.	Configuration	Ratio of Struts to Nodes in Unit Triangle (E_t/V_t)*
#1	TOROID1	3.75
#2	REDUCED1	3.5
#3	REDUCED2	3.75
#4	REDUCED3	3.5
#5	SKEW1	3.75
#6	MINIMUM1	3.43
#7	TOROID2	3.75
#8	TOROID3	3.67
#9	TOROID4	3.8
#10	OCTET1	4.5
#11	OCTET2	4.5

*For an infinite non-redundant truss, $E_t/V_t = 3.0$

Table 3. The Ratio of Struts to Nodes for a Unit Triangle Region of Each of the Eleven Truss Configurations.

Lowering the ratio of struts to nodes below 3.43 in infinite double-layered configurations would be an attractive goal to pursue. Though geometric configurations with a lower ratio may be found, the examples presented here are those which resulted in frequency reductions of 15-26%. This is an important constraint and makes the search for stiff and uniformly periodic structures a difficult challenge.

Morphological studies provide an important and systematic direction in this challenge for the discovery of structures with a reduced number of components. Towards this end, the fundamental region and the unit triangle method described here provides an expedient and economical way to derive new geometries for infinite, periodic space structures. This method also provides a compact way to derive the part count and

redundancy. Since a common approach is used for all space structures, independent of their geometry, symmetry or dimension, a comparative study is made possible. Though the examples described here are based on the octet truss, the approach described here is general and can be easily extended to other source geometries and symmetries in 2- and 3-dimensions. The generality of the approach opens up directions for further research in the morphology of novel space structures.

ACKNOWLEDGEMENTS

Dr. Martin M. Mikulas for many inspiring discussions and for Haresh Lalvani's sabbatical at NASA Langley Research Center.

To Neil Katz for providing visualization support through models and computer-aided drawings for the project during his month at Langley.

To the colleagues in the Spacecraft Structures Branch for their hospitality and for sharing their knowledge.

To Dr. Ahmed Noor and GWU staff for their support and cooperation.

To Pratt Institute for for Haresh Lalvani's sabbatical leave during the academic year of Fall1989 through Spring 1990.

REFERENCES

1. Fuller, Buckminster R.: *Synergetics : Exploration in the Geometry of Thinking.* McMillan, New York, 1975.

2. Mikulas, Martin M., Bush, Harold G., and Card, Michael F. : Structural Stiffness, Strength and Dynamic Characteristics of Large Tetrahedral Space Structures. NASA TM X-74001, March 1977.

3. Collins, Timothy J. and Fichter, W.F.: Support Trusses for Large Precision Segmented Reflectors: Preliminary Design and Analysis. NASA TM 101560, March 1989.

4. Bush, Harold G., Herstrom, Catherine L., Heard, Walter L., Jr., Collins, Timothy J., and Fichter, W.B.: Design and Fabrication of an Erectable Truss for Precision Segmented Reflector Application. AIAA Paper No. 90-099, April, 1990.

5. Mikulas, Martin M., Jr., Collins, Timothy J., and Hedgepeth, John M.: Preliminary Design Approach for Large High Precision Segmented Reflectors. NASA TM 102605, February 1990.

6. Coxeter, H.S.M., *Regular Polytopes.* Dover, New York, 1973, pp 63.

7. Lalvani, Haresh: *Multi-Dimensional Periodic Arrangements of Transforming Space Structures*, Ph.D. Thesis, University of Pennsylvania, 1981. University Microfilms, Ann Arbor, Michigan, 1982.

8. Calladine, C.R.: Buckminster Fuller's "Tensegrity" Structures and Clerk Maxwell's Rules for the Construction of Stiff Frames. International Journal of Solids and Structures, Permagon Press, Vol 14, pp 161-172, 1978.

9. Lalvani, Haresh: Coding and Generating Complex Periodic Patterns, *Visual Computer* Vol 5, pp 180-202, Springer-Verlag, Germany, 1989.

10. Buerger, Martin: *Elementary Crystallography.* M.I.T. Press, 1968.

11. Shubnikov A.V. and Koptsik V.A.: *Symmetry in Science and Art.* Plenum, New York , 1974.

12. Lalvani, Haresh: Continuous Transformations of Subdivided Surfaces. *Space Structures* , Multi-Science Publ., U.K., (in press).

13. Anderson, M.S. and Nimmo, N.A.: Dynamic Characteristics of Statically Determinate Space-Truss Platforms. *Journal of Spacecraft and Rockets*, Vol 23, No. 3, pp 303, 1986.

14. Collins, Timothy J. and Lalvani, Haresh: Generation and Analysis of Reduced-Part Count Truss Geometries for Space-Based Applications. AIAA/ASME/ASCE/AHS/ASC 32nd Structures, Structural Dynamics and Materials Conference, Baltimore, Maryland, AIAA Paper No. 91-1193, To be presented April,1991.

GLOSSARY OF TERMS

Frequency

The term "frequency" is used for number of linear divisions (or unit triangles) f1 of a fundamental region. In most cases this is along the edge of the fundamental region. It is also used for the number of divisions (fundamental regions) f along the edge of an entire periodic array. While the former provides the extent of subdivision of the fundamental region, the latter defines the extent of plane-filling of the entire array.

Full (structure, region,..... etc.)

The term "full" is used to identify a structure or region from which no struts have been removed. Full structure, full fundamental region, full layer, full top layer, etc. are configurations containing all struts from which derivatives are obtained by removing struts. The term is adapted from "full set" used in set theory.

Fundamental Region

The minimum region of a symmetrical configuration which can generate an entire periodic structure by symmetry operations (reflections, rotations, translations).

Inversion (Plane of Inversion)

The term "plane of inversion", represents a special type of symmetry plane which permits "inversion". By inversion, the region on the top left of this plane (and facing down) is transformed or "inverted" to the bottom right of the plane (and facing up). In the octet truss, the planes of inversion are perpendicular to the top and bottom layers of the truss.

Mechanism

An unstable pin-jointed structure.

Octet Configuration

The octet truss or the tetrahedral truss composed of a close-packed array of regular octahedra and tetrahedra.

Part Count

The number of component parts in a physical space structure, i.e. the number of nodes, struts, and other components.

Plane-filling

(adj.) Having the property of filling the entire (2-dimensional) plane completely without gaps, e.g. a plane-filling polygon, or a plane-filling procedure.

Space-filling

(adjective) Having the property of filling entire space (usually 3-dimensional) completely without gaps;

(noun) A structure which has the property of filling all space; alternatively also sometimes termed a "close-packing".

Space Structure

A generic term for a 3-dimensional configuration. Usually used for configurations composed of topological elements of different dimensions, namely, vertices, edges, faces and cells. In a physical structure, these topological elements translate into nodes, struts, panels, and 3-dimensional modules.

Symmetry Elements

The (abstract) component parts of a symmetrical structure. Symmetry elements include mirror planes, axes of symmetry, etc.

Symmetry Operations

Reflection, rotation, translation and their combinations.

3-fold Symmetry / 3-fold Rotation

The usage P-fold symmetry suggests a P-fold rotation, or the presence of a P-fold axis of rotation in a structure. A rotation of P times through an angle of $360^{o}/P$ about this axis brings the structure back to its original orientation. In structures with a 3-fold symmetry, $P=3_{\blacktriangle}$ and the structure is composed of three identical parts which can be brought in congruence with one another by a rotation of 120^{o} about the 3-fold axis.

Unit Triangle

The minimum equilateral triangle unit used for generating a periodic octet array. It is the plan view of the triangular prism unit of the octet truss, but is used here as a convenient 2-dimensional unit (of constant size) used for comparative studies of different double-layered truss configurations.

NOTES

1. Alternatively, all edges of the space-filling of octahedra and tetrahedra can be determined by "vectors" which are defined by lines joining the center of the cube to the mid-points of its edges. Since the cube has 12 edges, and the opposite two lie on the same vector, 6 distinct vectors can be specified this way. All edges of the octahedral-tetrahedral space-filling are parallel to these 6 vectors. The 6 vectors define a 6-dimensional Euclidean space, and the octet truss can be thought of as a 3-dimensional structure projected from 6-dimensional Euclidean space. The concept of seeing 3-dimensional structures as projections of n-dimensions broadens the definition of space structures and provides a more general way to classify and generate new space structures.

2. The symmetry of the octet truss corresponds to the symmetry group **p3m1** in the international crystallographic notation.

3. An interesting alternative to this procedure is to use "self-similarity" for plane-filling. By this method, one larger equilateral triangle is obtained from four smaller equilateral triangles such that the side of the larger triangle is twice the side of the smaller triangle. This procedure can be continued recursively and the value of f doubles at each stage of recursion.

4. These eight are a part of 16 double-layered symmetries associated with the triangular-hexagonal symmetry groups (see Fig.187 in [11], where the "unit mesh" number 75 corresponds to the double-layered octet truss).

5. Symmetry Type A is notated as **p3m1** in the international crystallographic system. Symmetry Type B has the crystallographic symbol **p31m,** and Symmetry Type C has the symbol **p3** (see [10]). Note that the single layer of the octet can also be associated with two other plane symmetry groups, **p6mm** and **p6**. These have 6-fold symmetry at each node; in the examples described later in Part 3, Figure 27a corresponds to p6 and Figure 28a to p6mm. However, since the double-layered octet has 3-fold axes of symmetry only, the introduction of these two additional symmetries was not considered necessary.

6. The two correspond to the two basic subdivisions of an equilateral triangle and are used in the derivation of geodesic domes. In spherical subdivisions based on the icosahedron, Alternative 1 described here corresponds to the 'alternate' breakdown, and Alternative 2 is the 'triacon' breakdown.

7. Incidentally, the rhombi with f1=3 in Figures 12c and 12d correspond to the crystallographic *unit cell* which can fill the entire plane by translations only. This gives us an alternative plane-filling procedure.

8. The structures described here are restricted to the removal of nodes and struts. The techniques of structure-generation described here can be extended to include removal of panels (faces) and 3-dimensional cells.

9. Note that in the method described here, the subdivision inside the fundamental region has the same geometry as the octet configuration. In this sense, there is a property of "self-similarity" associated with the procedure described here. This self-similarity can be used recursively to derive "fractal" trusses with a reduced part count.

10. This particular derivative, which will be used later in two different derivatives, is also a part of an infinite series of tessellations composed of Sierpinski triangles. Sierpinski triangles are characterized by a recursive self-similarity and are thus fractals. Periodic tessellations using these triangles and their 3-dimensional extension into an infinite class of 'fractal tetrahedra' have been suggested concurrently in a separate project (Non Redundant Space Structures, unpublished report to Joint Institute of Flight Sciences, George Washington University, NASA LaRC, May 1990, available from authors). The inherent property of non-redundancy in these fractal polyhedra and the Sierpinski triangle have also been pointed out; details are being prepared at the time of this writing.

11. An alternative approach is to determine the number of equilateral triangular regions of frequency f1 within a triangular array of frequency f. Such equilateral triangles correspond to the fundamental regions of frequency f1. For a fixed f1, the number of such triangular regions in an array of frequency f equals f^2 for each Symmetry Type.

12. This zig-zag array is a layer through the "diamond lattice", a lattice which can be visualized as an array of 4 struts meeting at every node at co-equal angles of 109°28'. This makes TOROID2 a double-layered slice of a 3-dimensional "infinite polyhedron" based on the diamond lattice. Infinite polyhedra have been described in *Infinite Polyhedra* by B. Wachman and M. Kleinman (Technion, Israel Institute of Technology, Haifa, Israel, 1974). In the present work, TOROID1 is obtained by a different procedure, i.e. by removing struts from an octet truss.

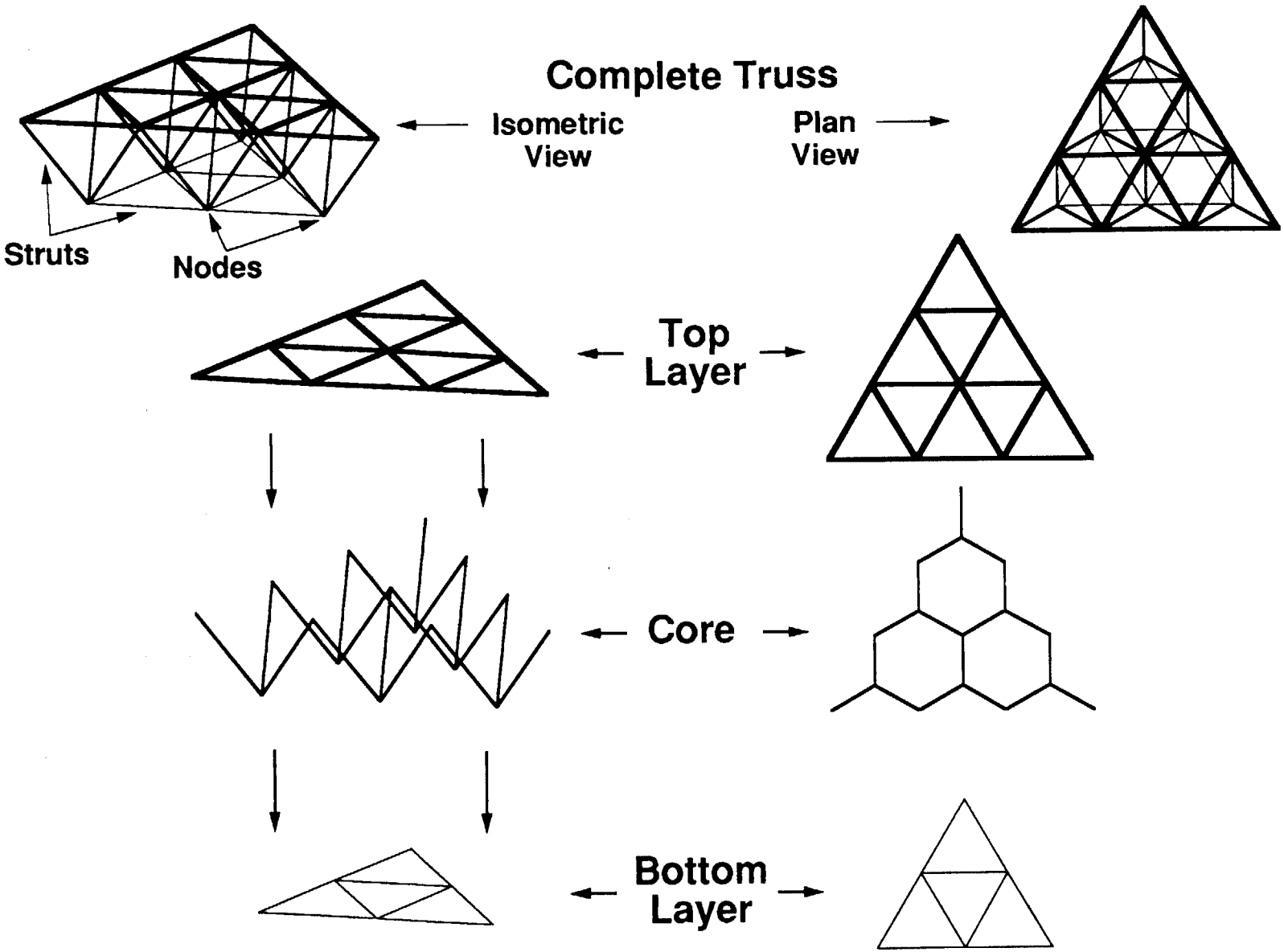

Figure 1. Representative Portion of the Octahedral-Tetrahedral (Octet) Truss.

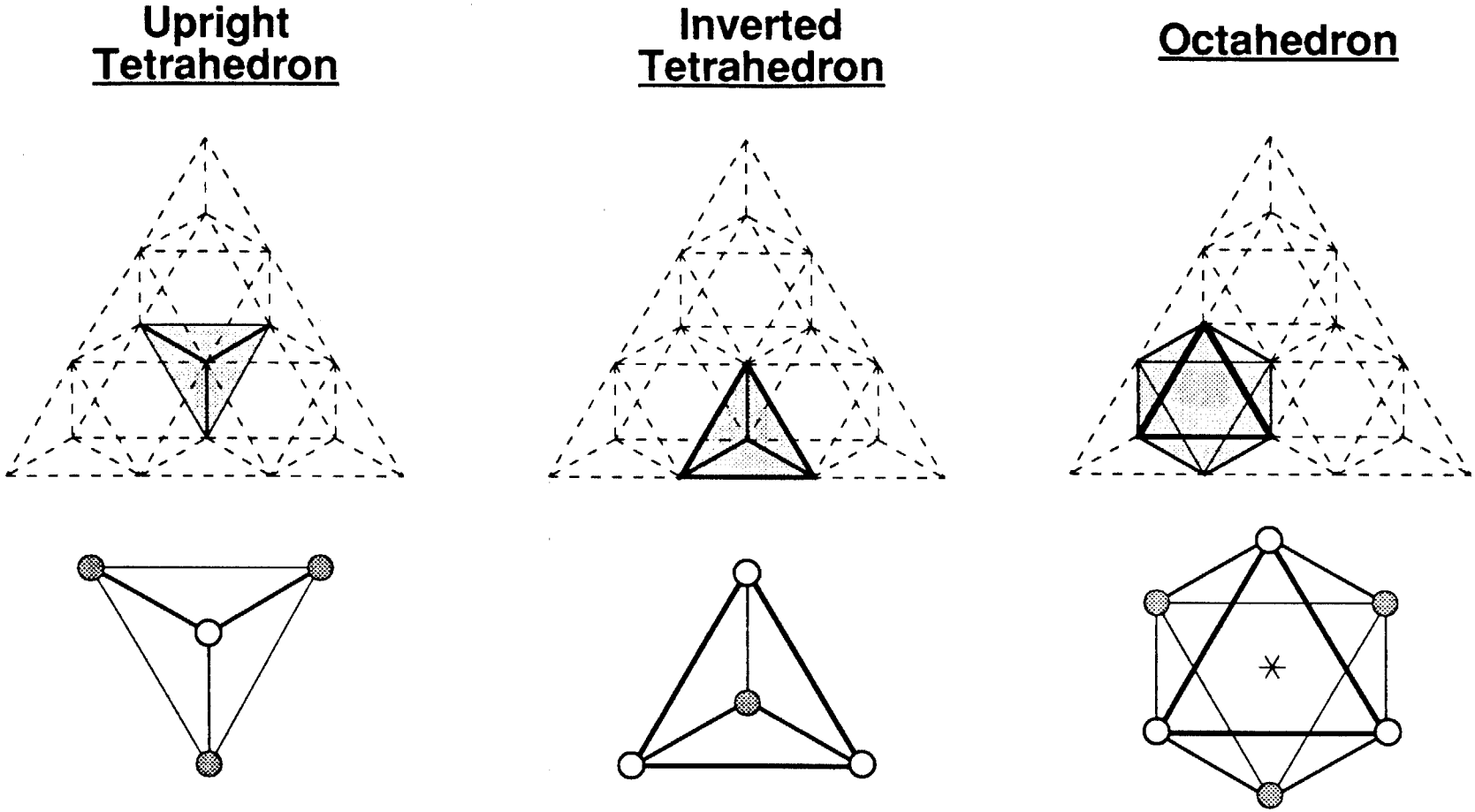

Figure 2. The Three Basic Polyhedra in the Octet Truss.

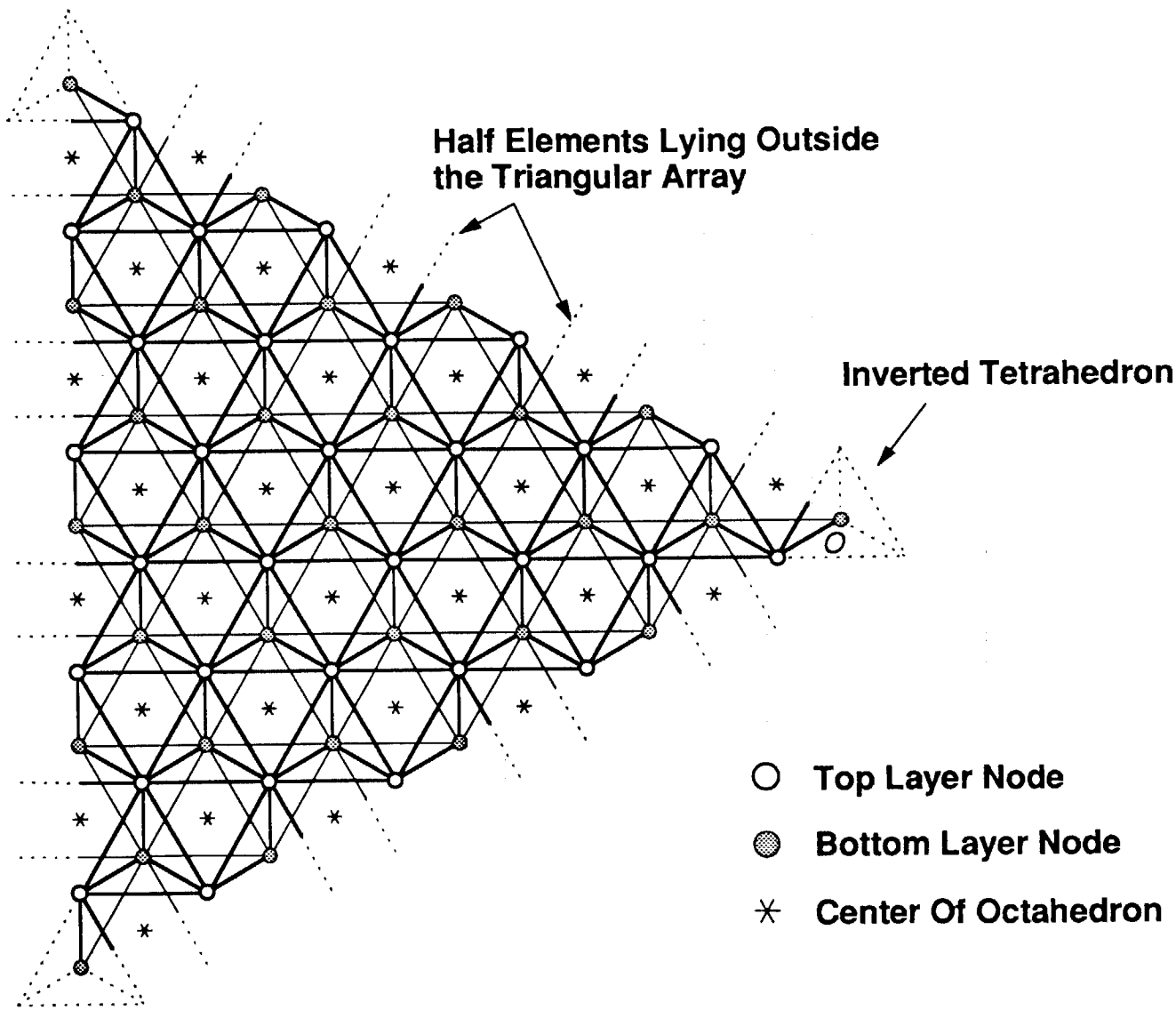

Figure 3a. A Triangular Array of the Octet Truss Configuration With Inverted Tetrahedrons at the Vertices (Configuration OCTET1).

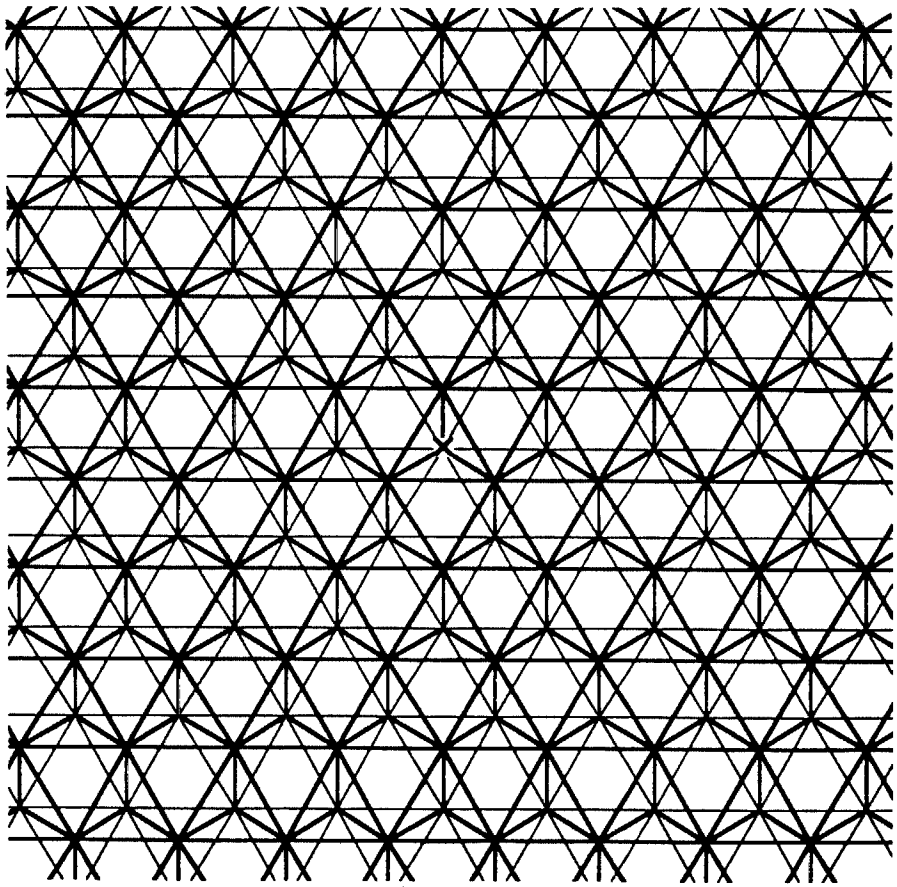

Figure 3b. A Portion of the Infinite Configuration OCTET1.

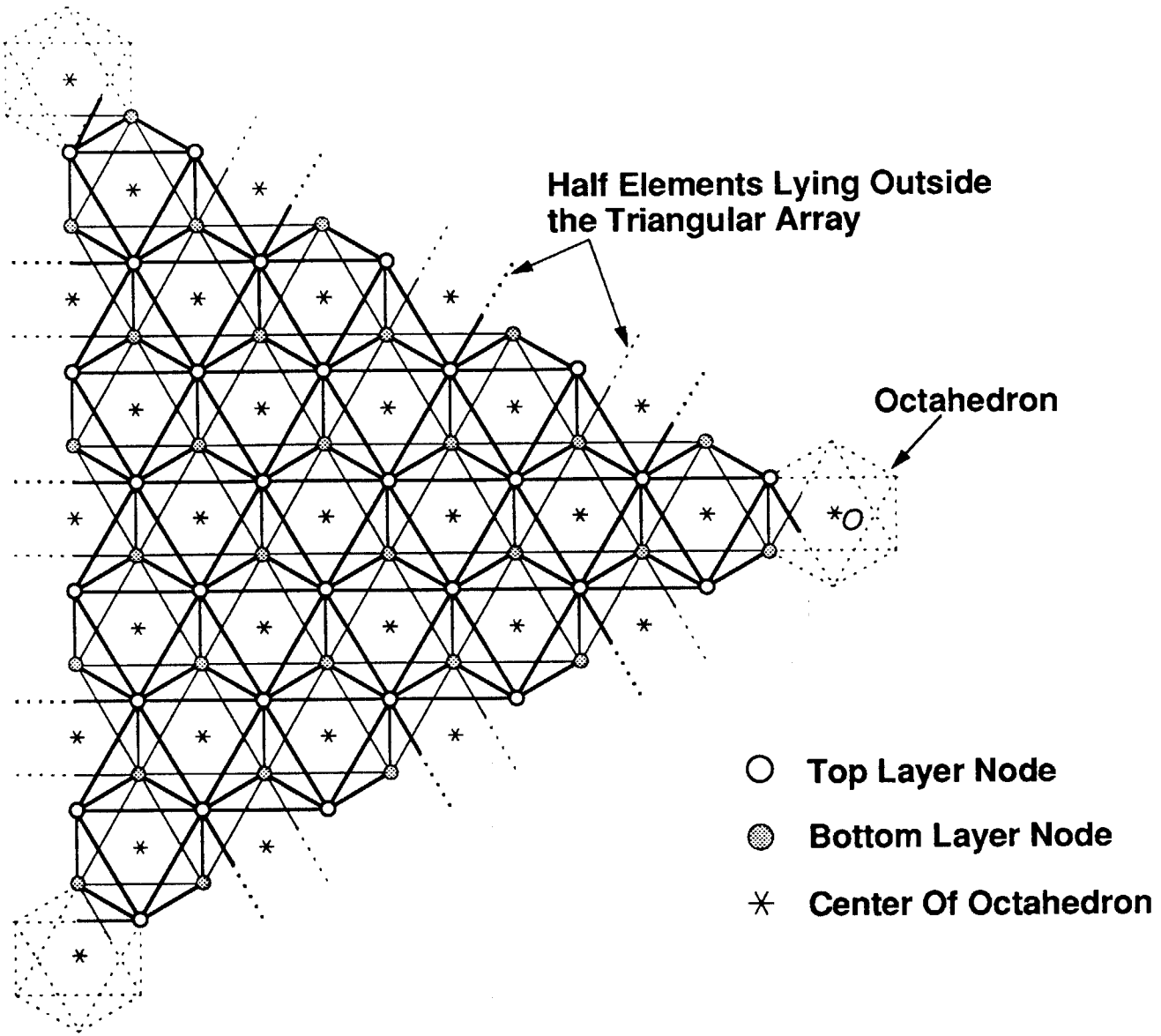

Figure 4a. A Triangular Array of the Octet Truss Configuration With Octahedrons at the Vertices (Configuration OCTET2).

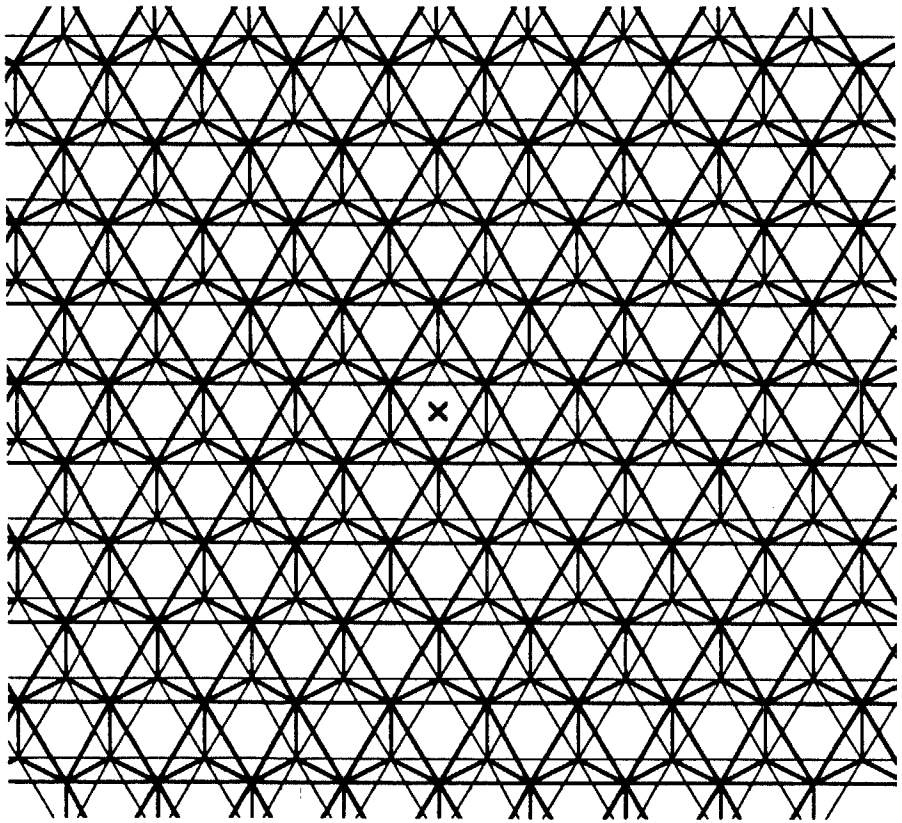

Figure 4b. A portion of the infinite configuration OCTET2

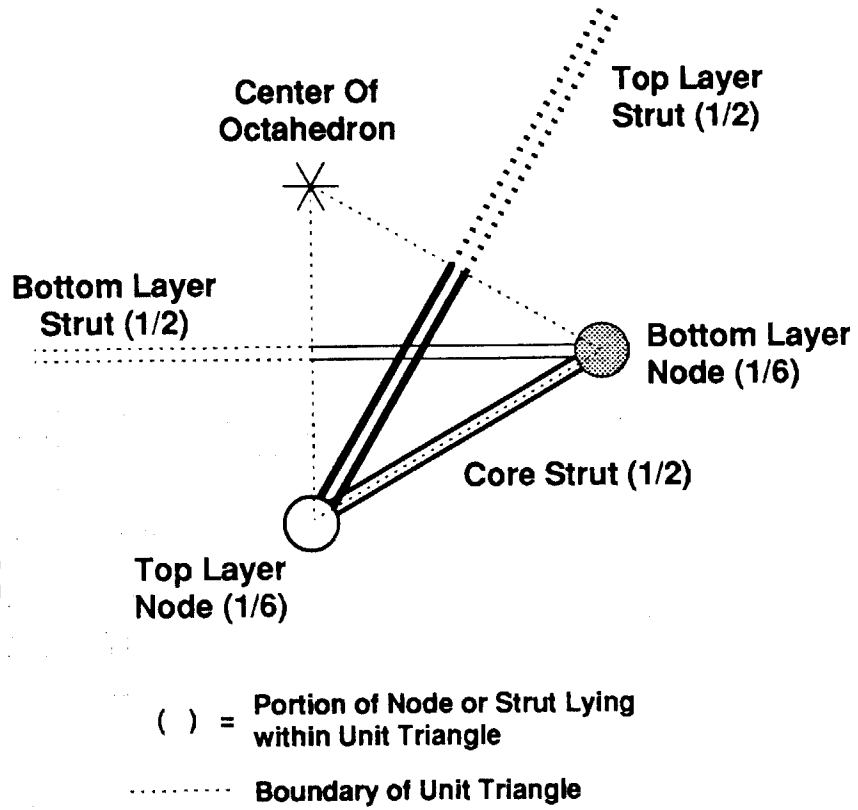

Truss Elements

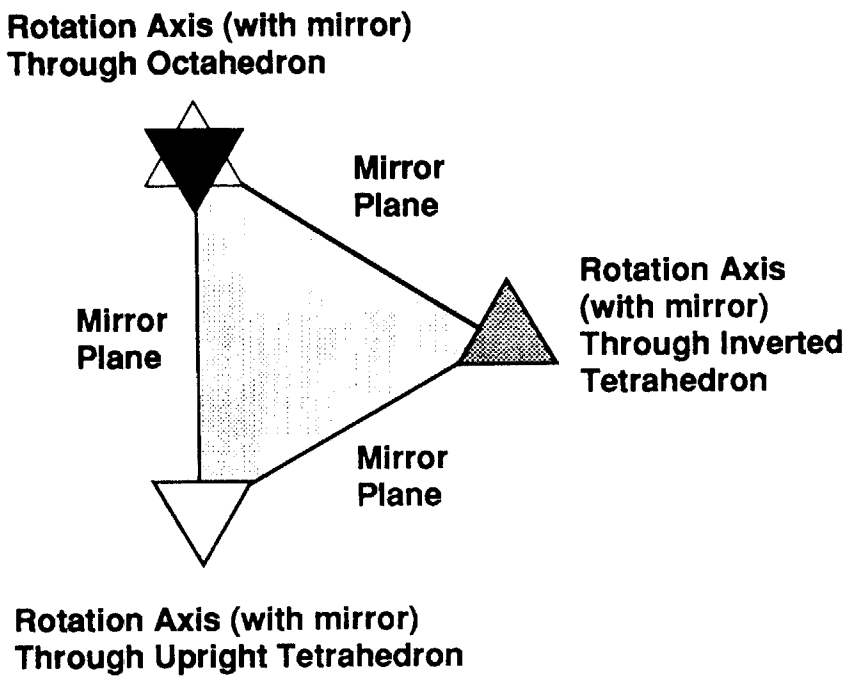

Symmetry Elements

Figure 5. The "Unit Triangle" of the Octet Truss Configuration Depicted Using Truss Elements, or Alternatively Symmetry Elements.

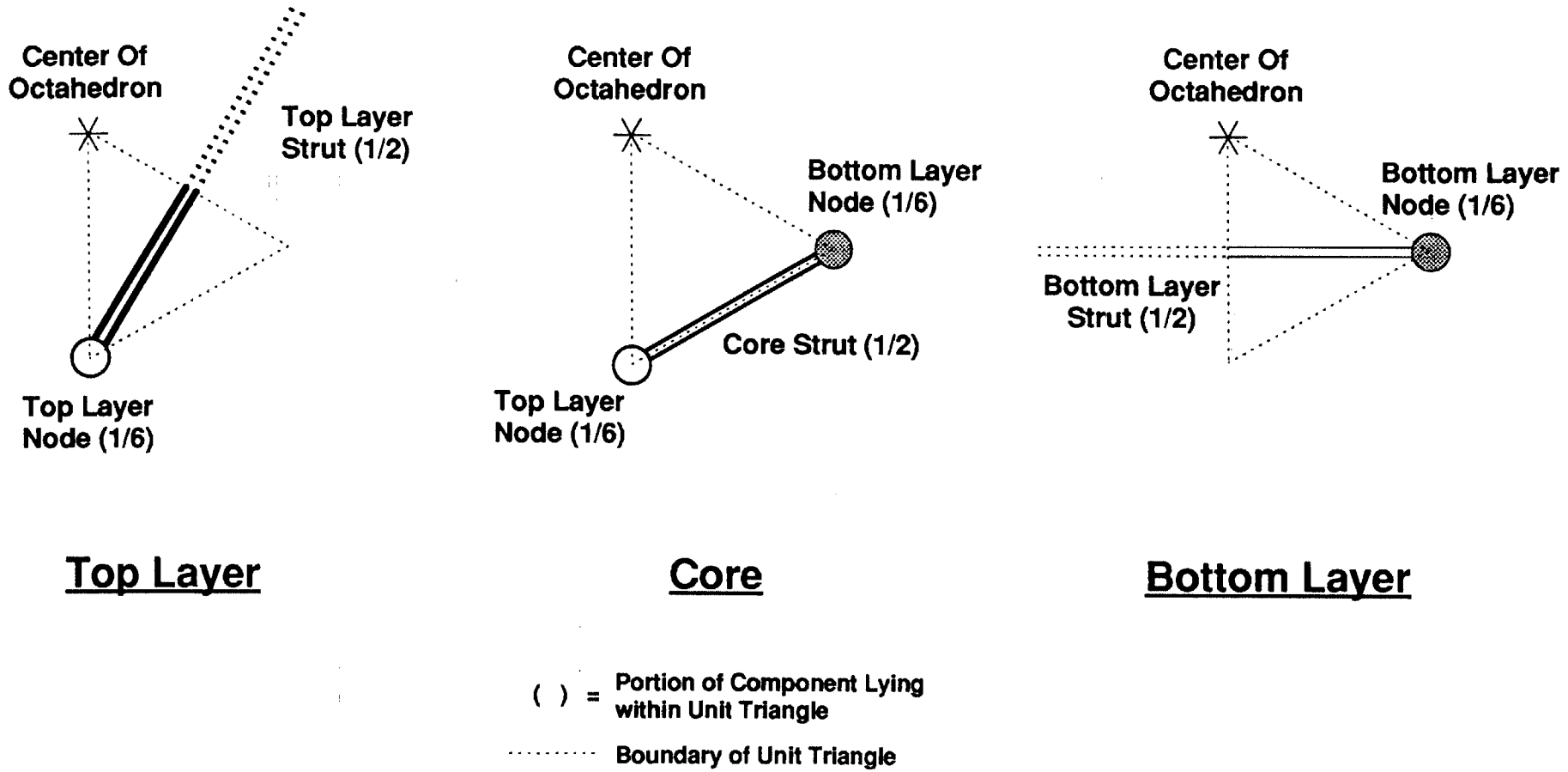

Figure 6. The Top Layer, Core, and Bottom Layer Portions of the Octet Truss Unit Triangle.

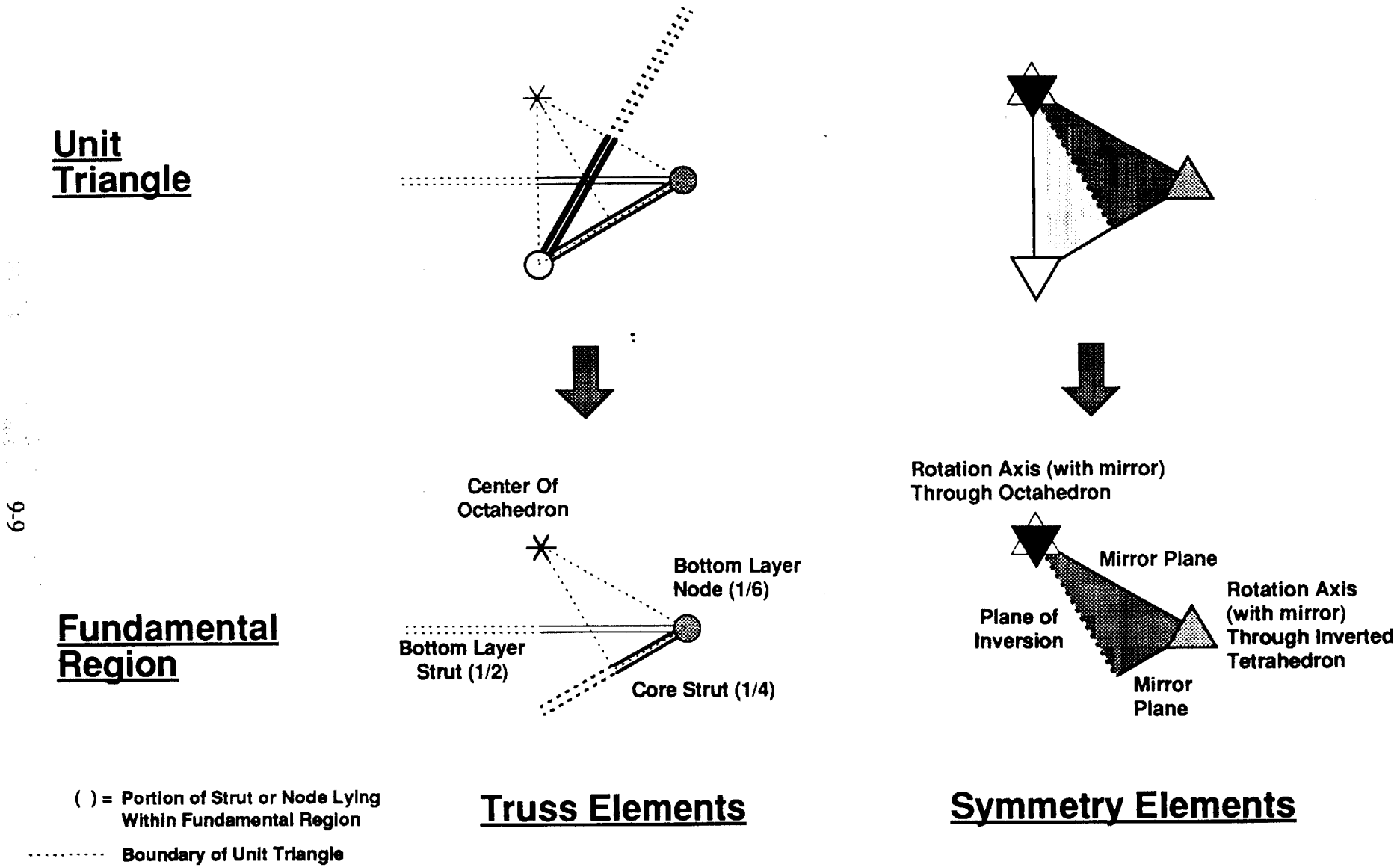

Figure 7. The Relationship Between the Unit Triangle and the Fundamental Region of the Octet Truss Configuration.

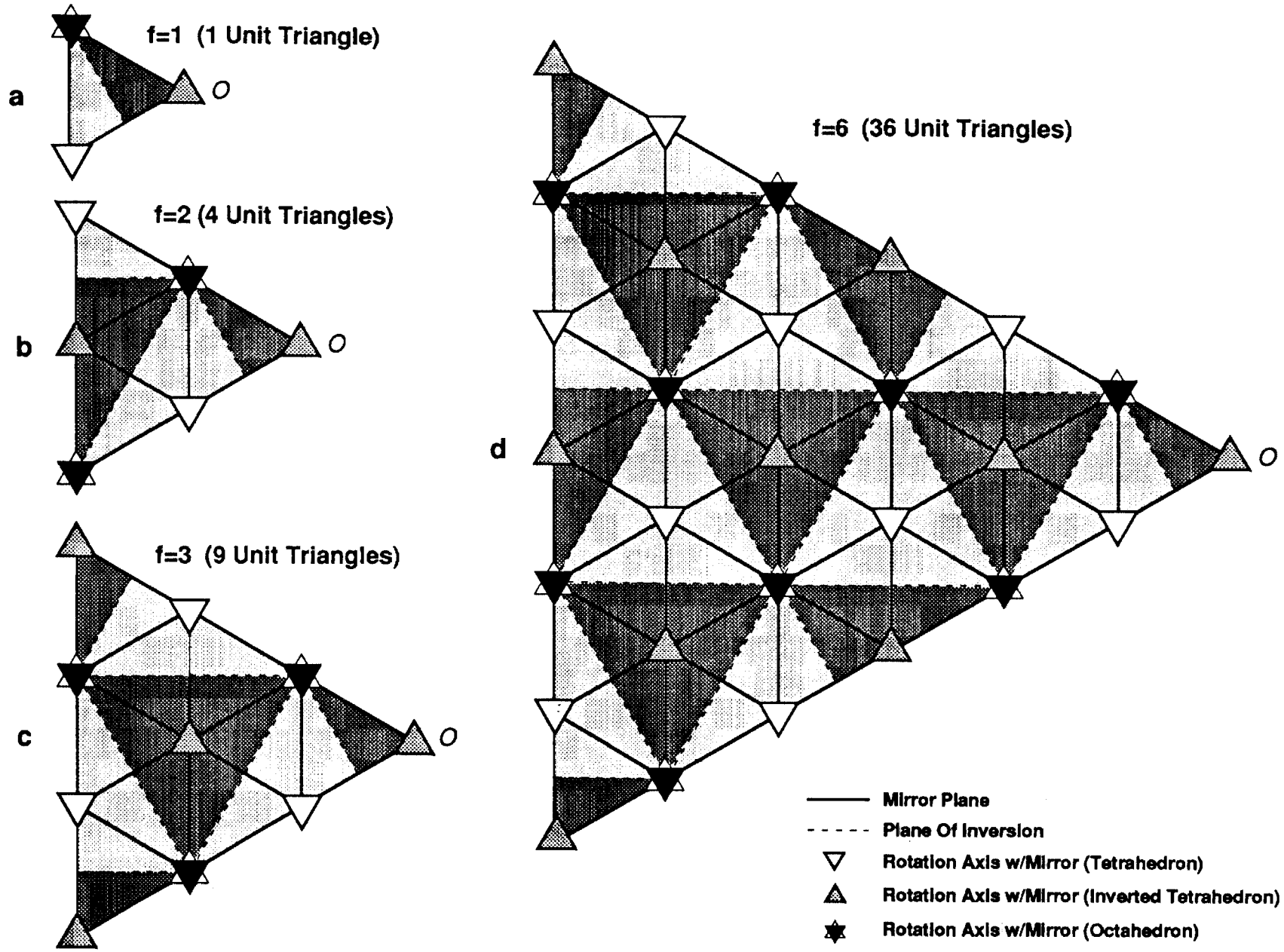

Figure 8. Stages of Plane Filling Through Multiple Replicas (Reflections) of the Octet Truss Unit Triangle (the Apex *O* is Fixed for Each Stage).

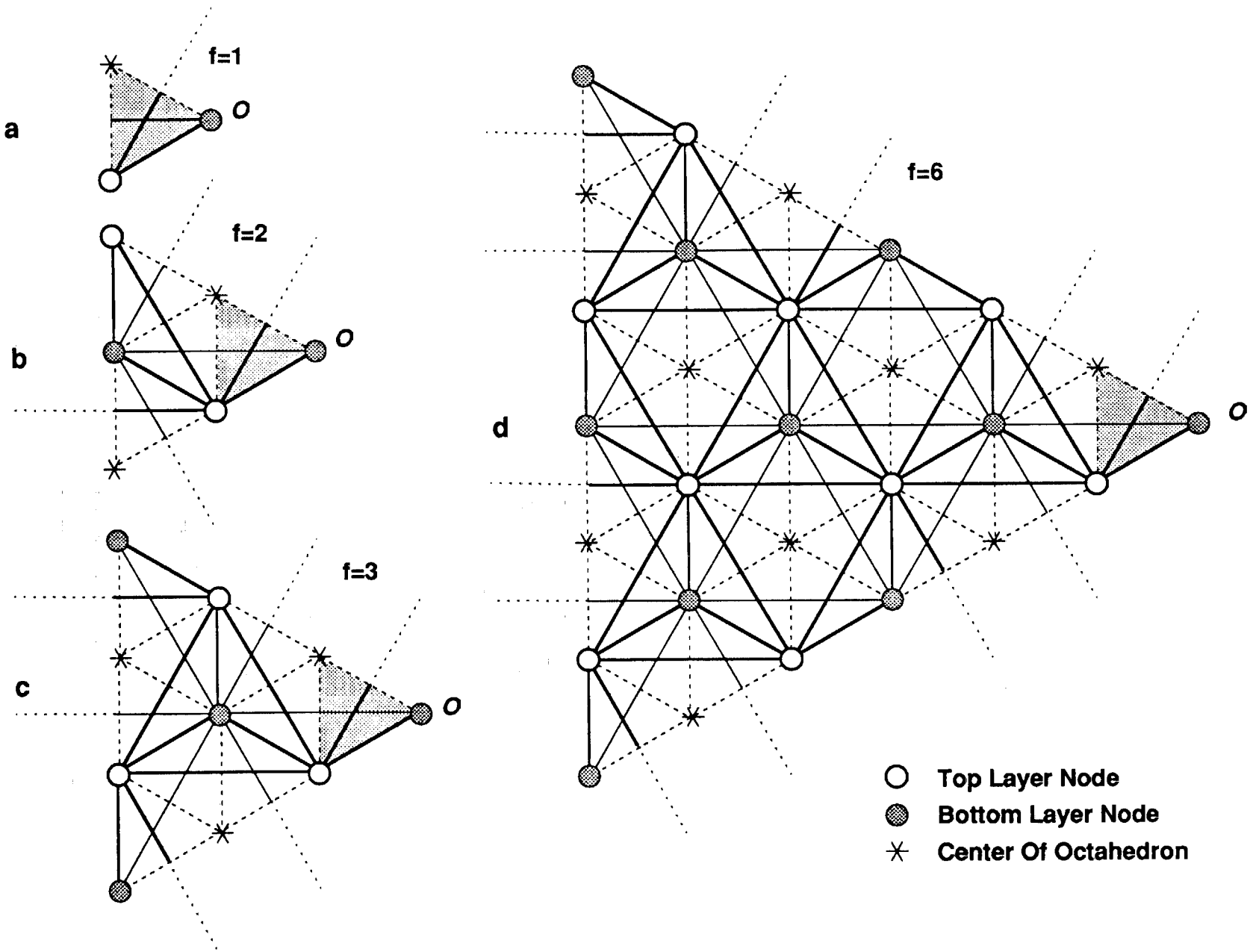

Figure 9. Stages of Growth of the Octet Truss Using the Unit Triangle Plane Filling Method as Shown in Figure 8.

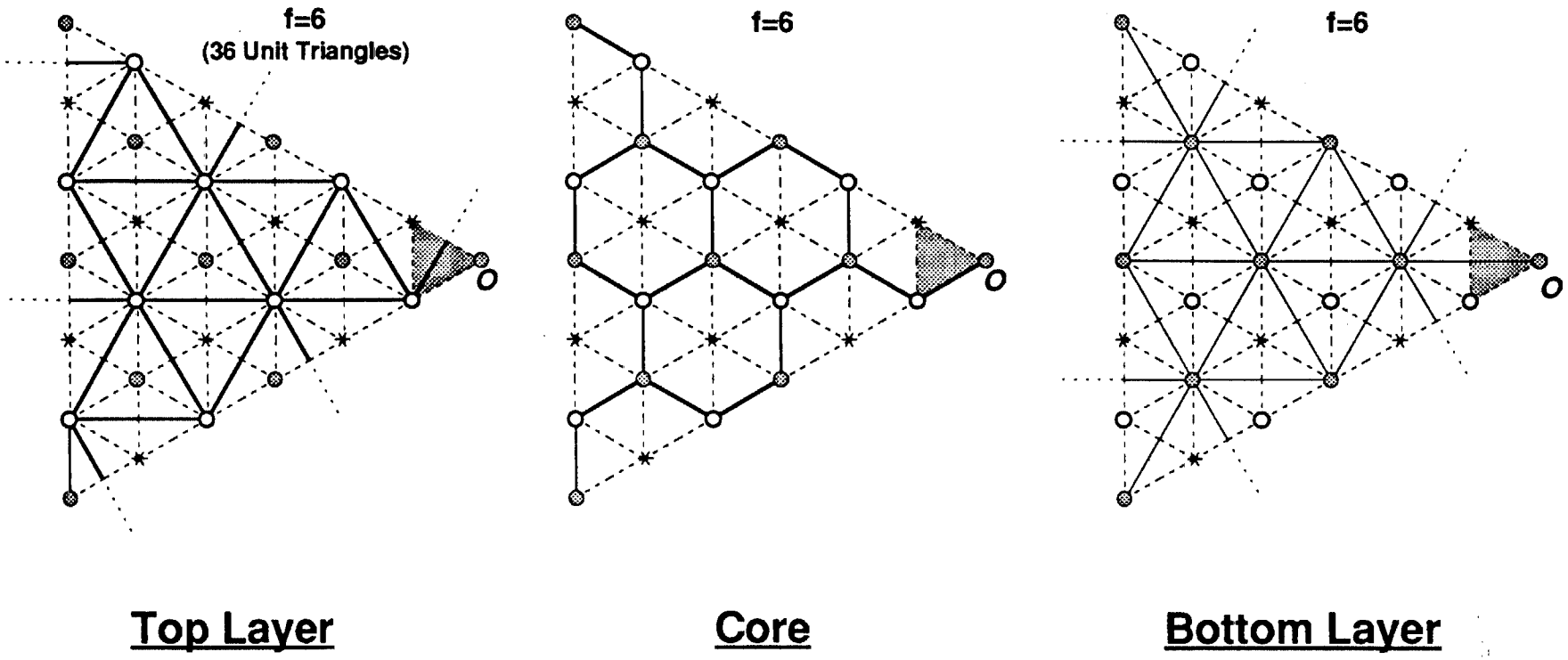

Figure 10. The Three Layers of the Octet Truss Configuration Produced by Reflections of the Unit Triangle and Corresponding to Figure 9d.

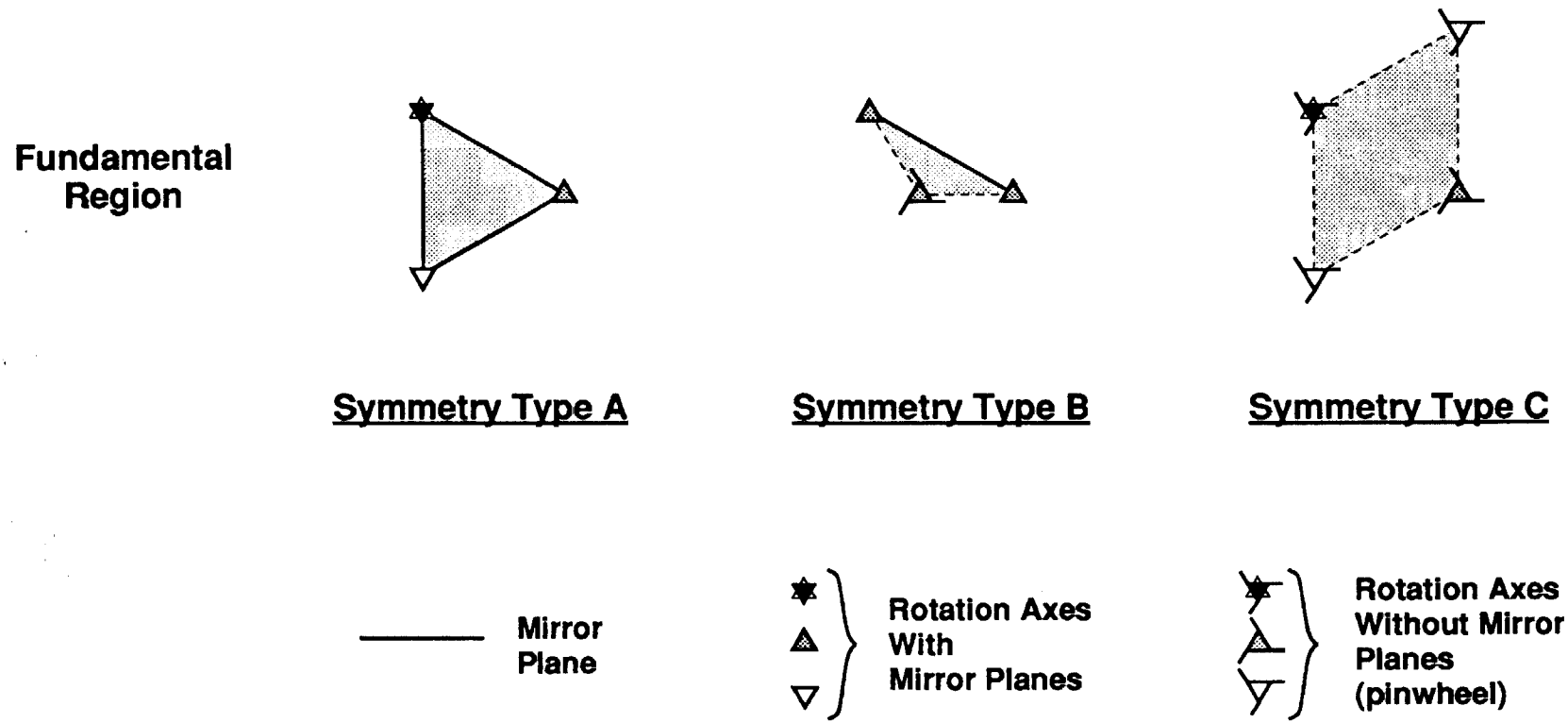

Figure 11. The Fundamental Region of the Three Permissible Symmetry Types for Single Layer Truss Configurations.

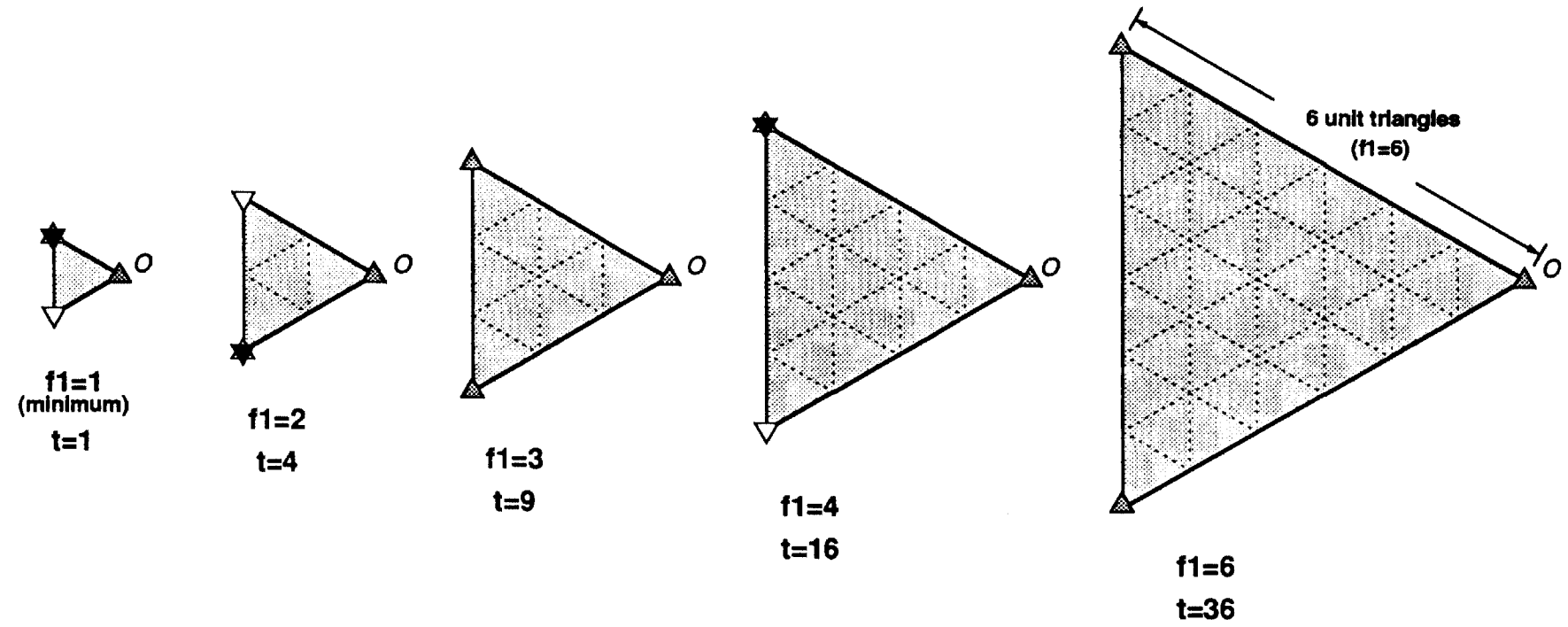

Figure 12a. Fundamental Regions with Increasing f1 for Symmetry Type A Subdivided into Arrays of Unit Triangles.

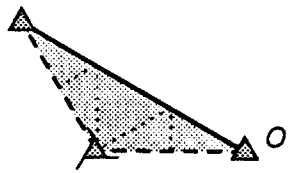

f1=3
(minimum)
t=3

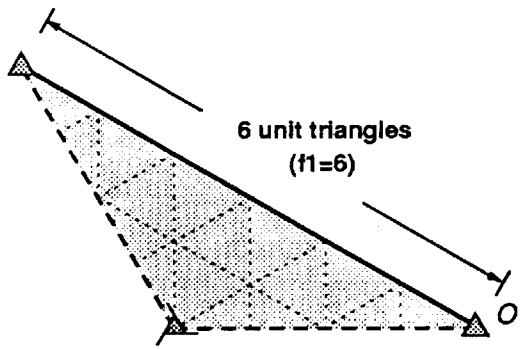

f1=6
t=12

Figure 12b. Fundamental Regions with Increasing f1 for Symmetry Type B Subdivided into Arrays of Unit Triangles (f1 is restricted to multiples of 3).

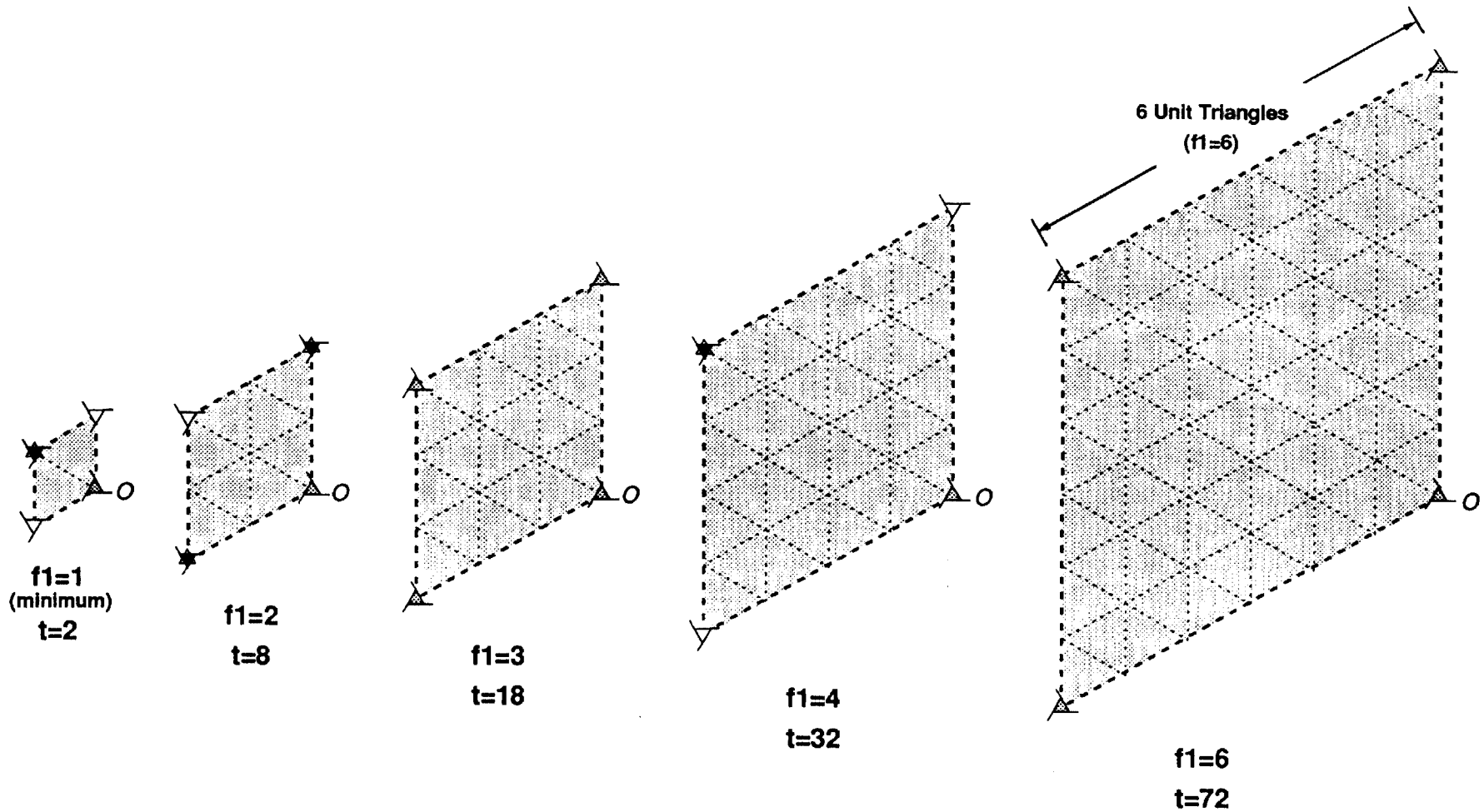

Figure 12c. Fundamental Regions with Increasing f1 for Symmetry Type C (Alternate 1) Subdivided into Arrays of Unit Triangles.

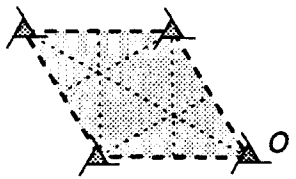

f1=3
(minimum)
t=6

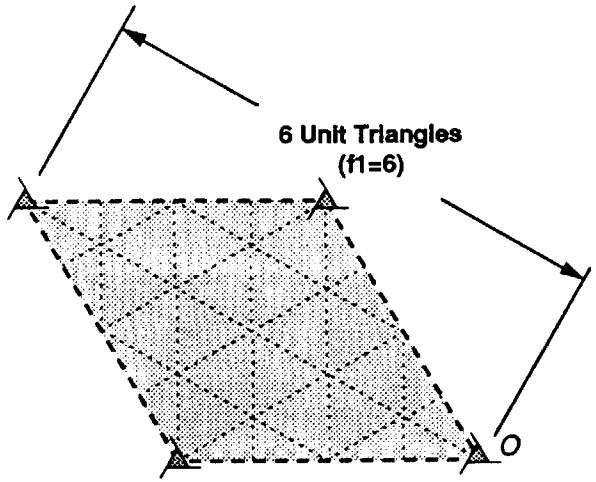

f1=6
t=24

Figure 12d. Fundamental Regions with Increasing f1 for Symmetry Type C (Alternate 2) Subdivided into Arrays of Unit Triangles (f1 is restricted to multiples of 3).

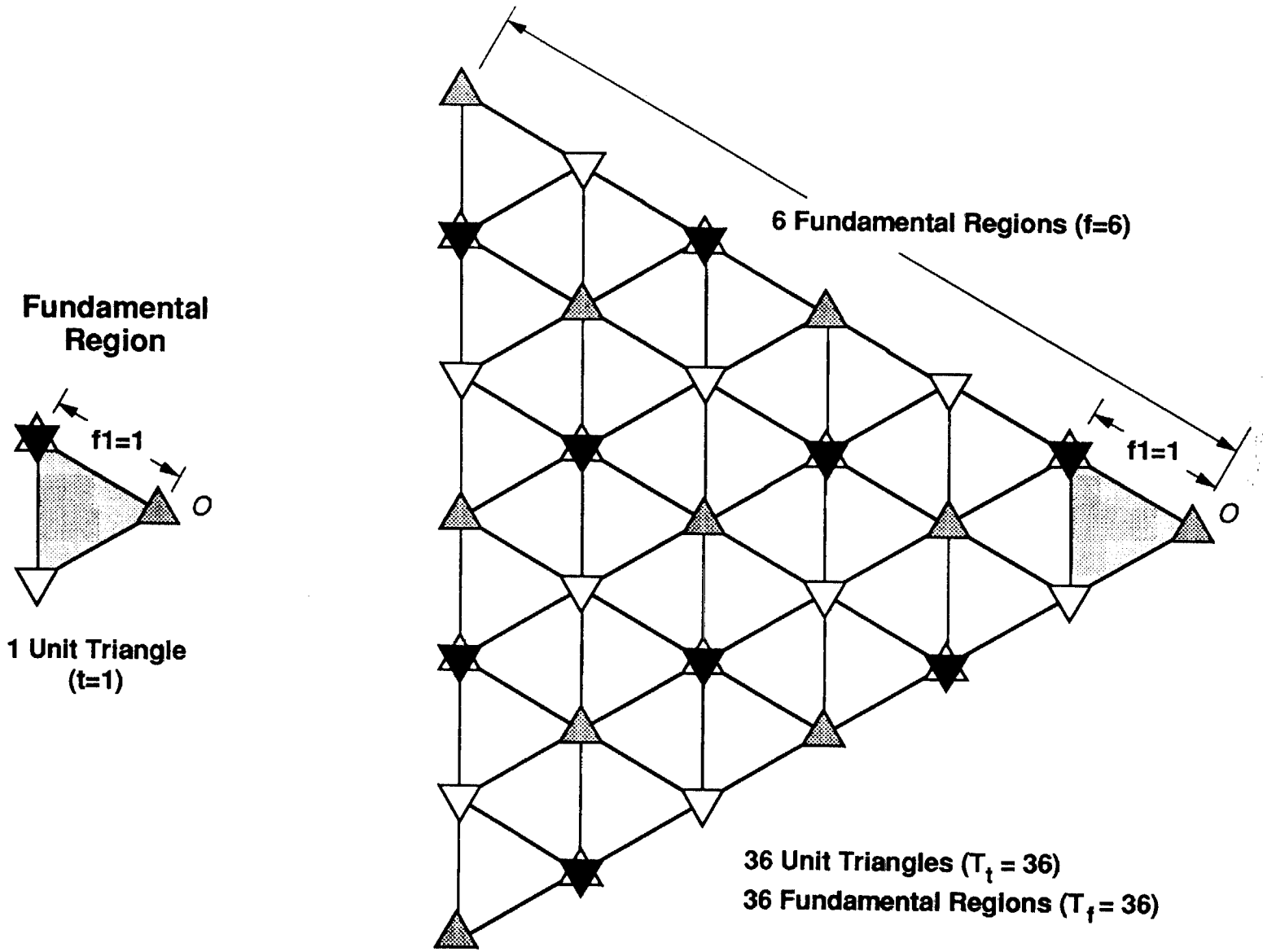

Figure 13. A Triangular Array of Symmetry Type A with a Fundamental Region having f1 = 1.

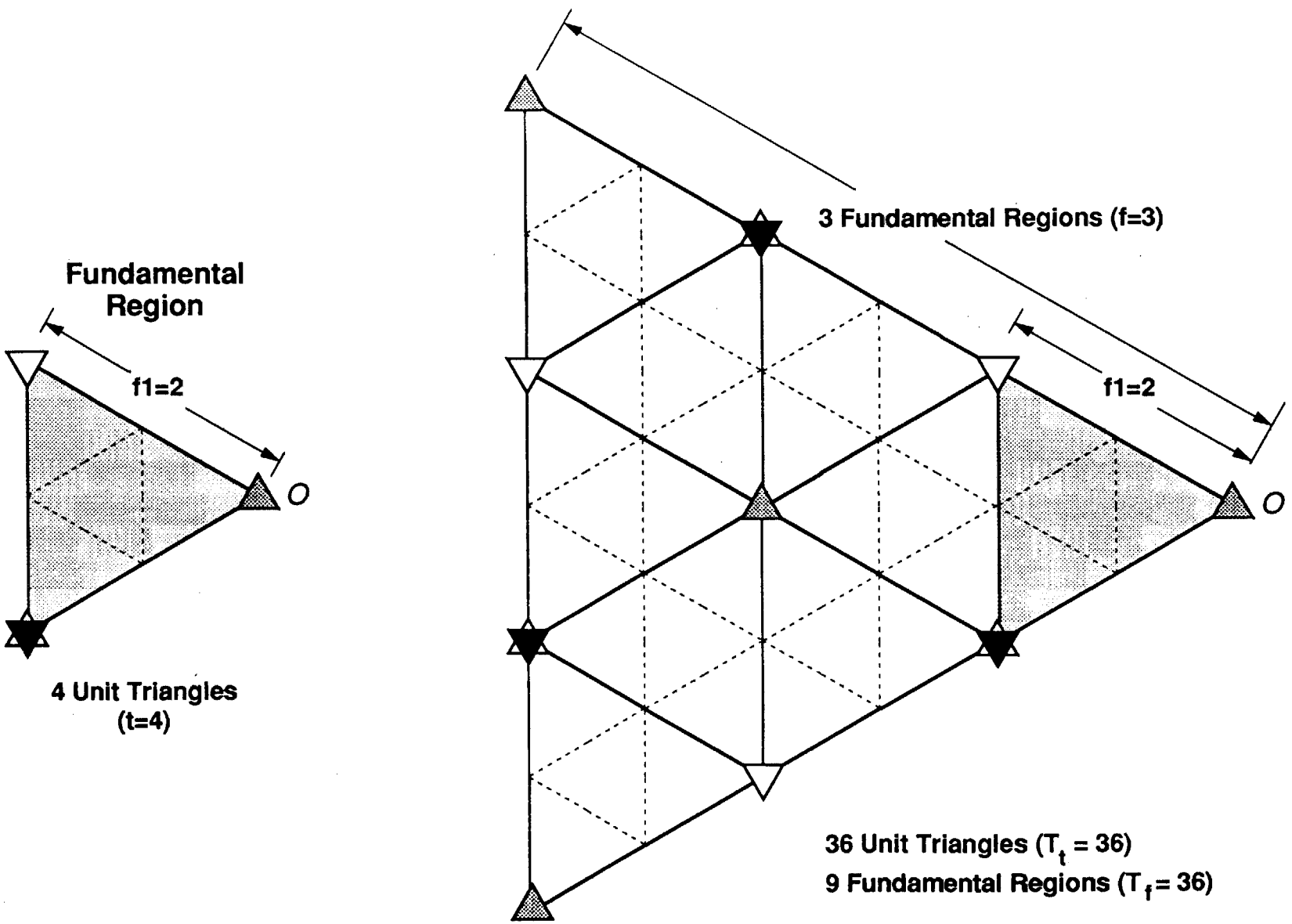

Figure 14. A Triangular Array of Symmetry Type A with a Fundamental Region having f1=2.

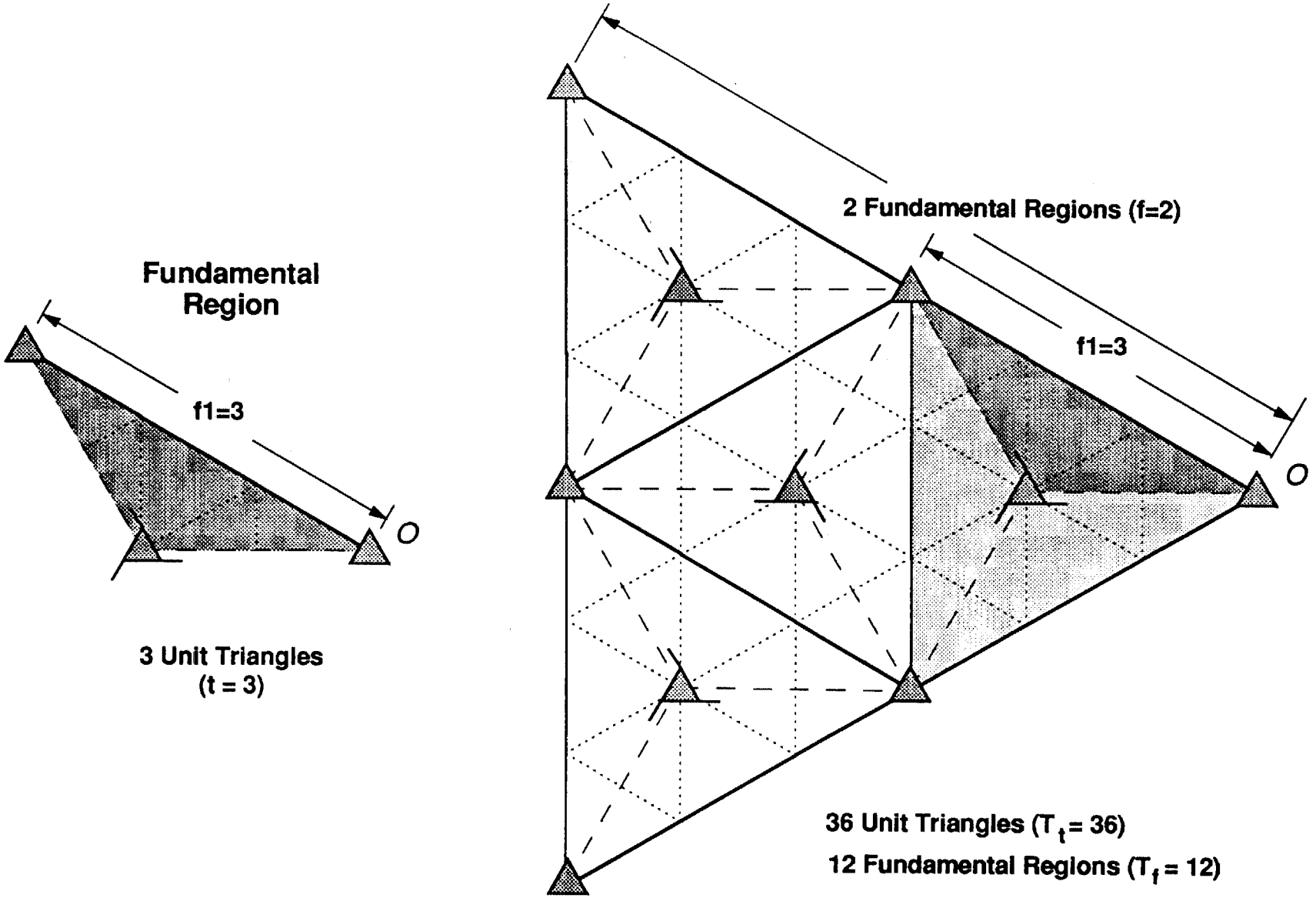

Figure 15. A Triangular Array of Symmetry Type B with a Fundamental Region Having f1=3.

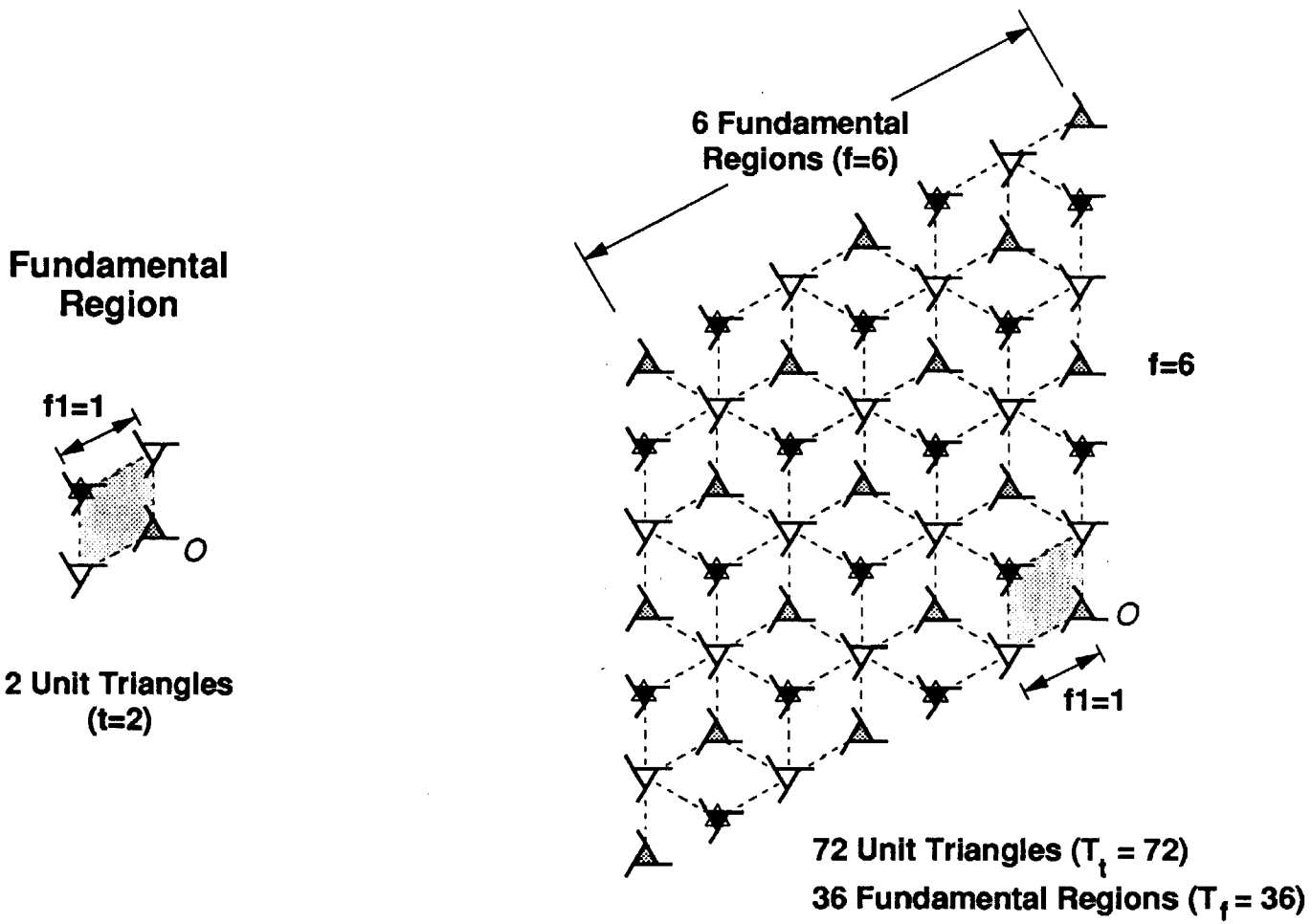

Figure 16. A Rhombic Array of Symmetry Type C (Alternate 1) with a Fundamental Region having f1=1.

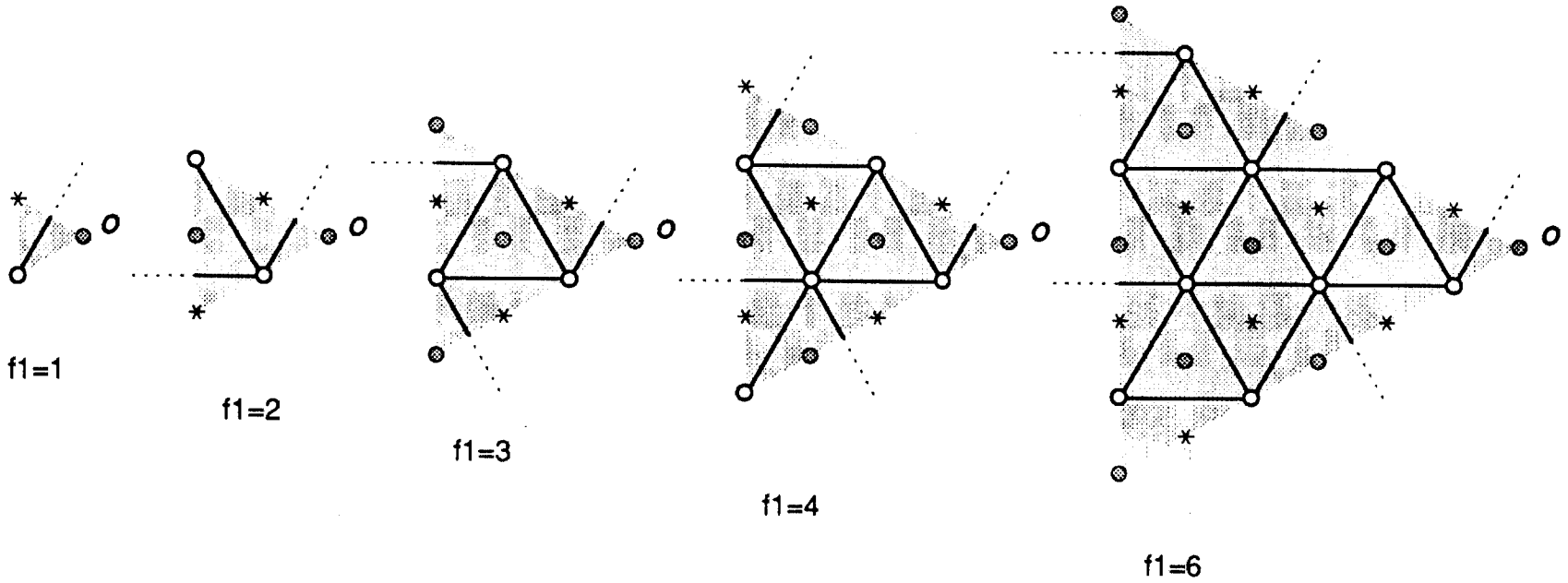

Figure 17. Examples of Fundamental Regions with Increasing f1 for Symmetry Type A Derived from the Top Layer of the Truss Configuration OCTET1.

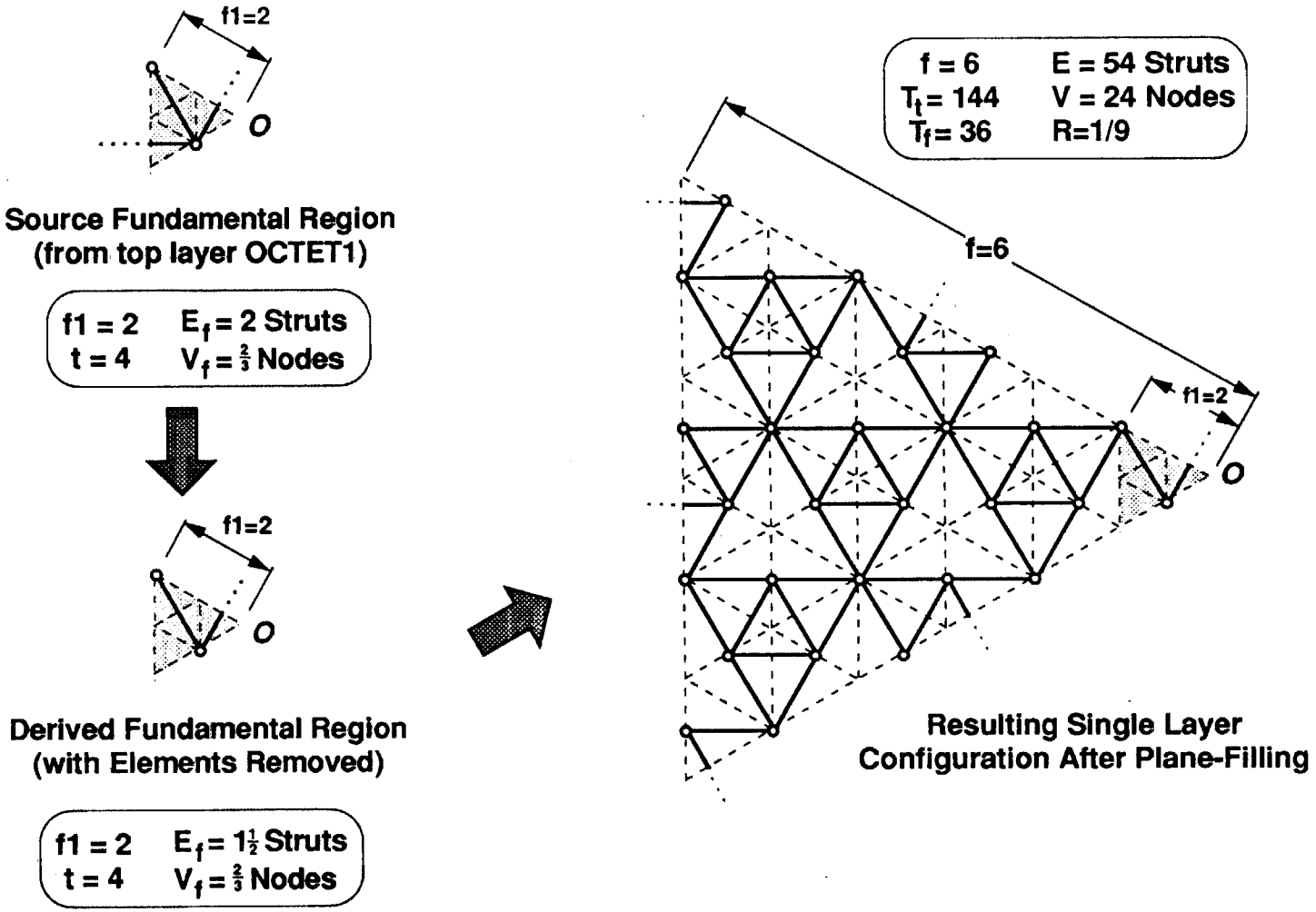

Figure 18. Example of a Single Layer Truss Configuration of Symmetry Type A Derived by Removing Struts from the Top Layer of OCTET1.

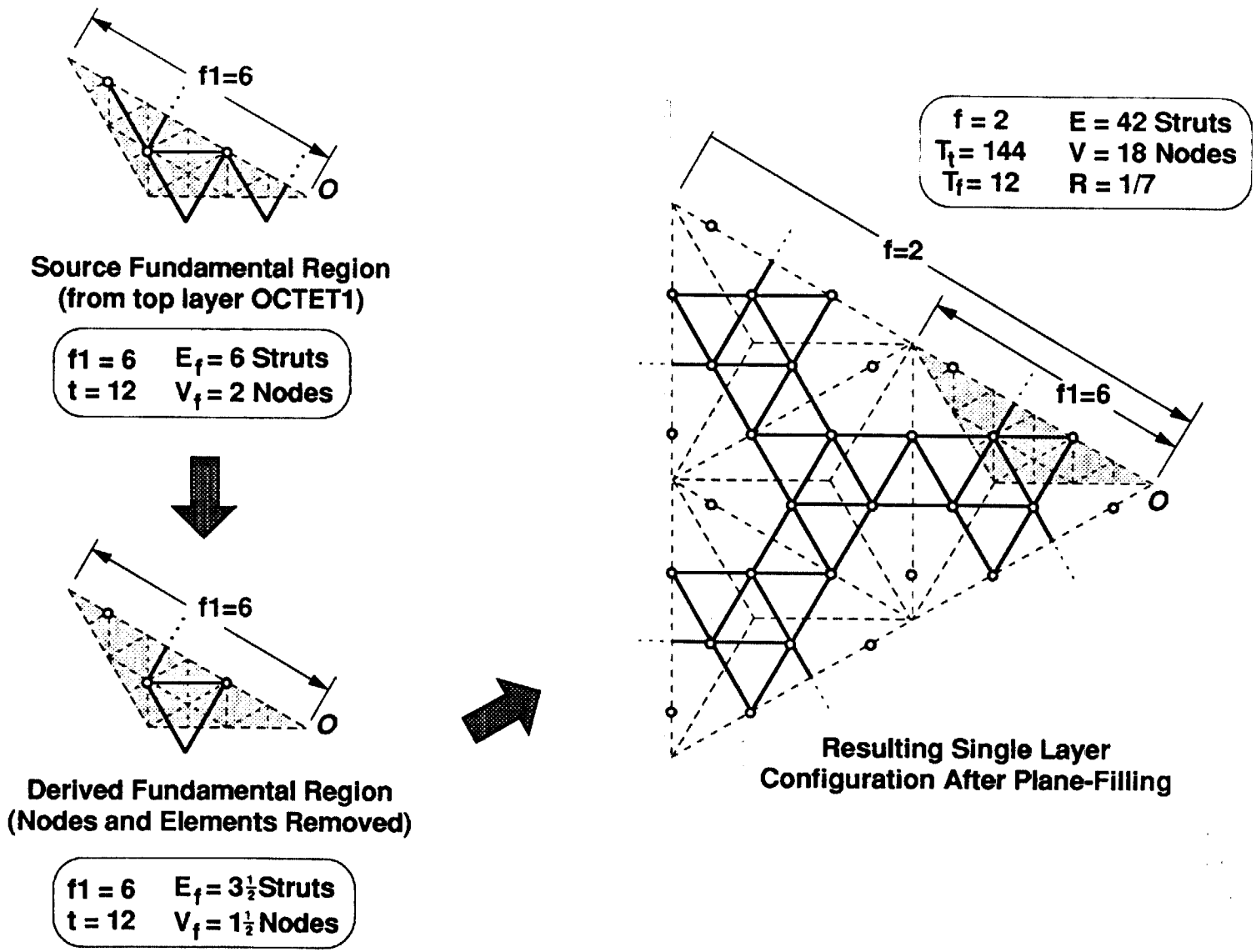

Figure 19. Example of a Single Layer Truss Configuration of Symmetry Type B Derived by Removing Nodes and Struts from the Top Layer of OCTET1.

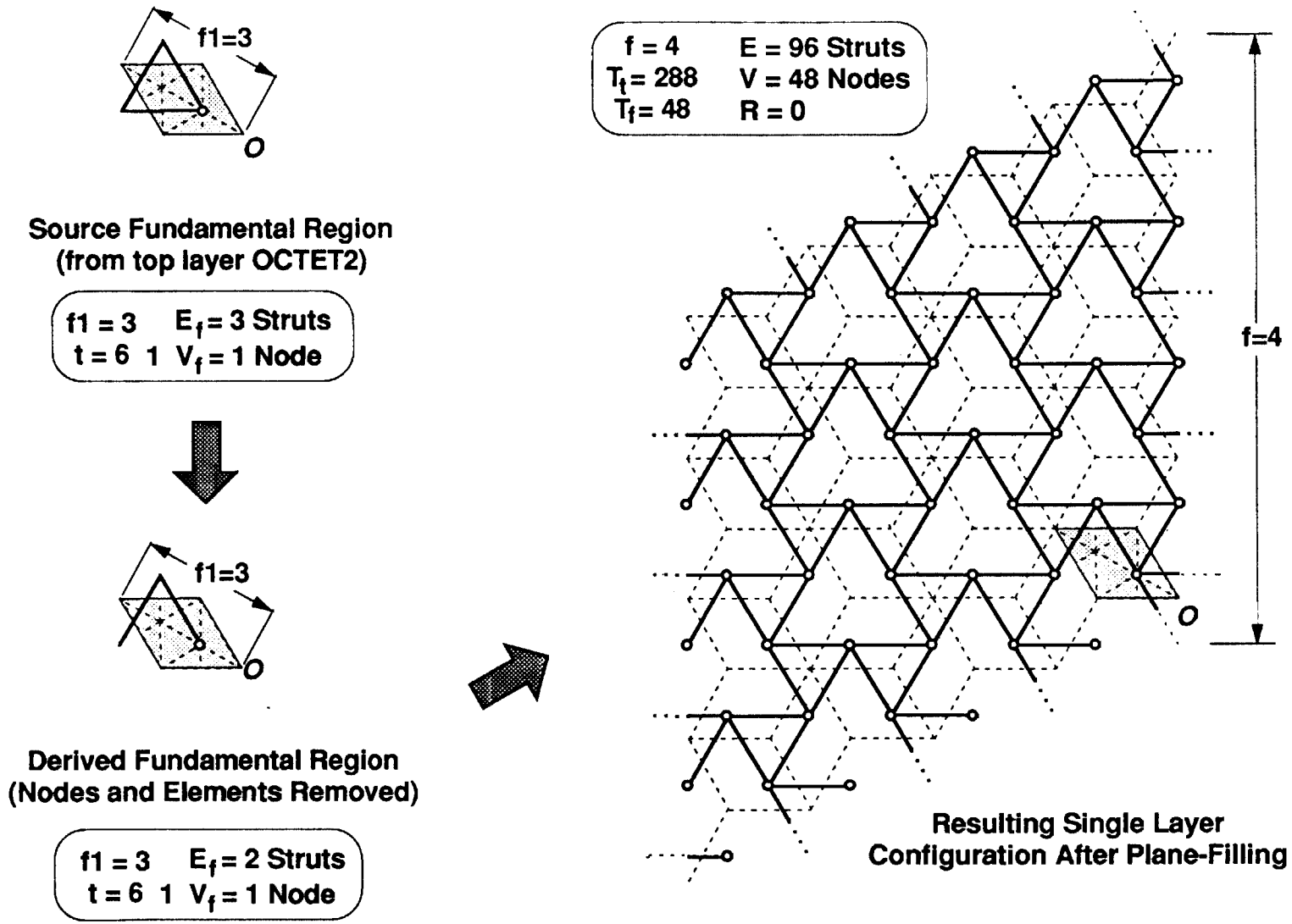

Figure 20. Example of a Single Layer Truss Configuration of Symmetry Type C (Alternate 2) Derived by Removing Elements from the Top Layer of OCTET2.

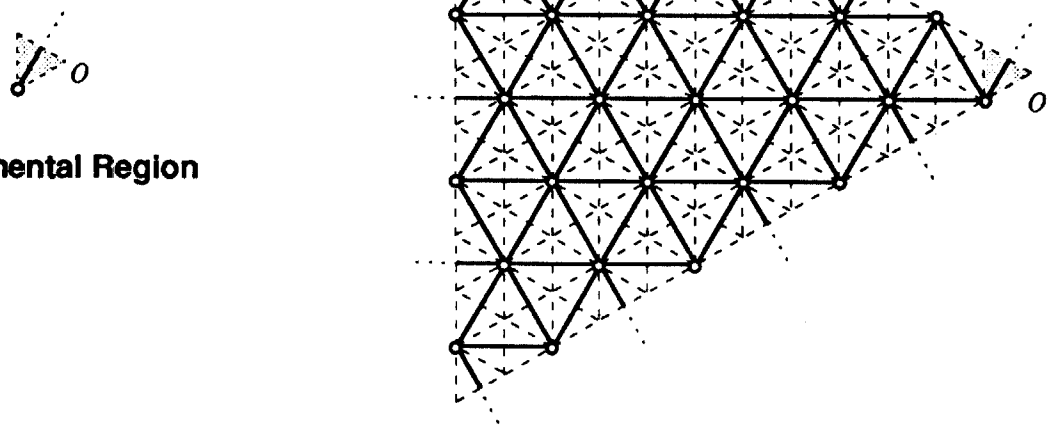

Figure 21a. The Source Top Layer Taken from the Octet Configuration OCTET1.

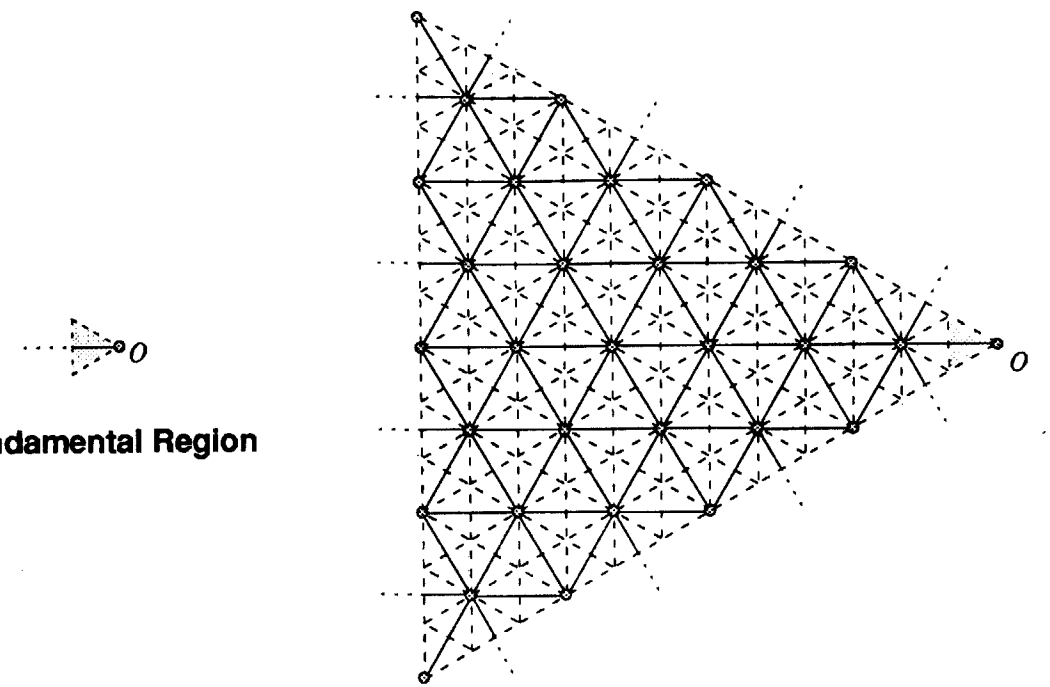

Figure 21b. The Source Bottom Layer Taken from the Octet Configuration OCTET1

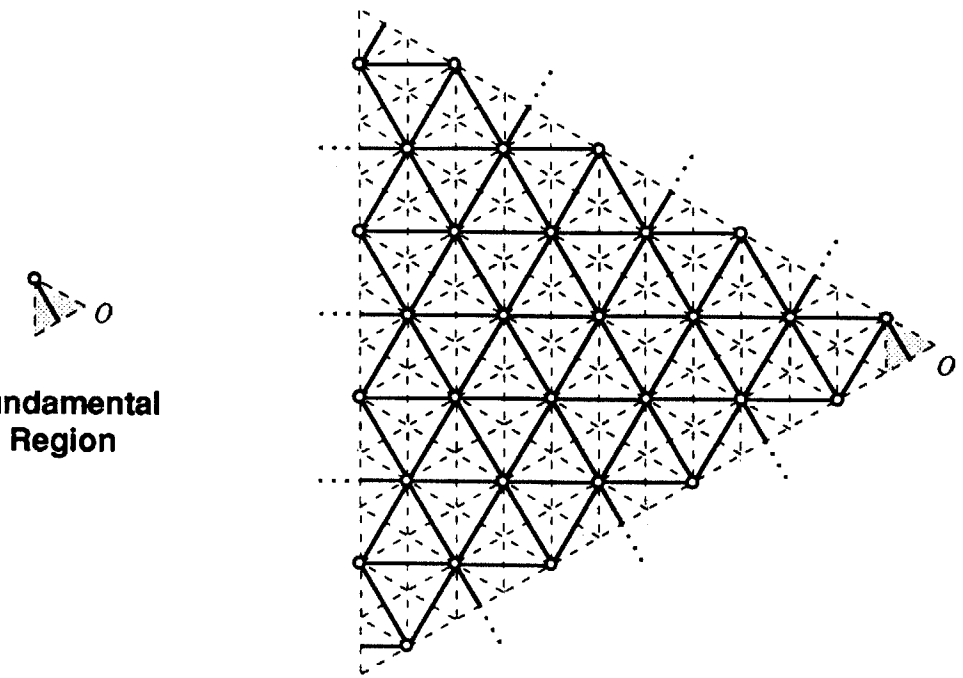

Figure 22a. The Source Top Layer Taken from the Octet Configuration OCTET2 .

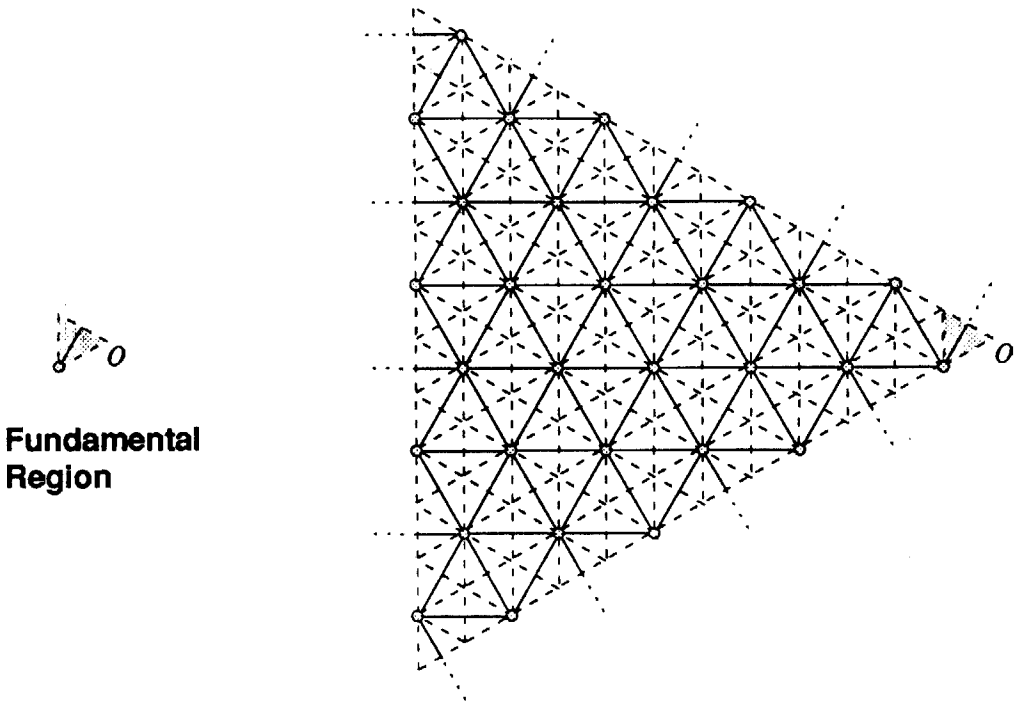

Figure 22b. The Source Bottom Layer Taken from the Octet Configuration OCTET2.

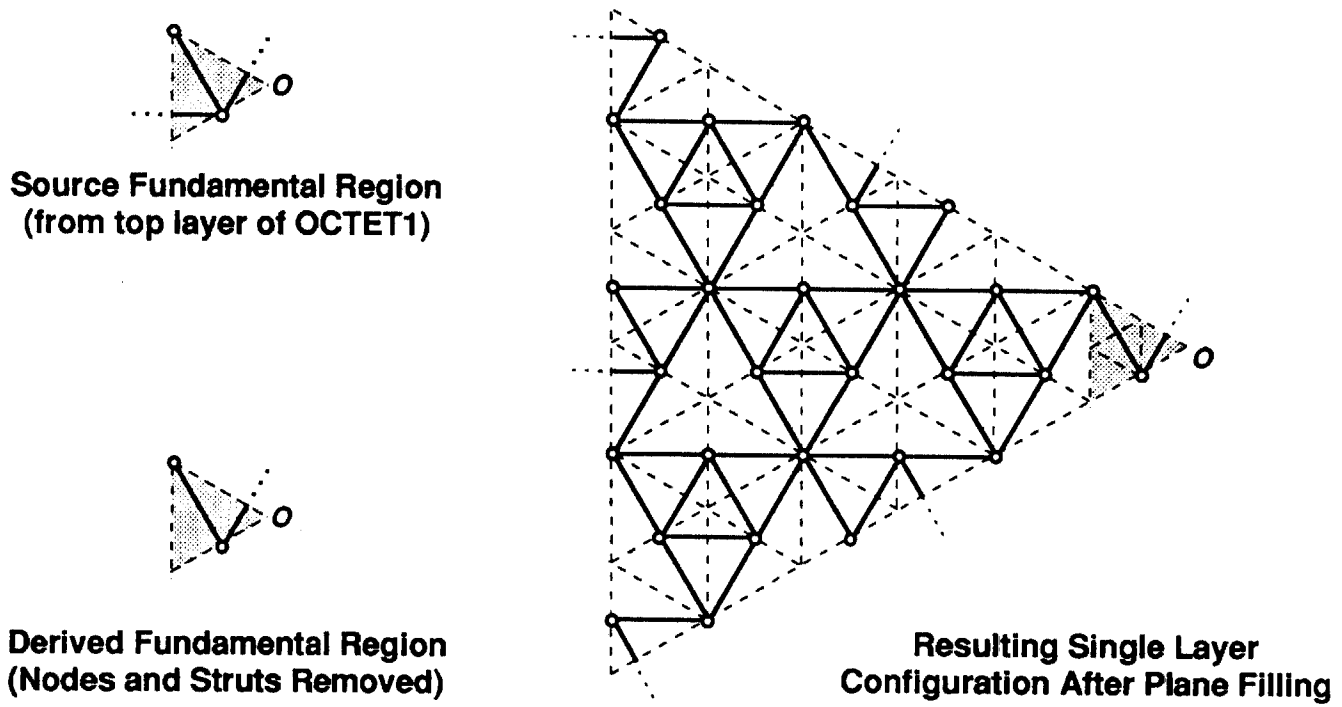

Figure 23a. The Top Layer of **TOROID1** Derived from theTop Layer of OCTET1.

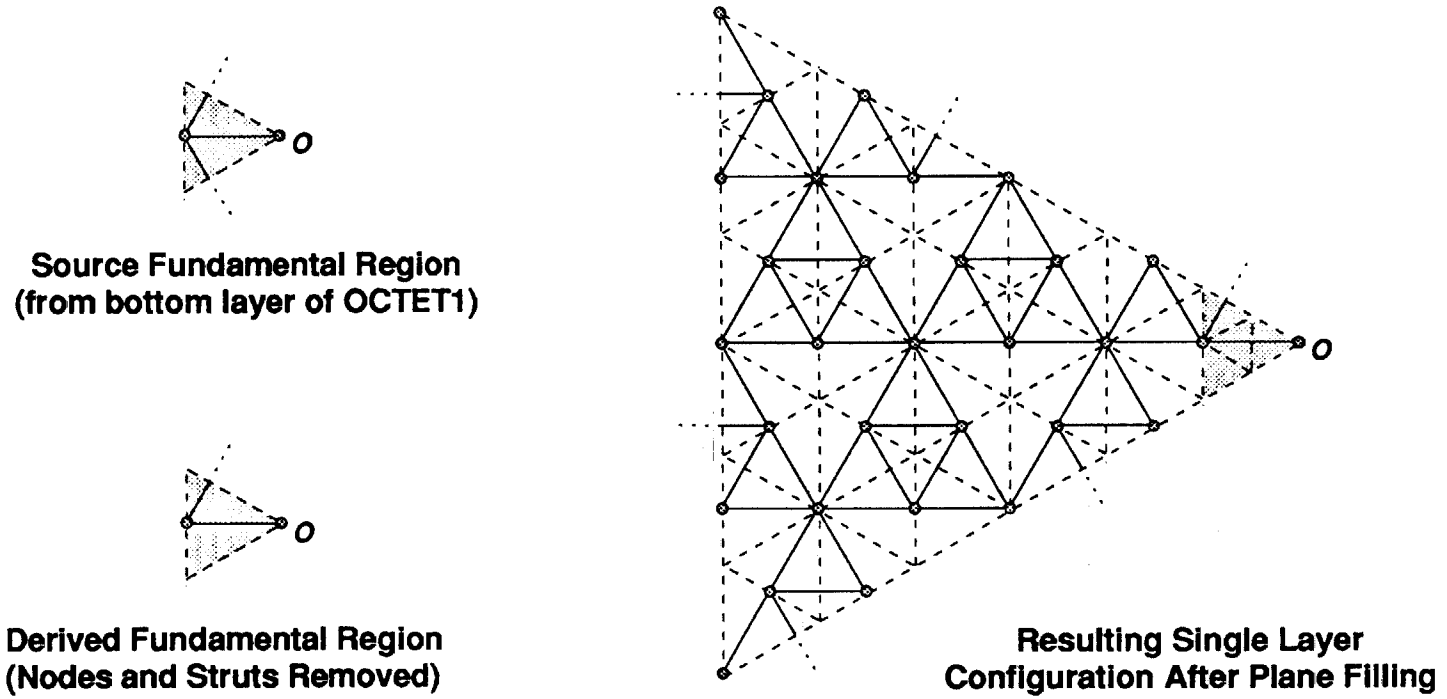

Figure 23b. The Bottom Layer of **TOROID1** Derived from the Bottom Layer of OCTET1.

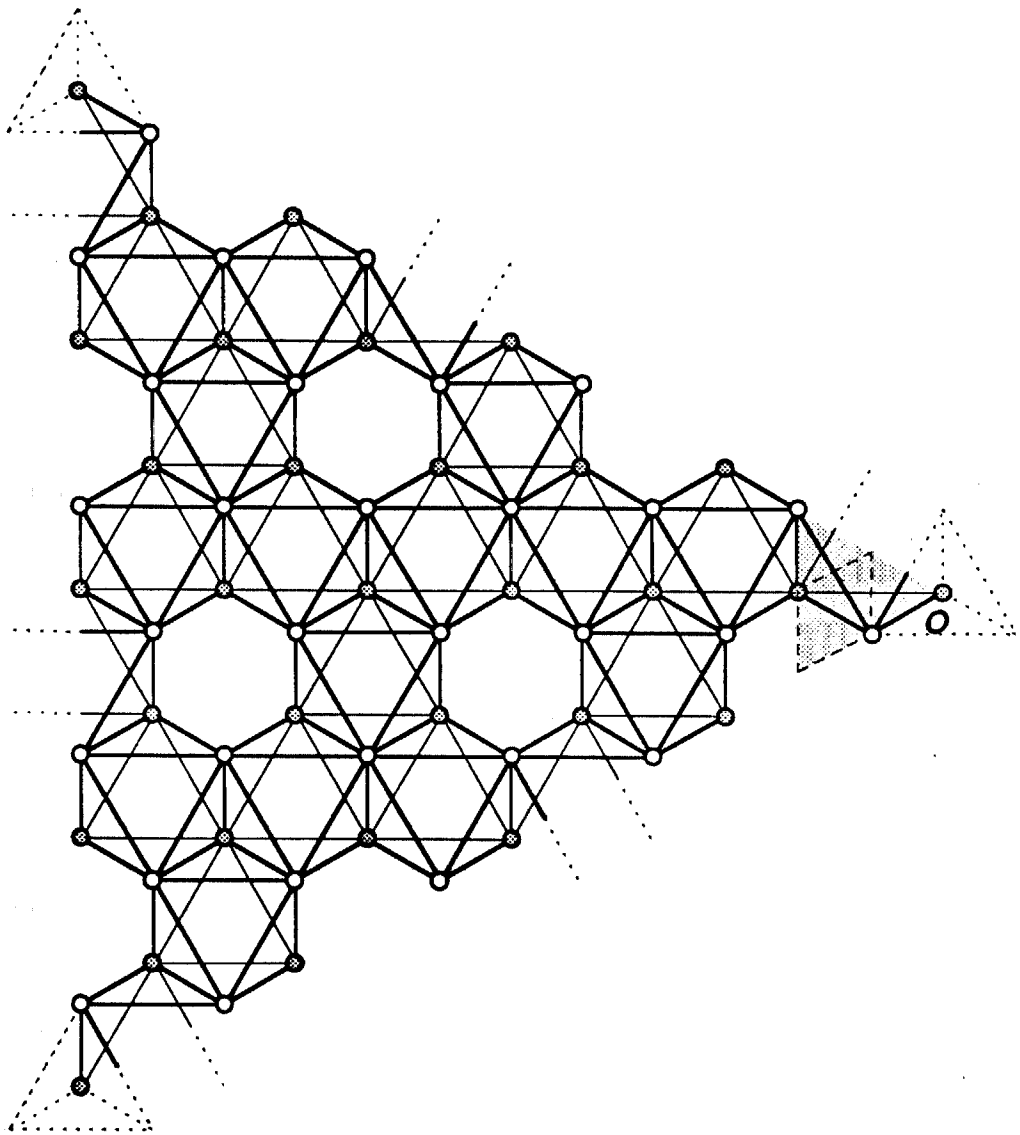

Figure 23c. The Double-Layered Configuration **TOROID1** Derived from the Octet Configuration OCTET1 by Removing Struts Only.

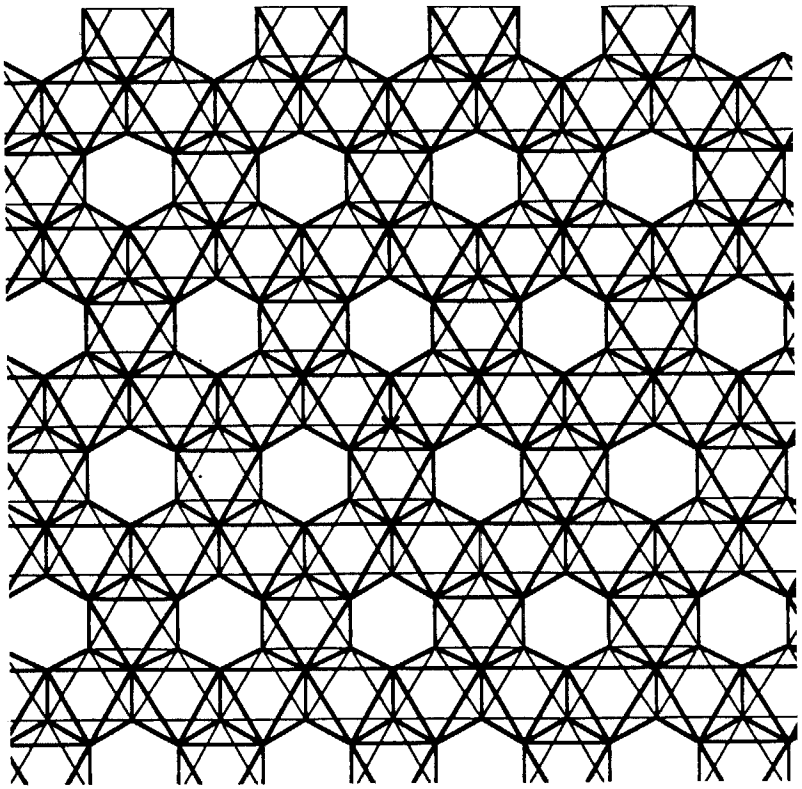

Figure 23d. A Portion of the Infinite Configuration **TOROID1.**

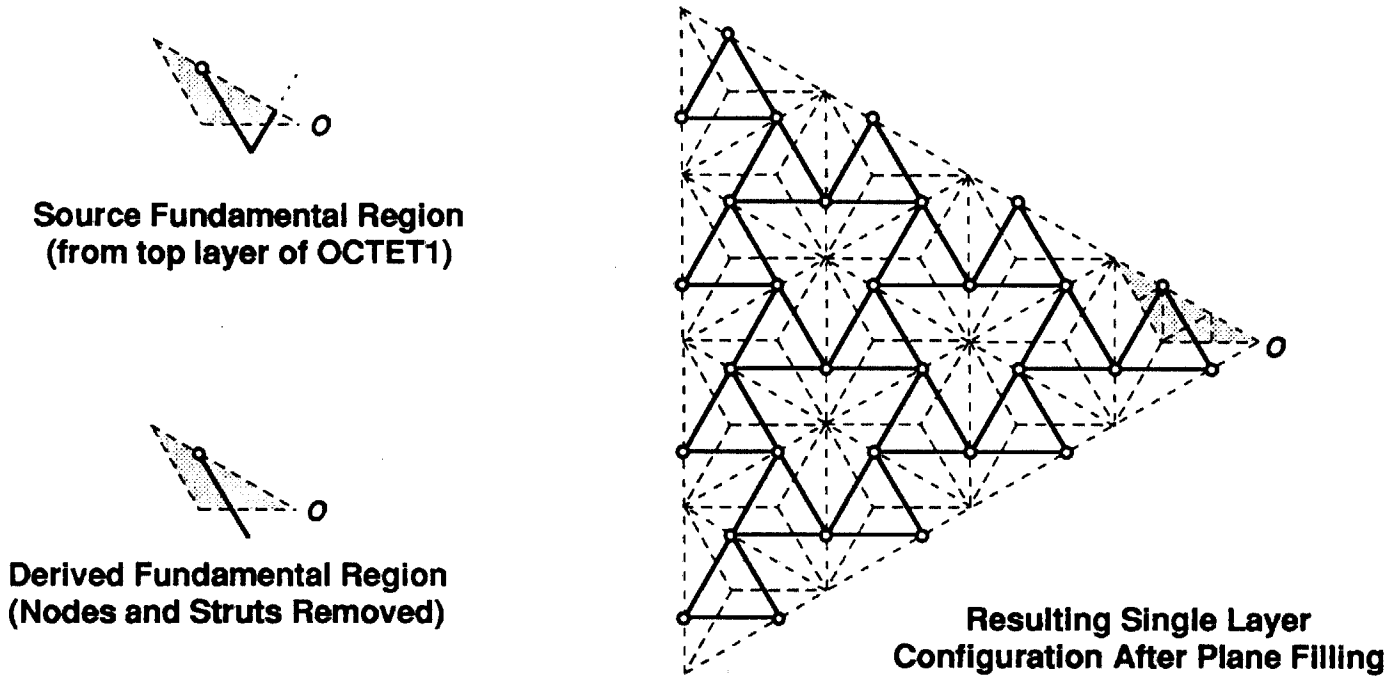

Figure 24a. The Top Layer of **REDUCED1** Derived from the Top Layer of OCTET1.

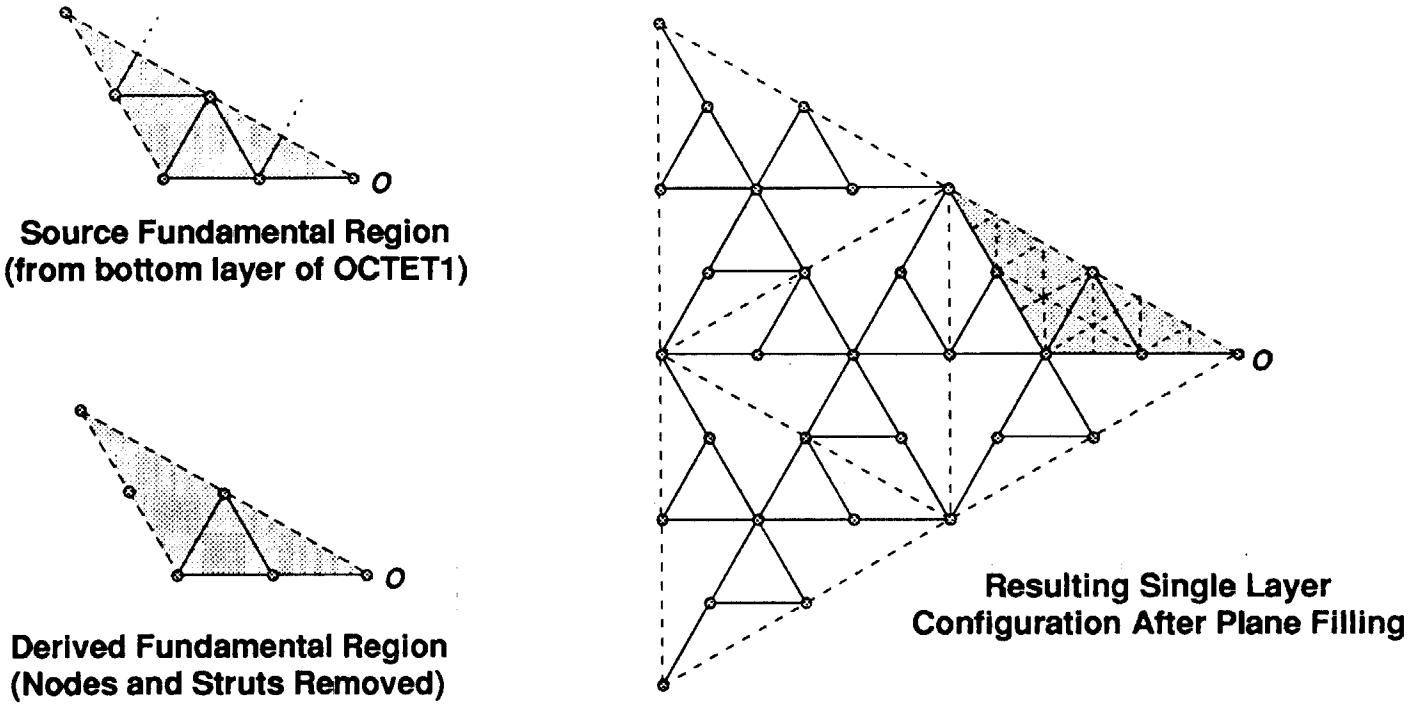

Figure 24b. The Bottom Layer of **REDUCED1** Derived from the Bottom Layer of OCTET1.

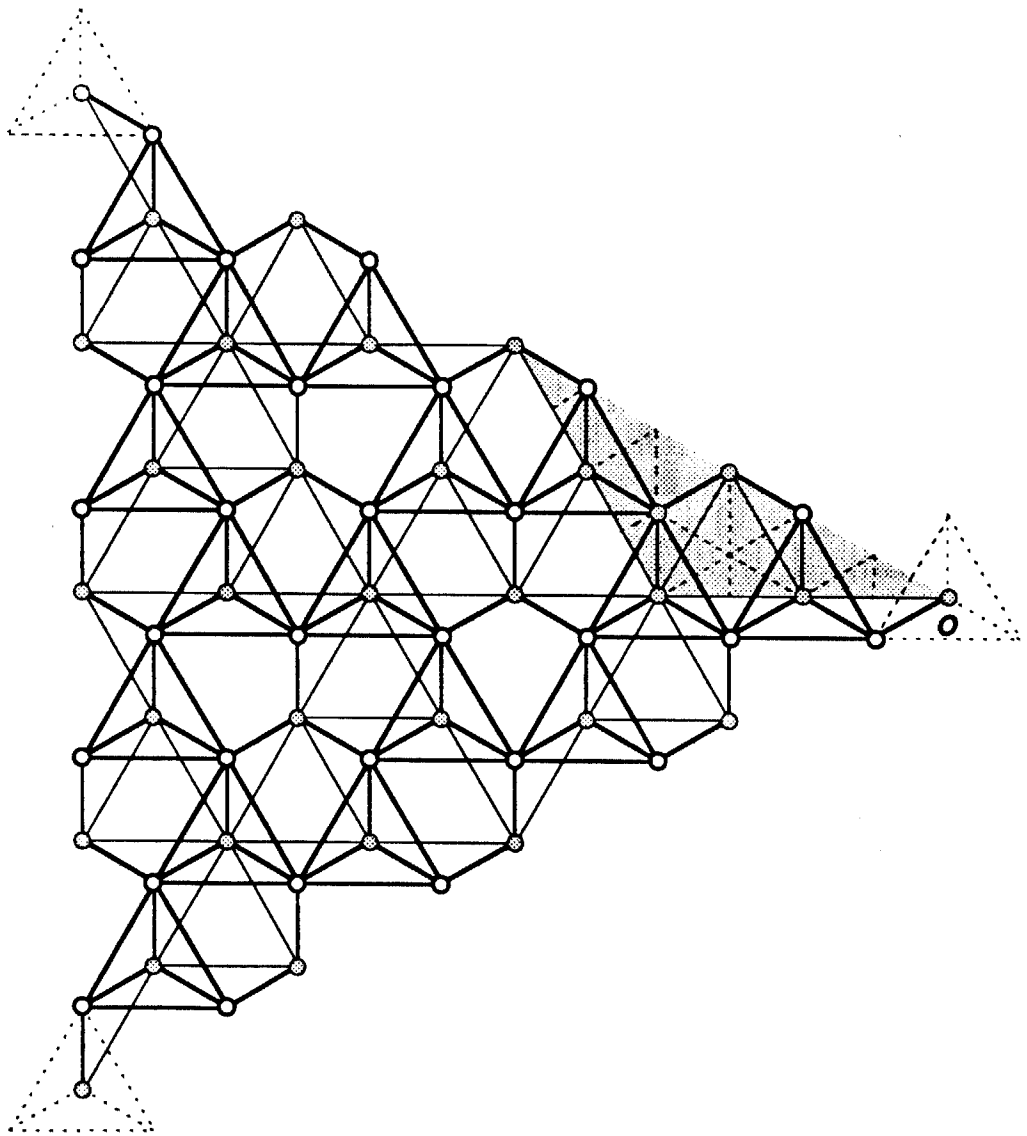

Figure 24c. The Double-Layered Configuration **REDUCED1** Derived from the Octet Configuration OCTET1 by Removing Struts Only.

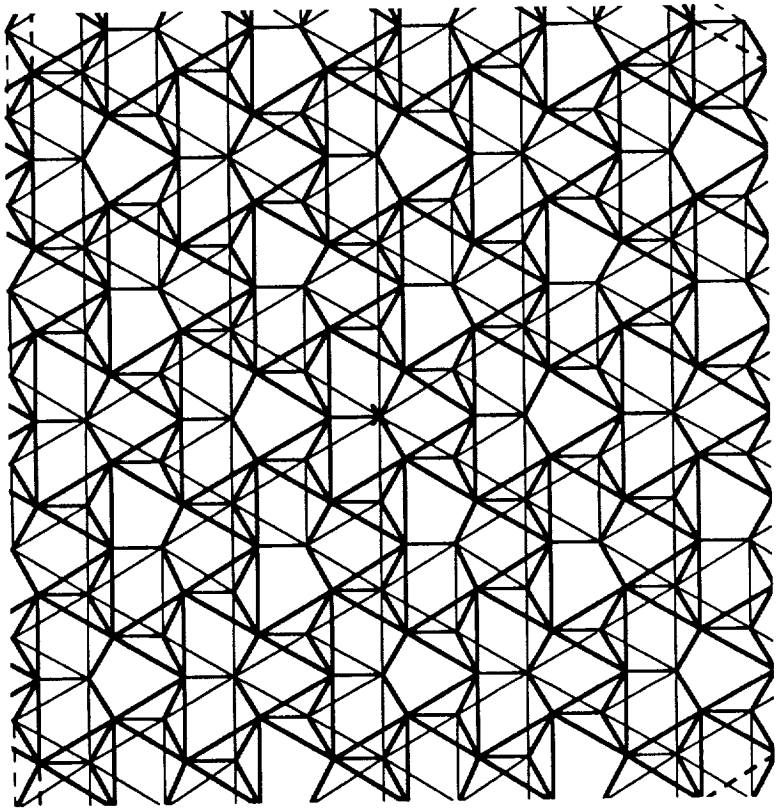

Figure 24d. A Portion of the Infinite Configuration **REDUCED1**

C-2

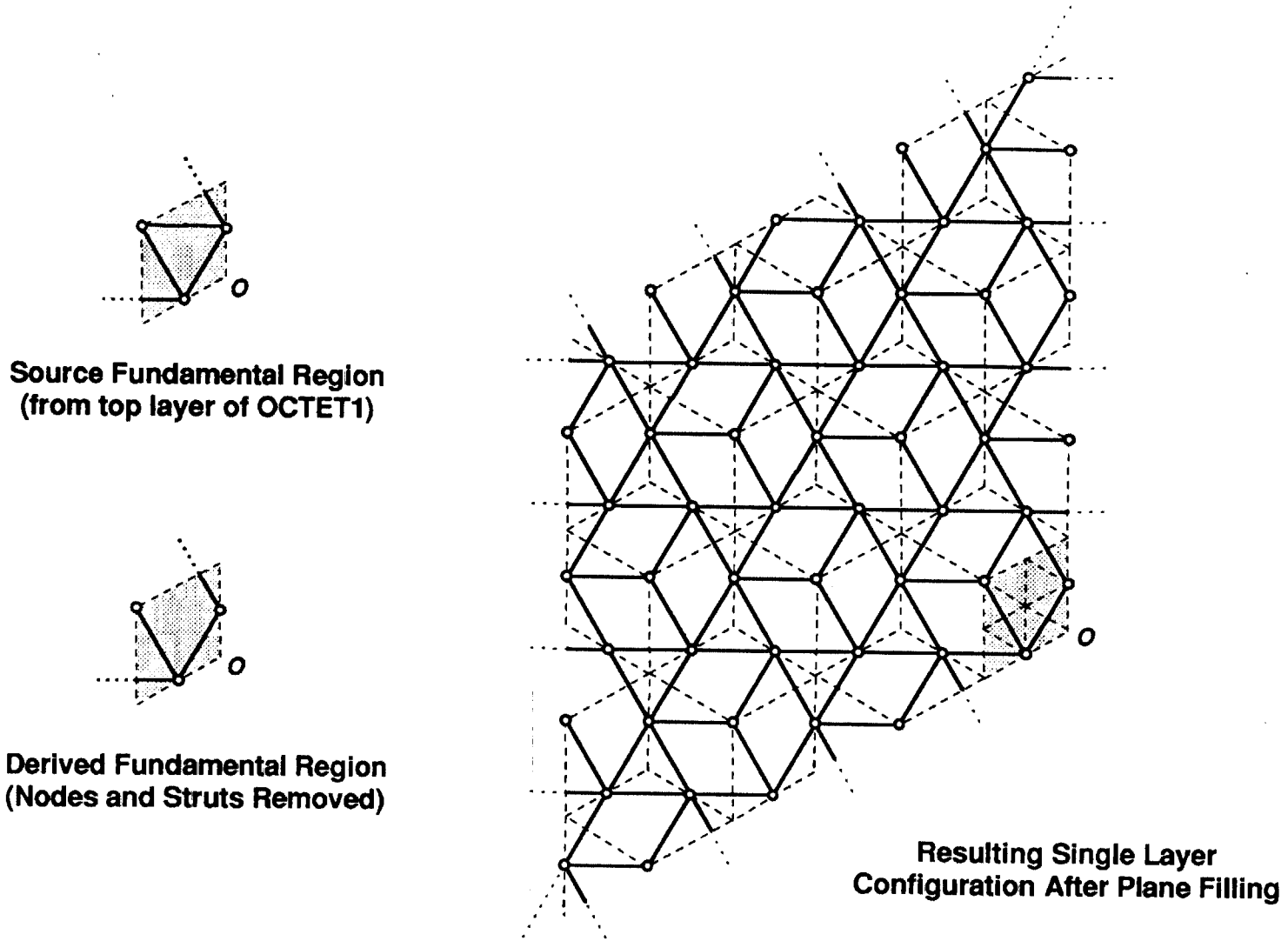

Figure 25a. The Top Layer of **REDUCED2** Derived from the Top Layer of OCTET1.

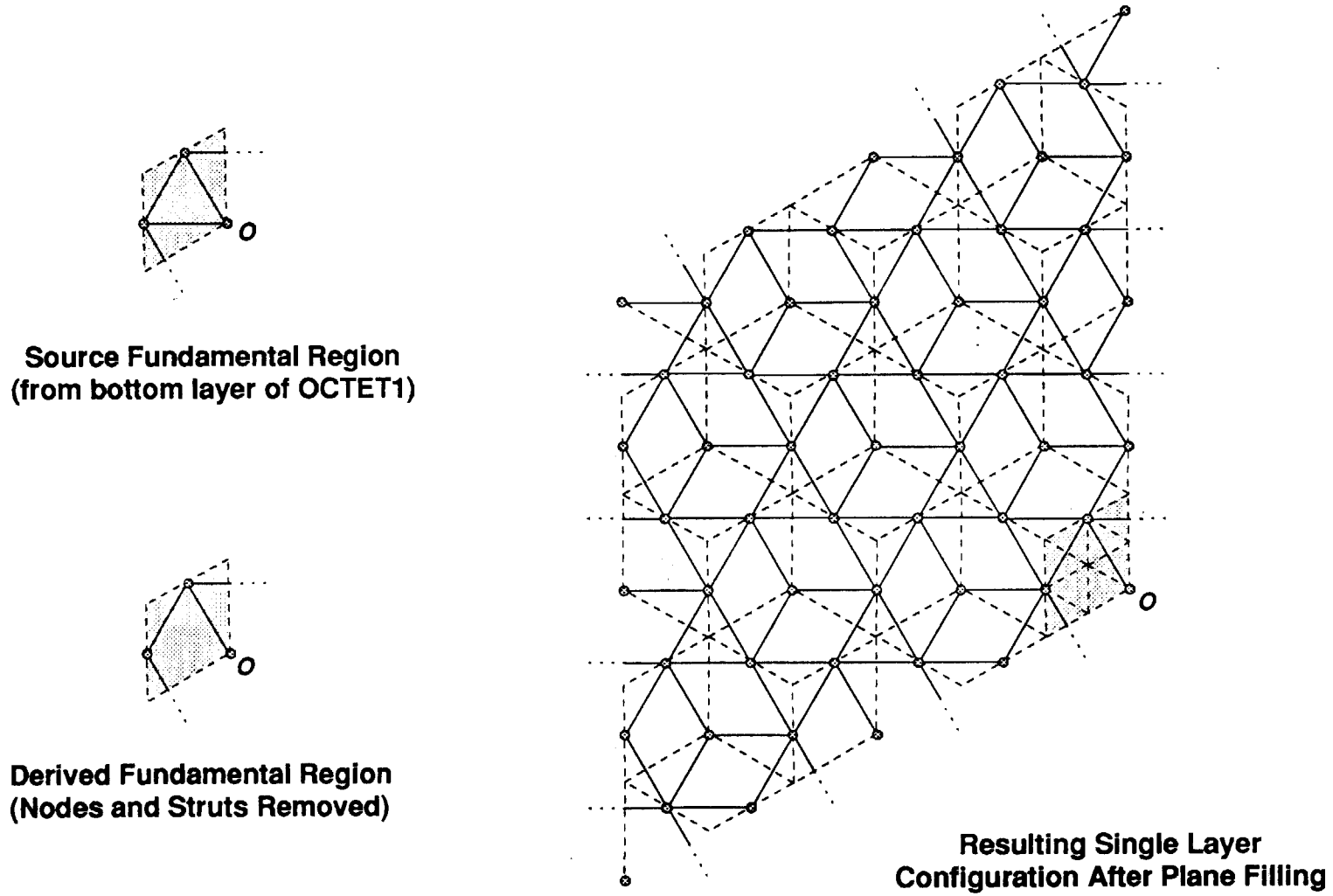

Figure 25b. The Bottom Layer of **REDUCED2** Derived from the Bottom Layer of OCTET1.

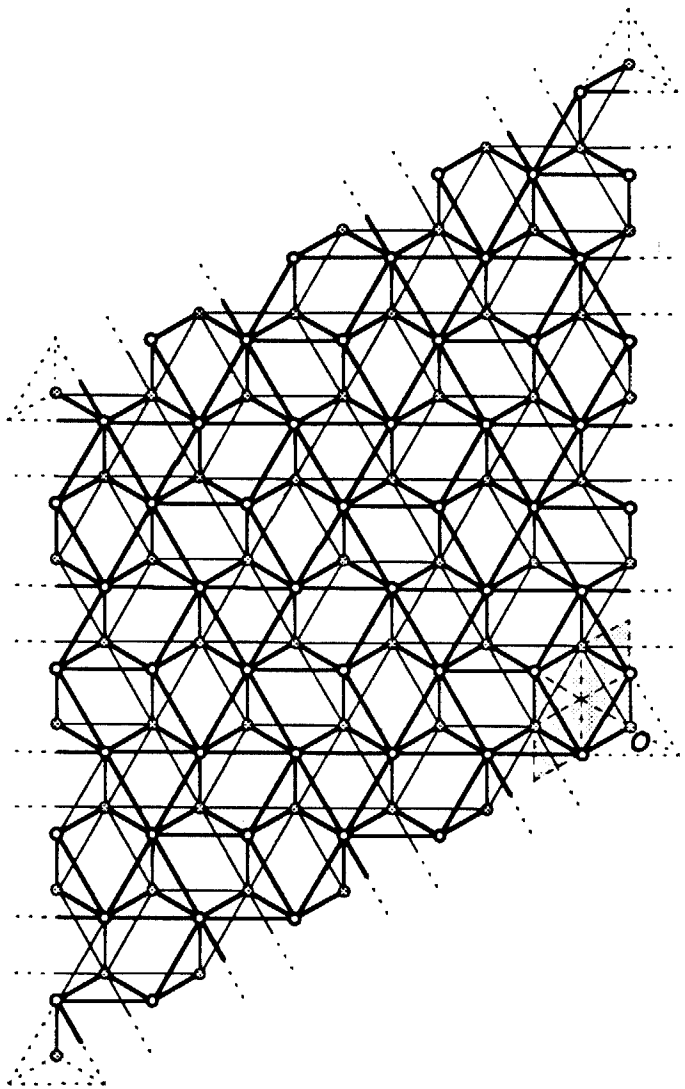

Figure 25c. The Double-Layered Configuration **REDUCED2** Derived from the Octet Configuration OCTET1 by Removing Struts Only.

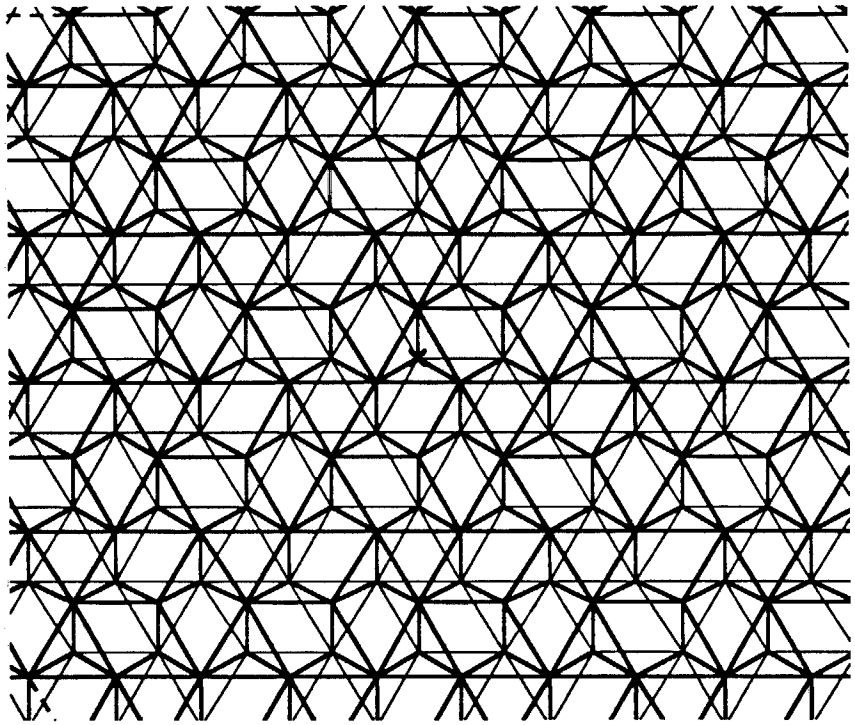

Figure 25d. A Portion of the Infinite Configuration **REDUCED2**

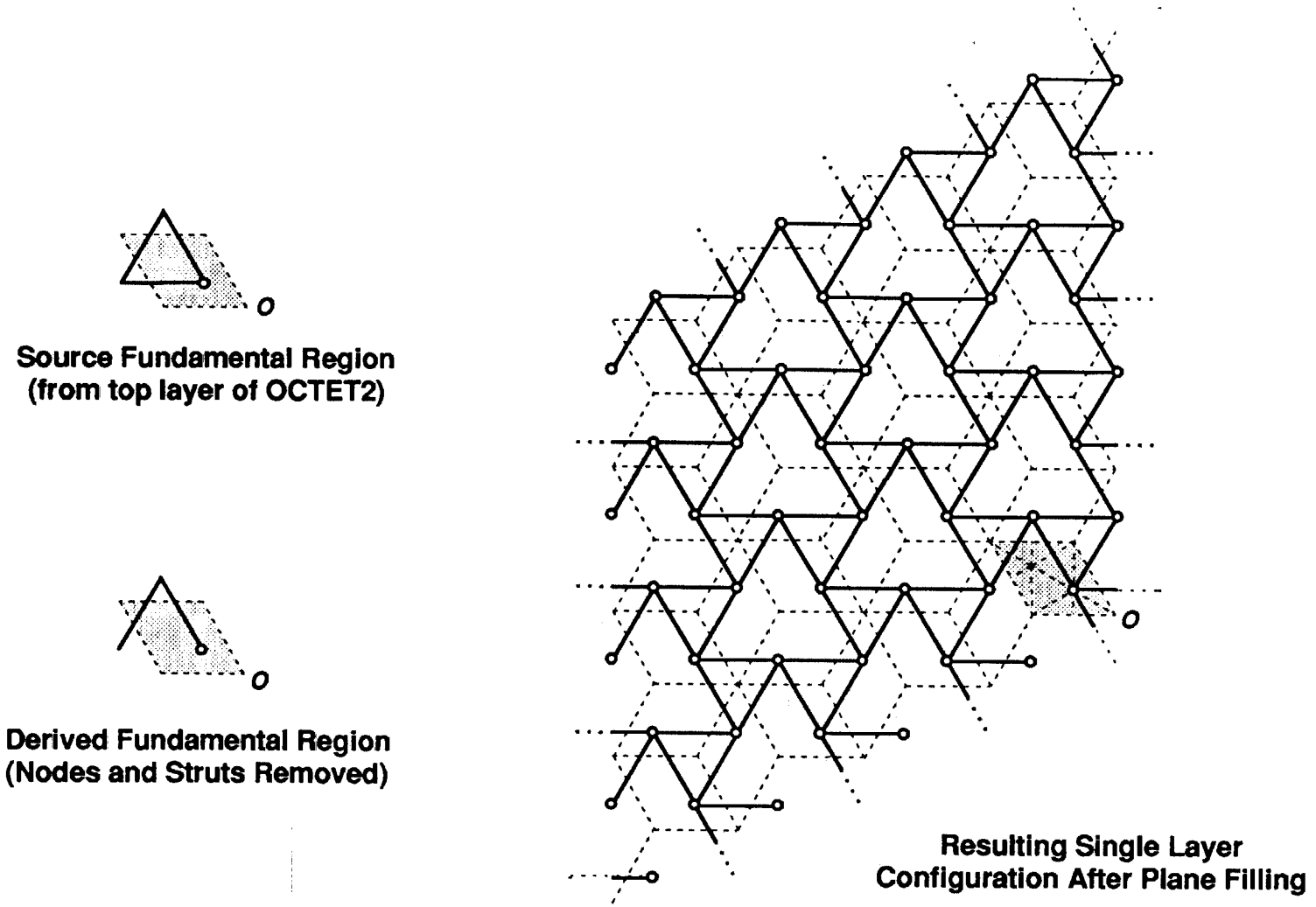

Figure 26a. The Top Layer of **REDUCED3** Derived from the Top Layer of OCTET2

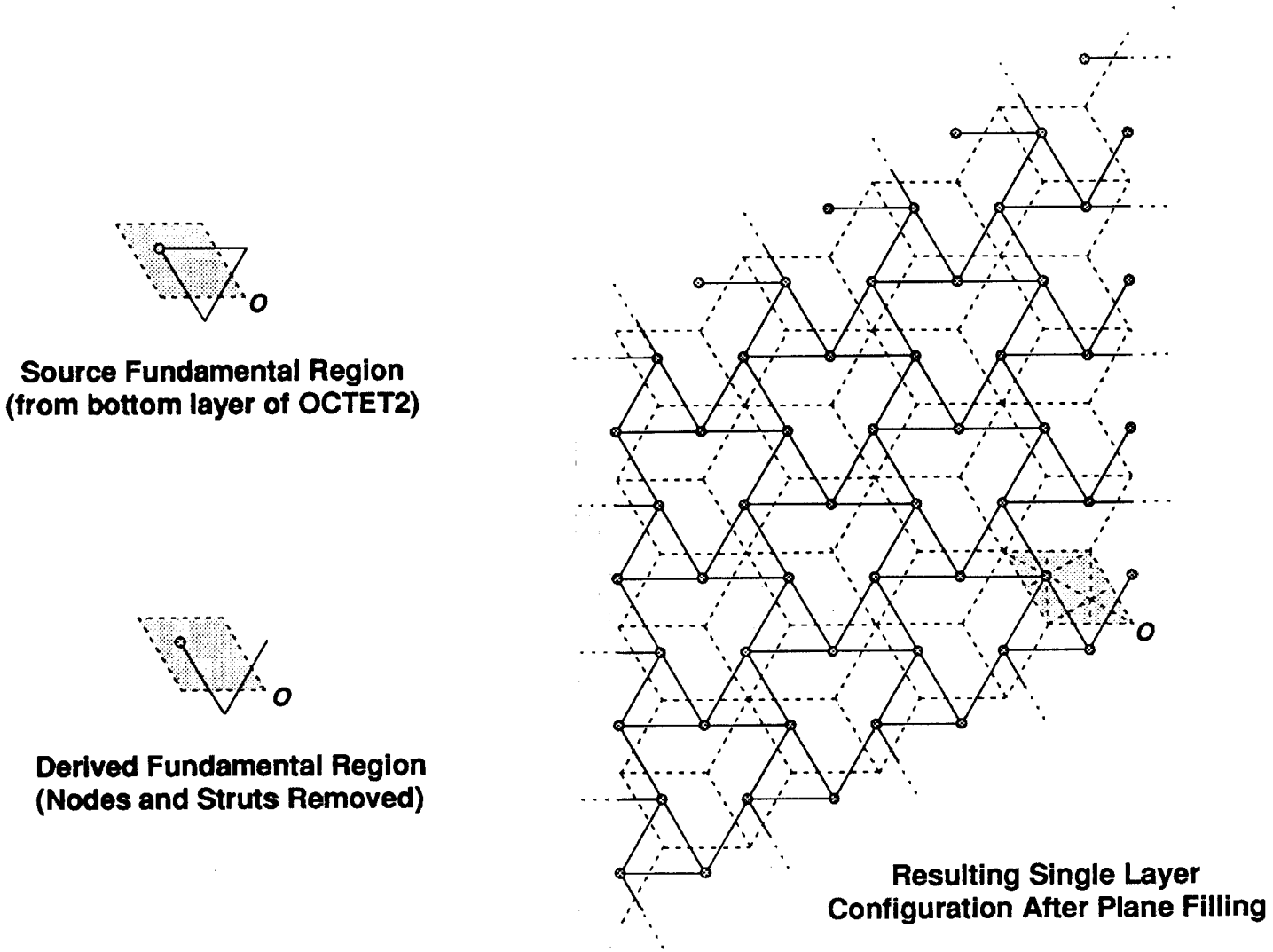

Figure 26b. The Bottom Layer of **REDUCED3** Derived from the Bottom Layer of OCTET2.

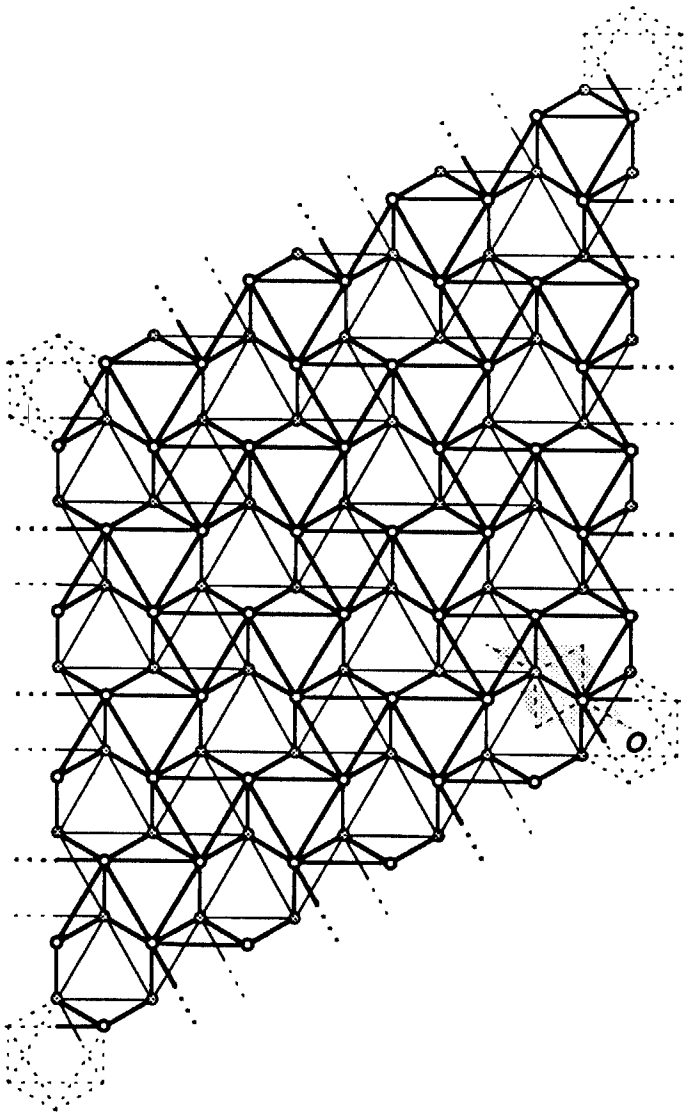

Figure 26c. The Double-Layered Configuration **REDUCED3** Derived from the Octet Configuration OCTET2 by Removing Struts Only.

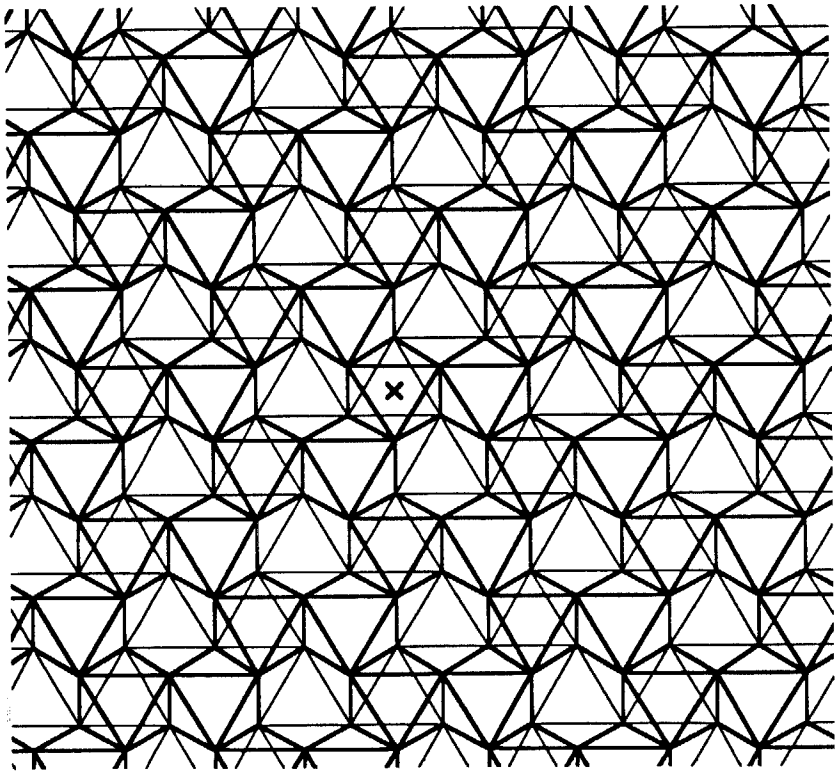

Figure 26d. A Portion of the Infinite Configuration **REDUCED3.**

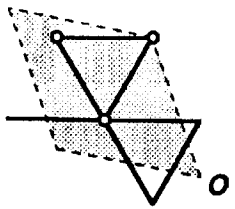

Source Fundamental Region
(from top layer of OCTET1)

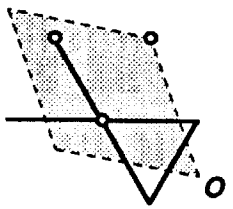

Derived Fundamental Region
(Nodes and Struts Removed)

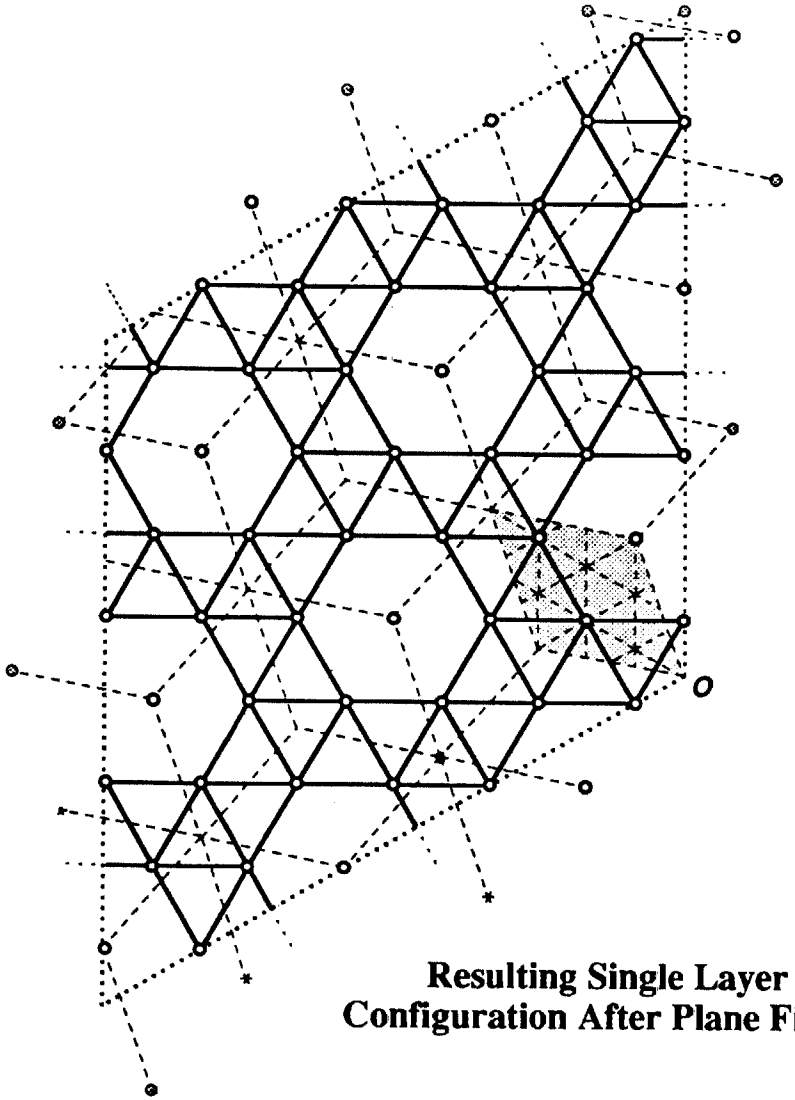

Resulting Single Layer
Configuration After Plane Filling

Figure 27a. The Top Layer of **SKEW1** Derived from the Top Layer of OCTET1.

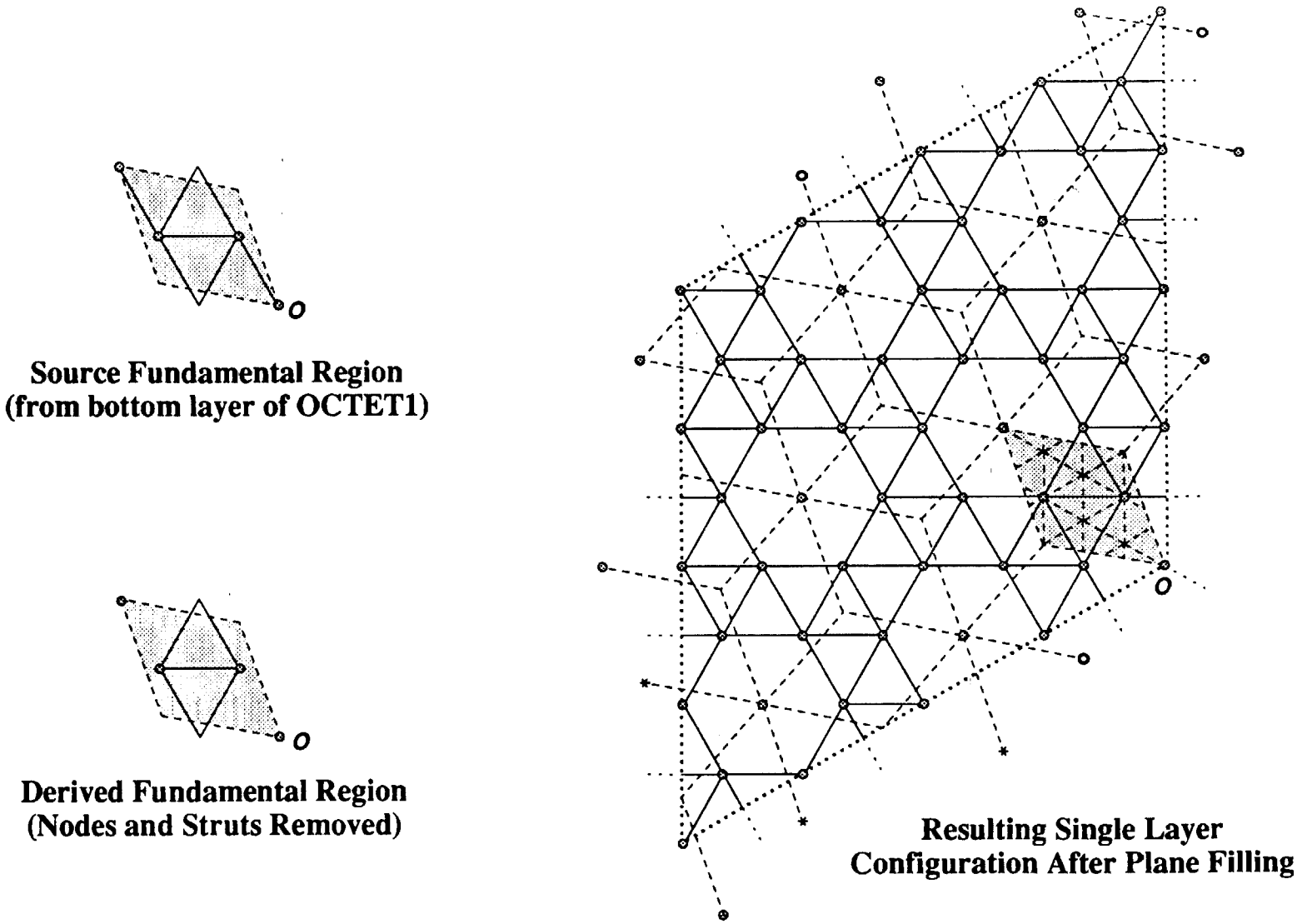

Figure 27b. The Bottom Layer of **SKEW1** Derived from the Bottom Layer of OCTET1.

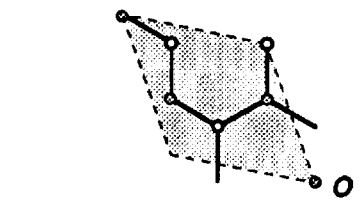

Source Fundamental Region
(from core of OCTET1)

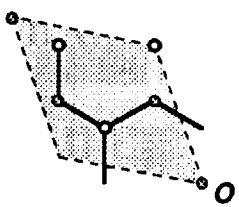

Derived Fundamental Region
(Nodes and Struts Removed)

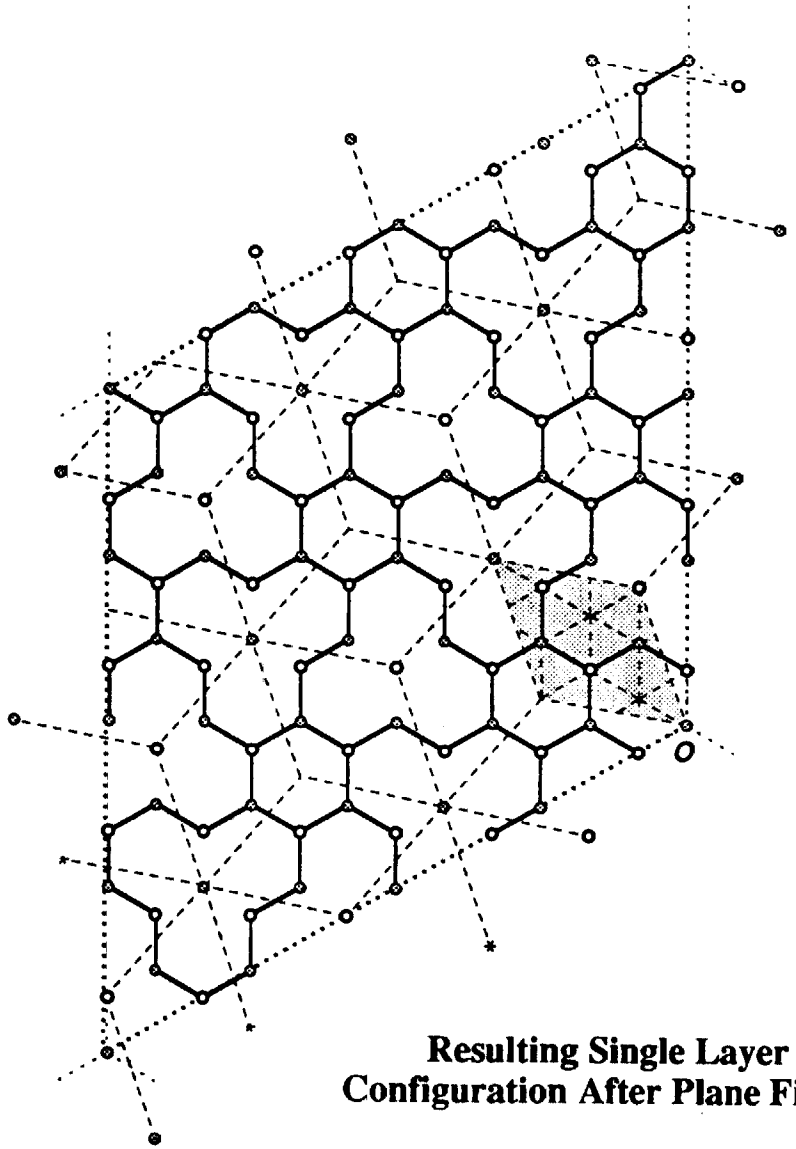

Resulting Single Layer
Configuration After Plane Filling

Figure 27c. The Core of **SKEW1** Derived from the Core of OCTET1.

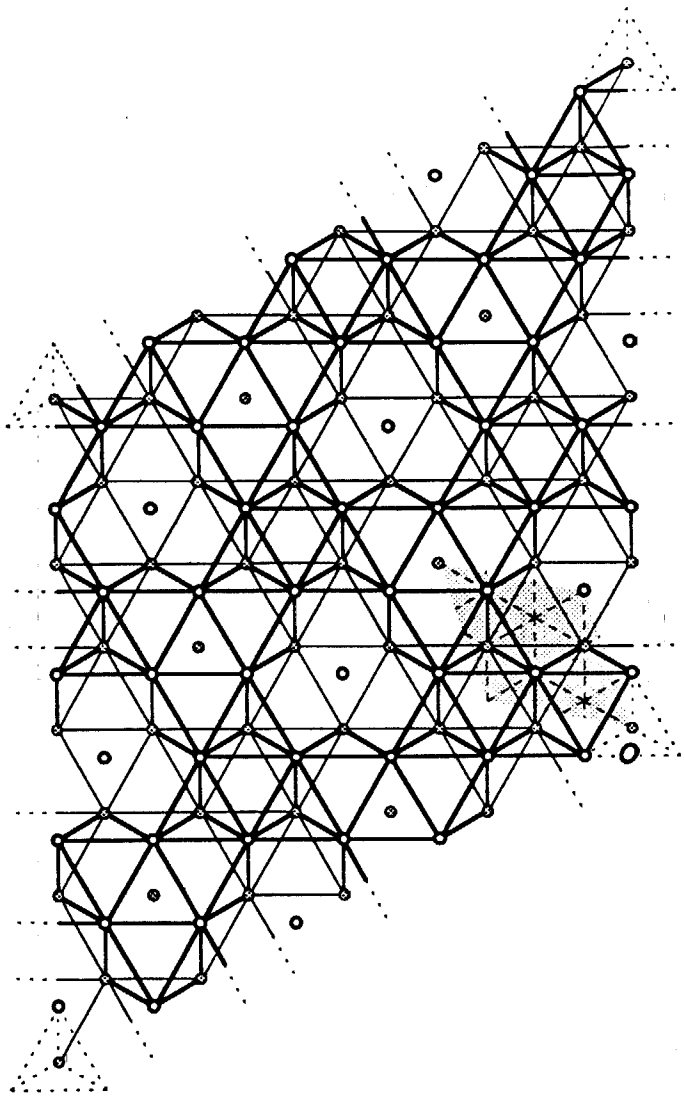

Figure 27d. The Double-Layered Configuration **SKEW1** Derived from the Octet Configuration OCTET1 by Removing Nodes and Struts.

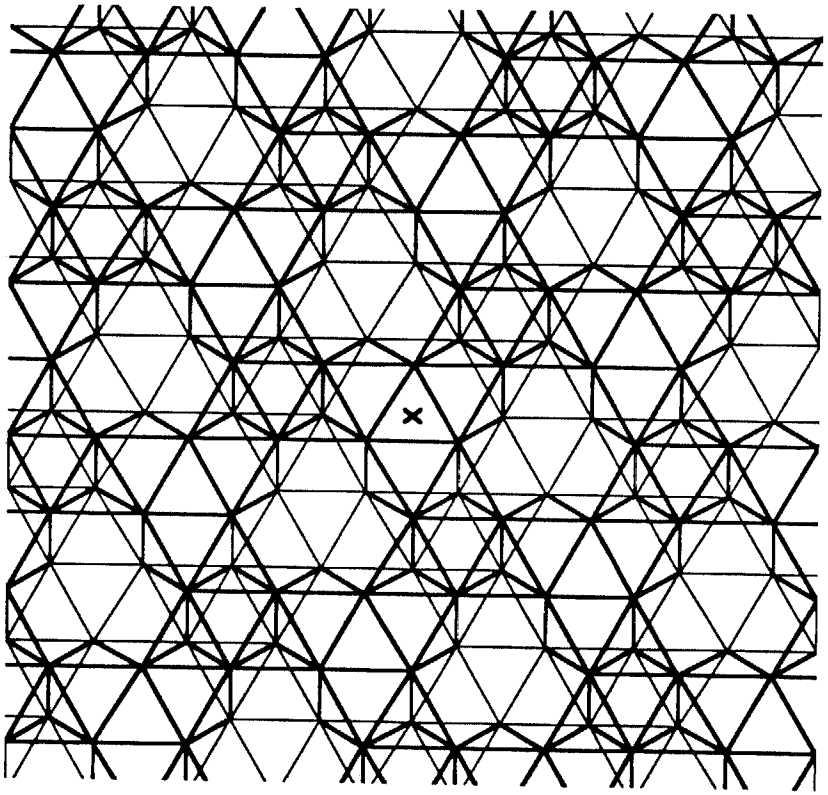

Figure 27e. A Portion of the Infinite Configuration **SKEW1.**

Source Fundamental Region
(from top layer of OCTET2)

Derived Fundamental Region
(Nodes and Struts Removed)

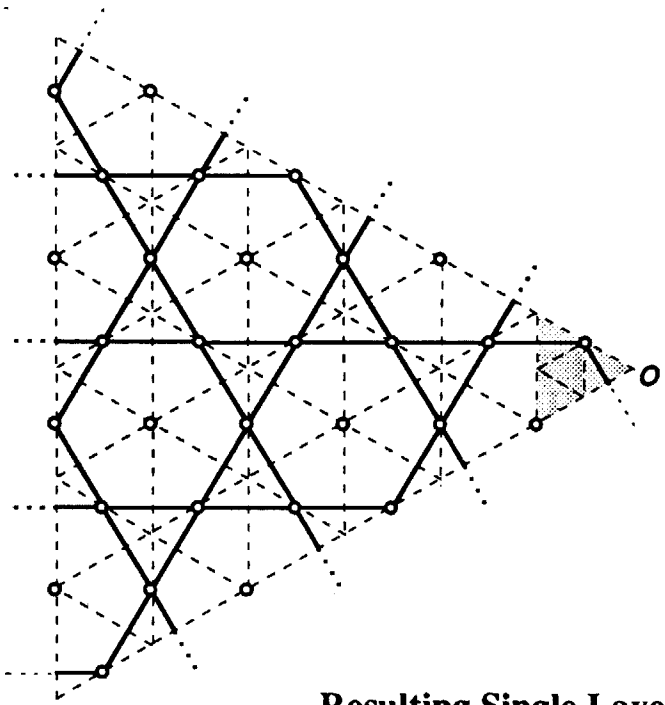

Resulting Single Layer
Configuration After Plane Filling

Figure 28a. The Top Layer of **MINIMUM1** Derived from the Top Layer of OCTET2.

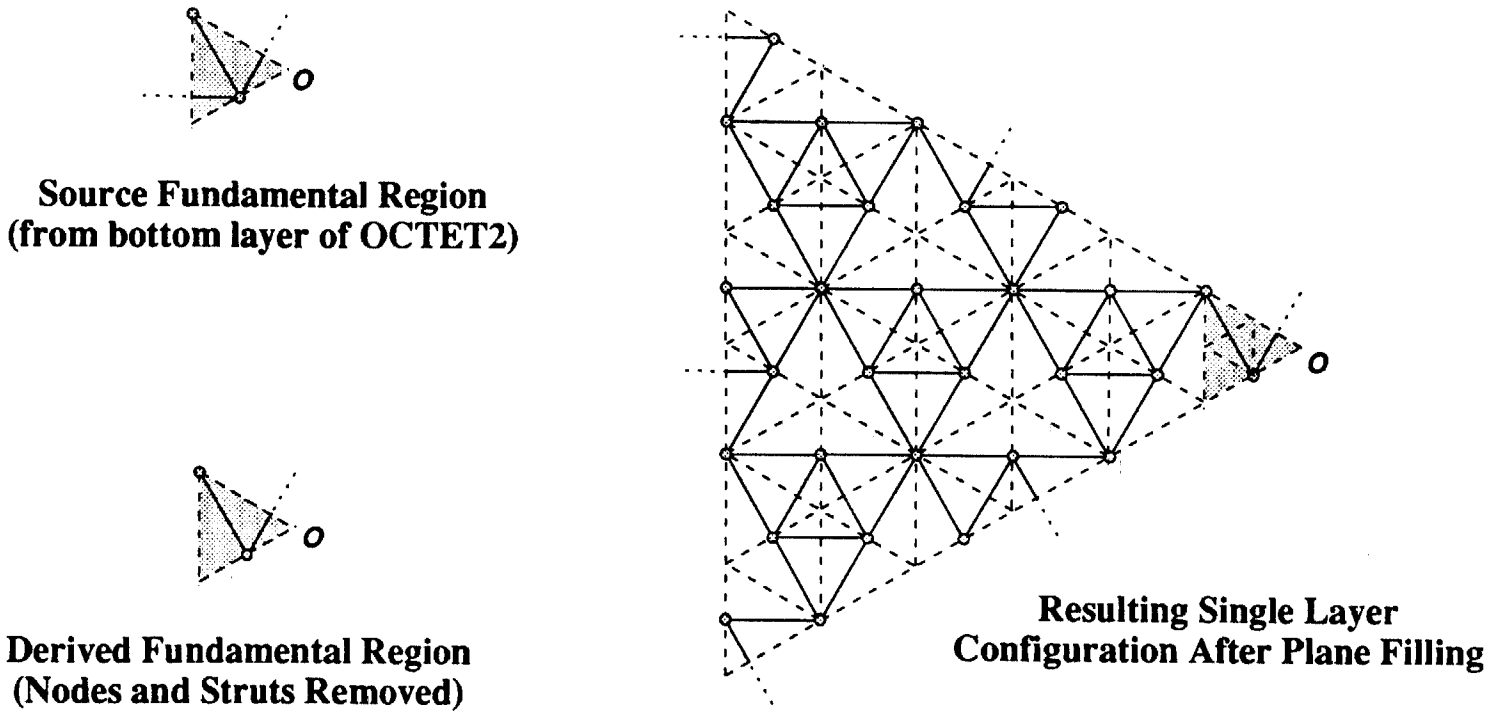

Figure 28b. The Bottom Layer of **MINIMUM1** Derived from the Bottom Layer of OCTET2.

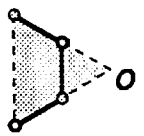

Source Fundamental Region
(from core of OCTET2)

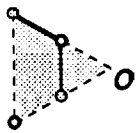

Derived Fundamental Region
(Nodes and Struts Removed)

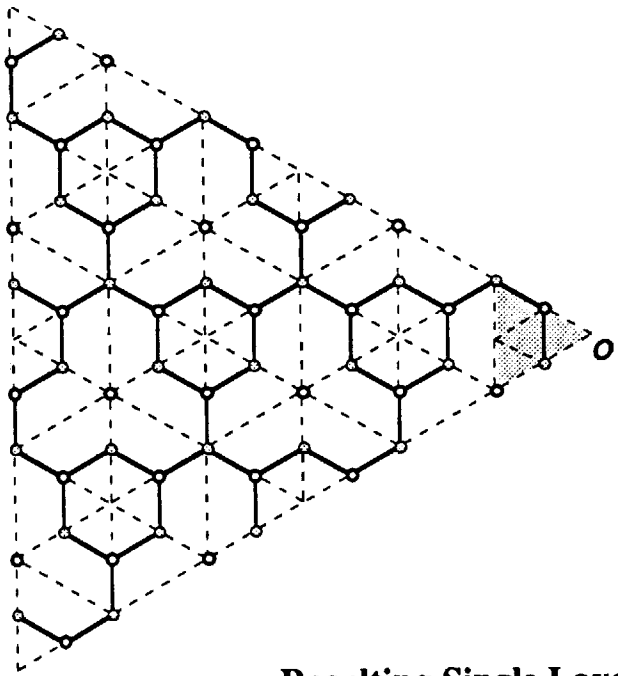

Resulting Single Layer
Configuration After Plane Filling

Figure 28c. The Core of **MINIMUM1** Derived from the Core of OCTET2.

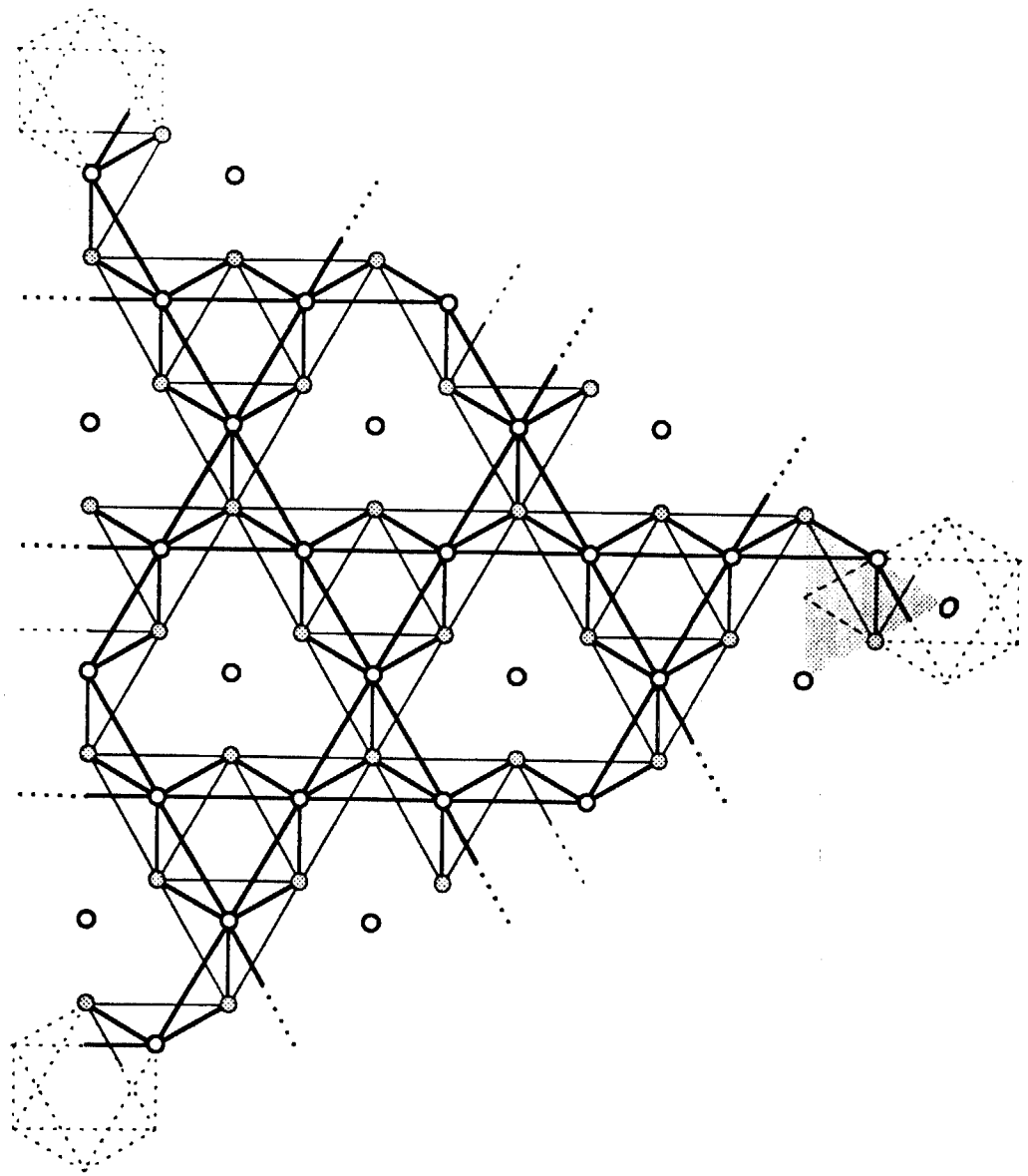

Figure 28d. The Double-Layered Configuration **MINIMUM1** Derived from OCTET2 by Removing Nodes and Struts.

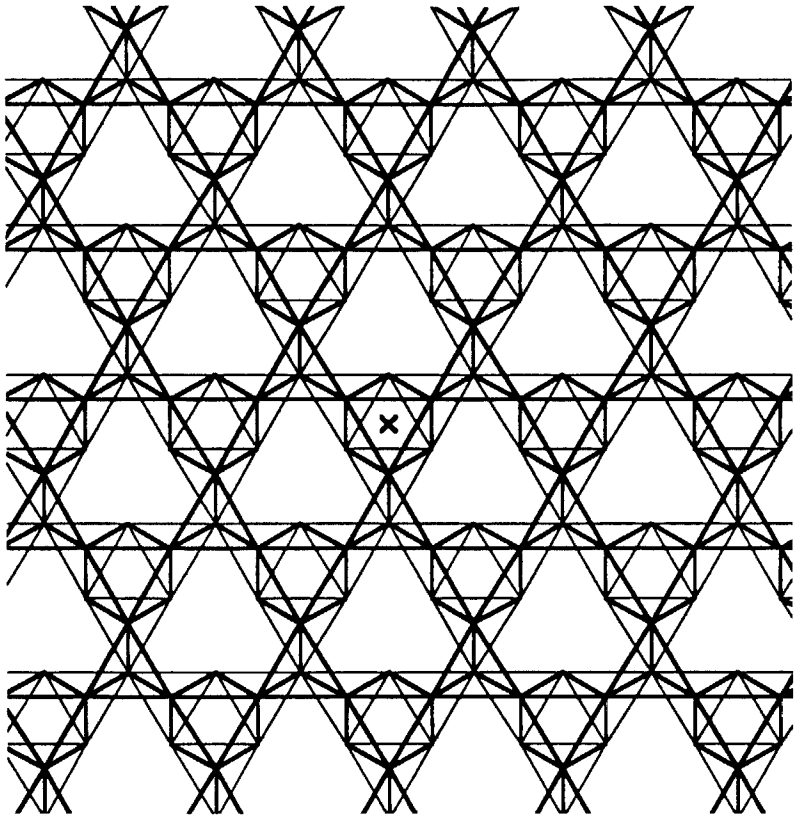

Figure 28e. A Portion of the Infinite Configuration **MINIMUM1.**

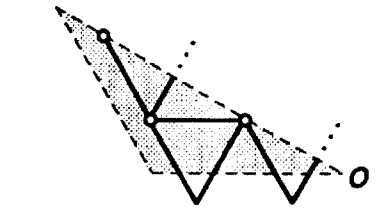

Source Fundamental Region
(from top layer of OCTET1)

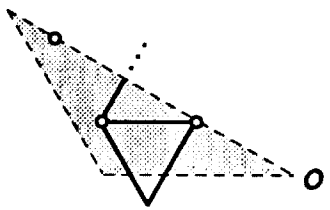

Derived Fundamental Region
(Nodes and Struts Removed)

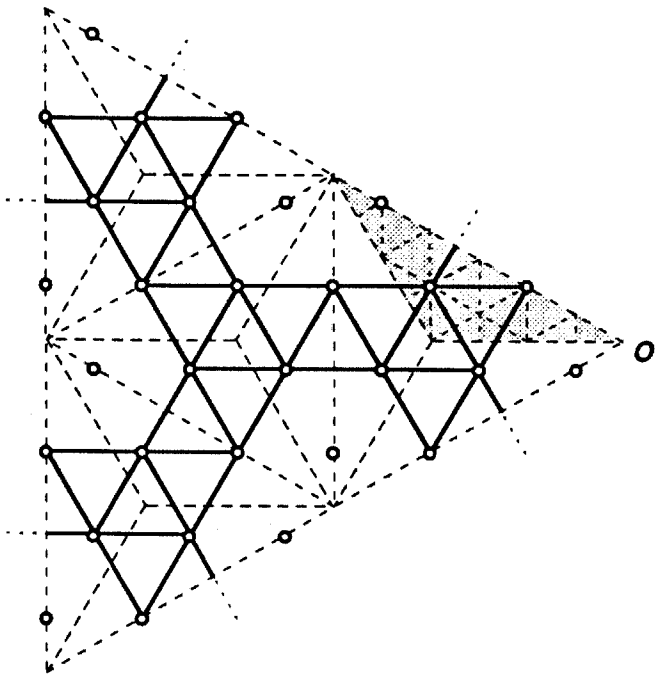

Resulting Single Layer
Configuration After Plane Filling

Figure29a. The Top Layer of **TOROID2** Derived from the Top Layer of OCTET1.

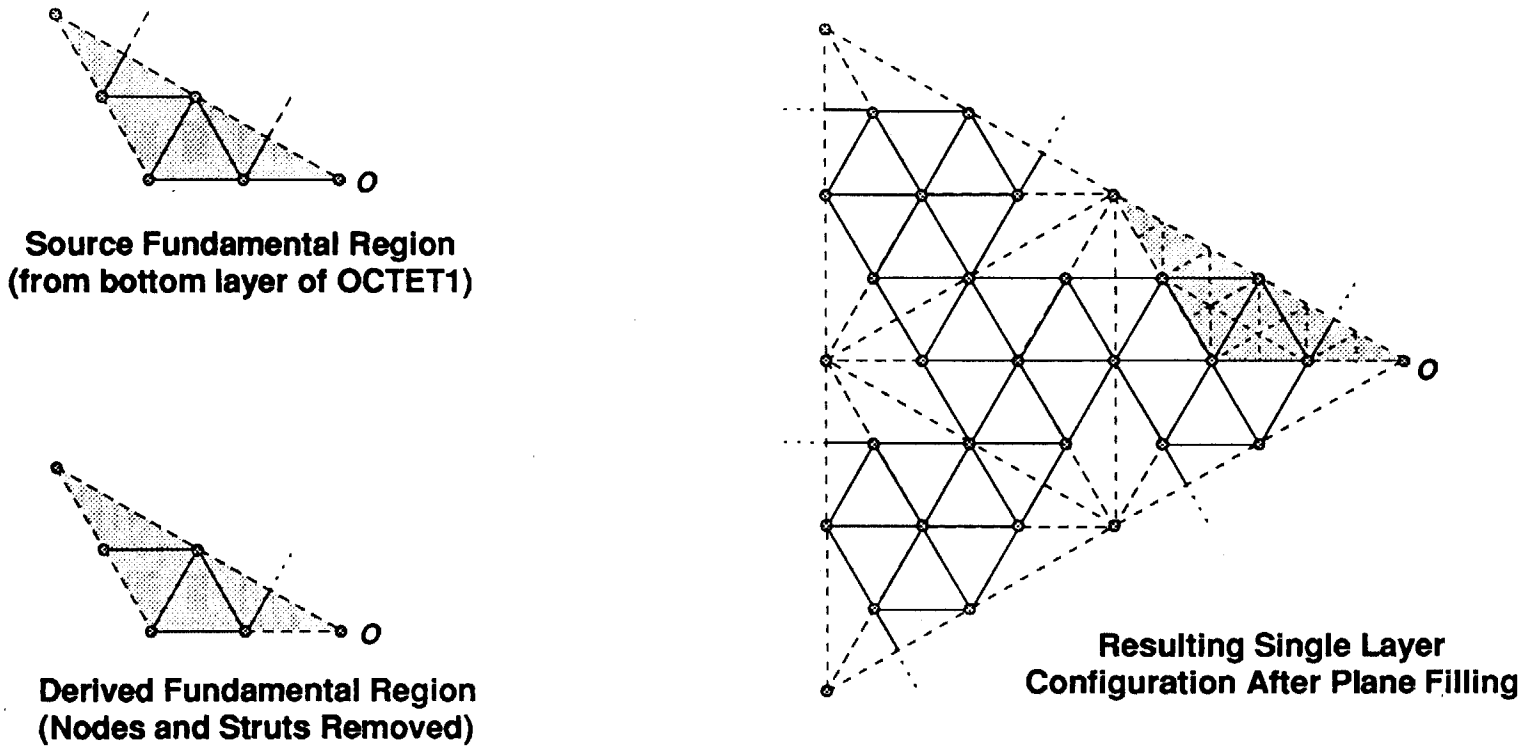

Figure 29b. The Bottom Layer of **TOROID2** Derived from the Bottom Layer of OCTET1.

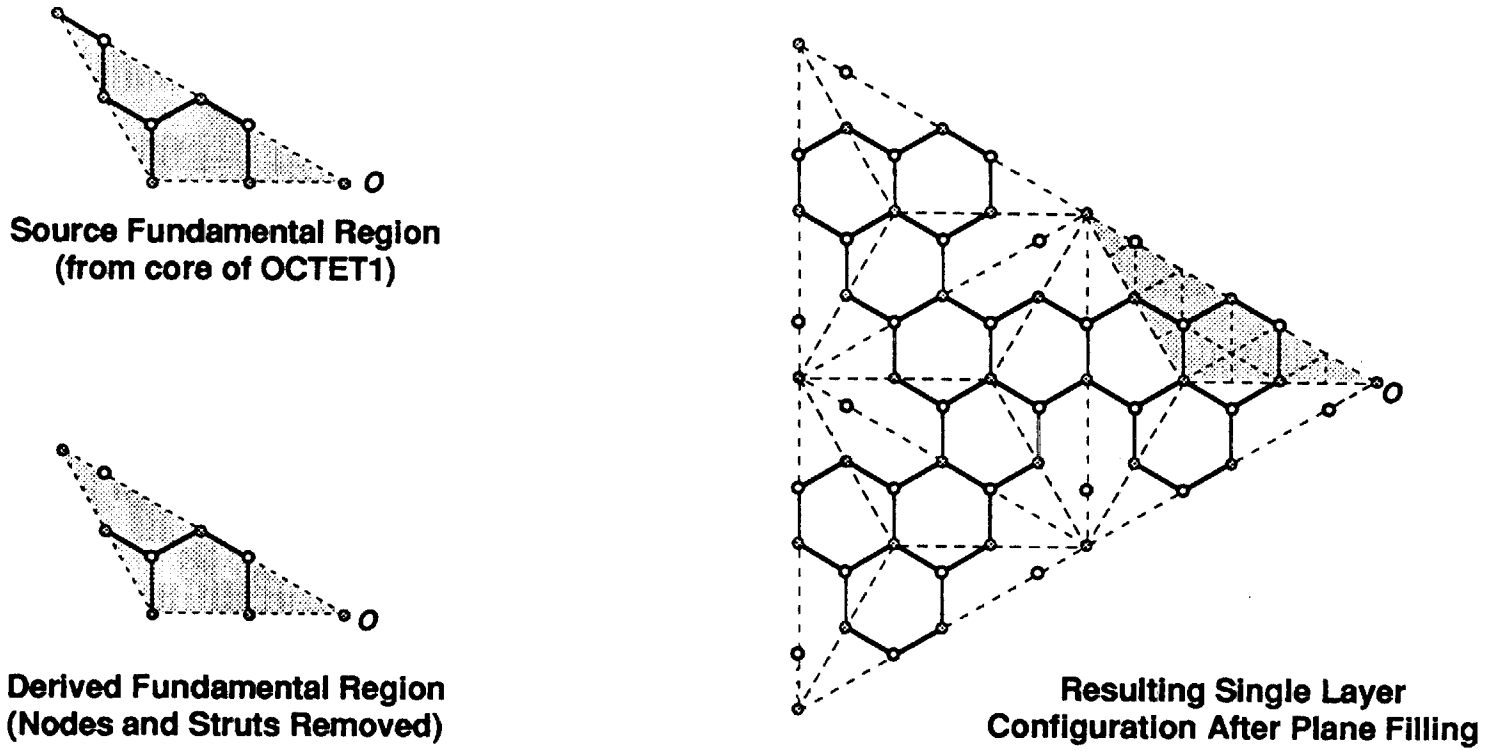

Figure 29c. The Core of **TOROID2** Derived from the Core of OCTET1.

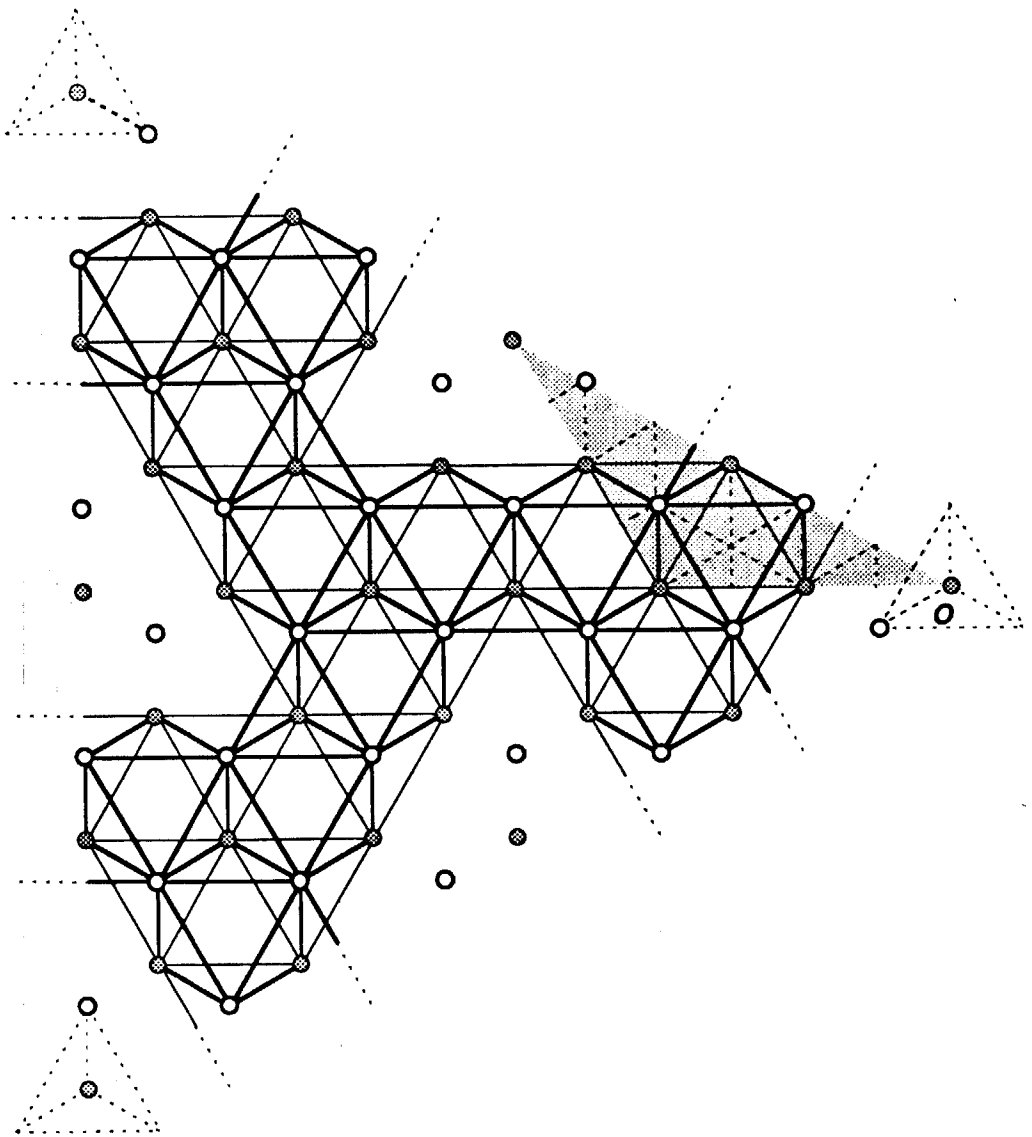

Figure 29d. The Double-Layered Configuration **TOROID2** Derived from the Octet Configuration OCTET1 by Removing Nodes and Struts.

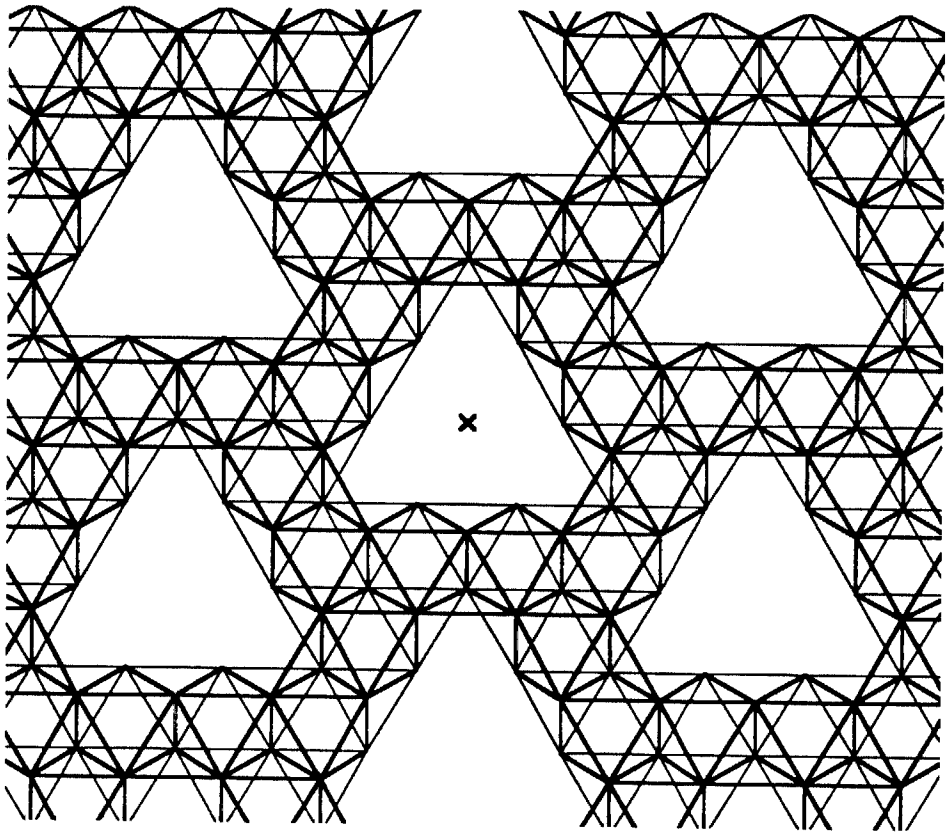

Figure 29e. A Portion of the Infinite Configuration **TOROID2.**

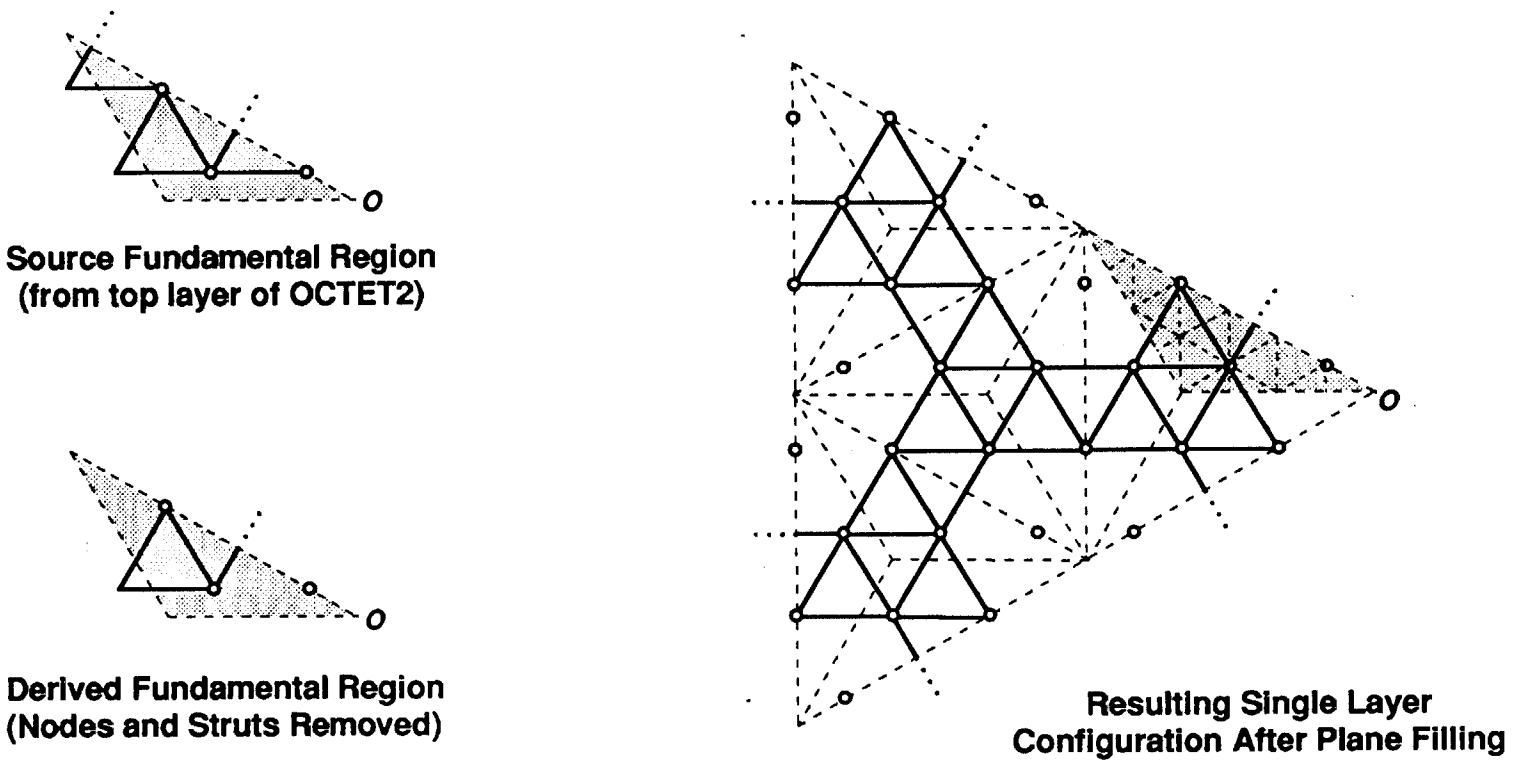

Figure 30a. The the Top Layer of **TOROID3** Derived from the Top Layer OCTET2.

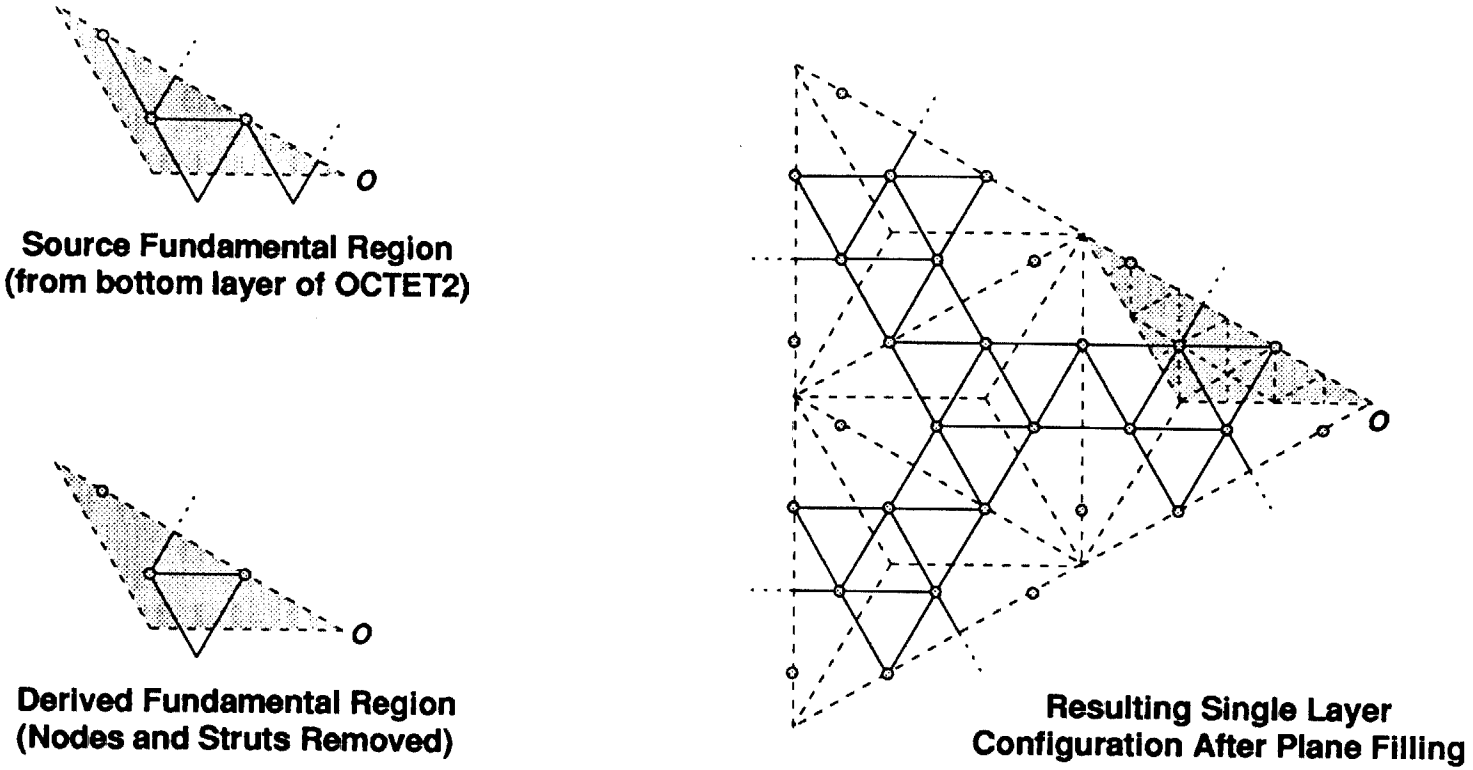

Figure 30b. The Bottom Layer of **TOROID3** Derived from the Bottom Layer of OCTET2.

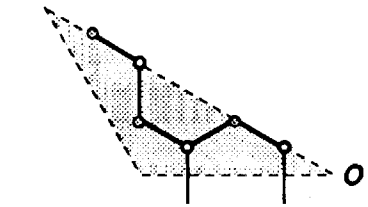

Source Fundamental Region
(from core of OCTET2)

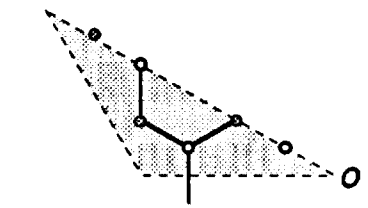

Derived Fundamental Region
(Nodes and Struts Removed)

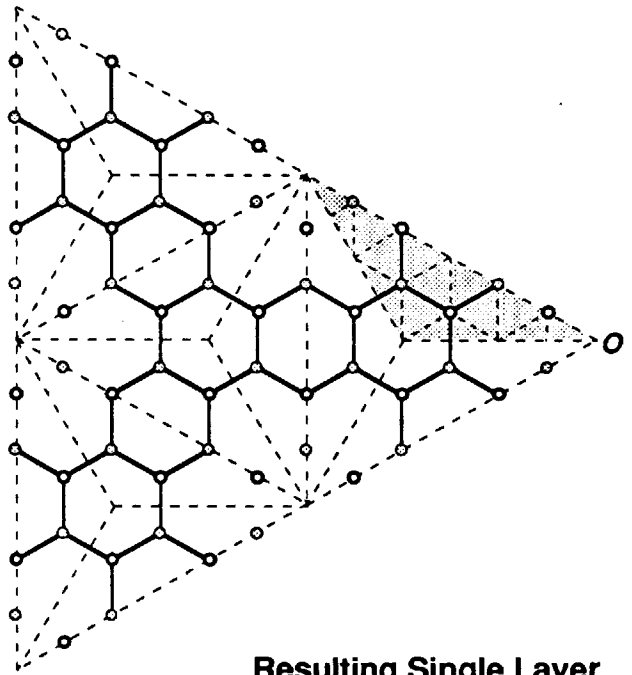

Resulting Single Layer
Configuration After Plane Filling

Figure 30c. The core of **TOROID3** Derived from the Core of OCTET2.

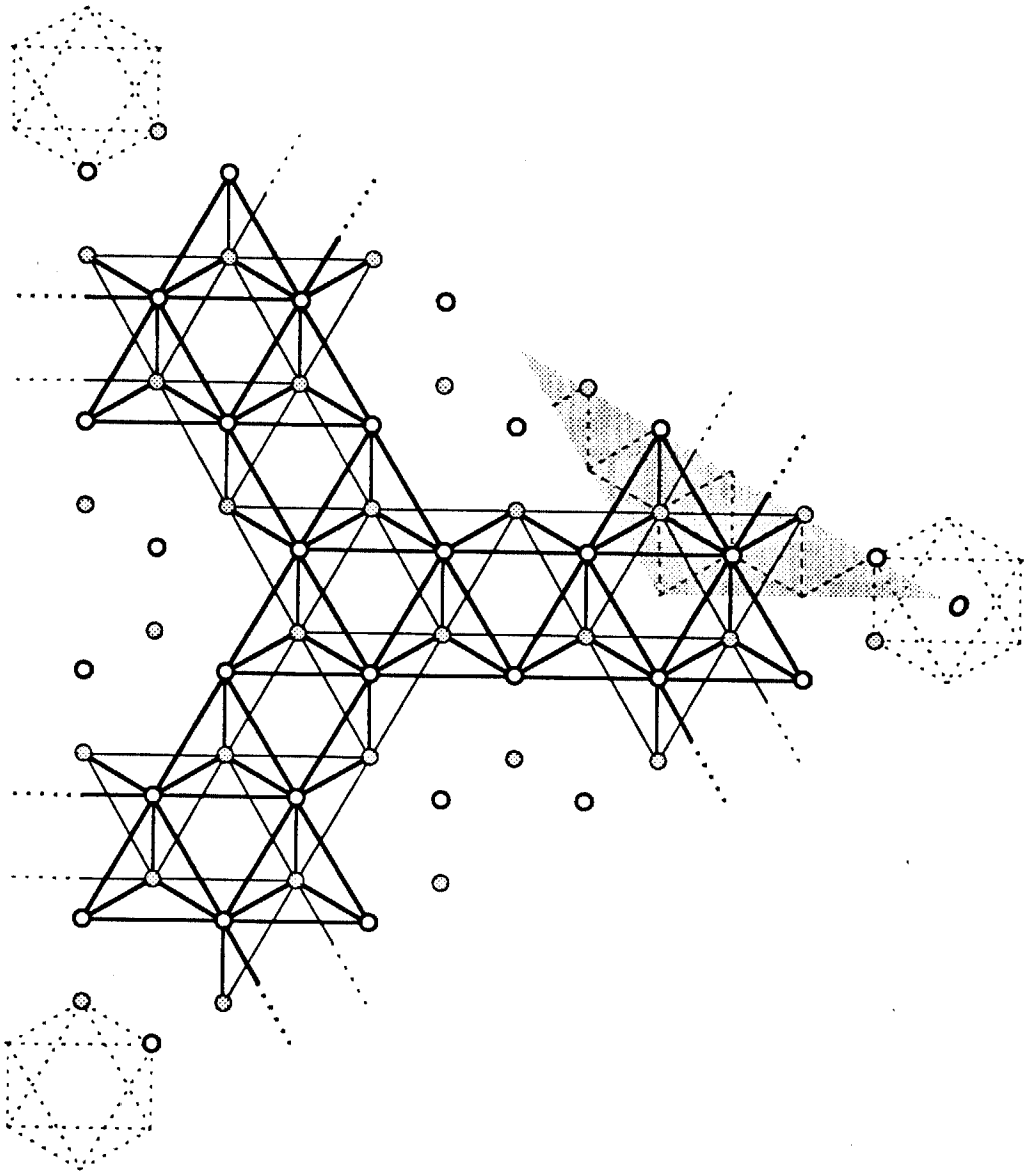

Figure 30d. The Double-Layered Configuration **TOROID3** Derived from the Octet Configuration OCTET2 by Removing Nodes And Struts.

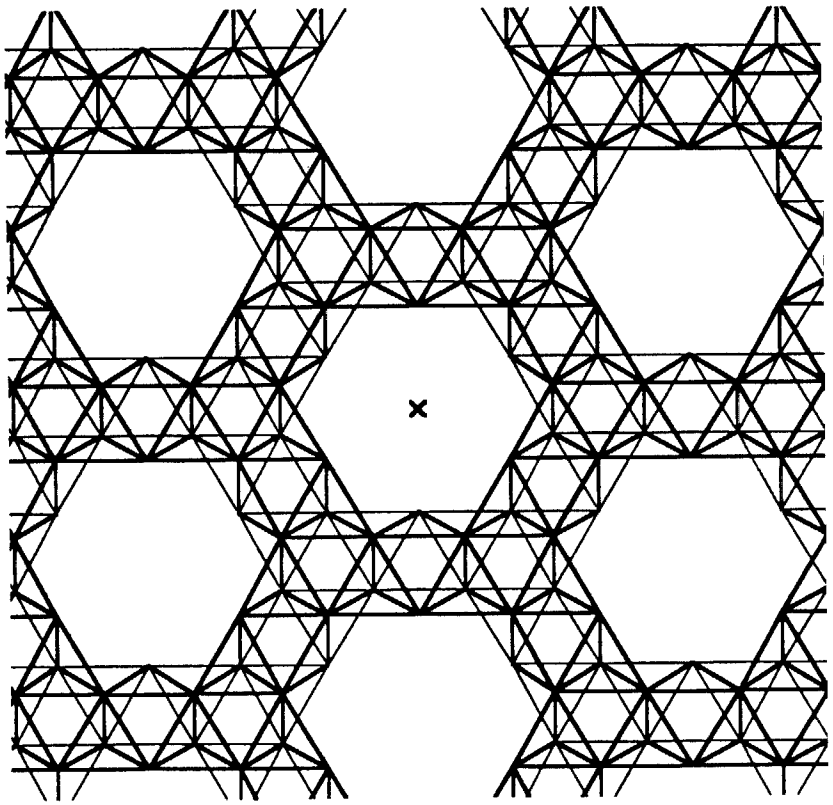

Figure 30e. A Portion of the Infinite Configuration **TOROID3.**

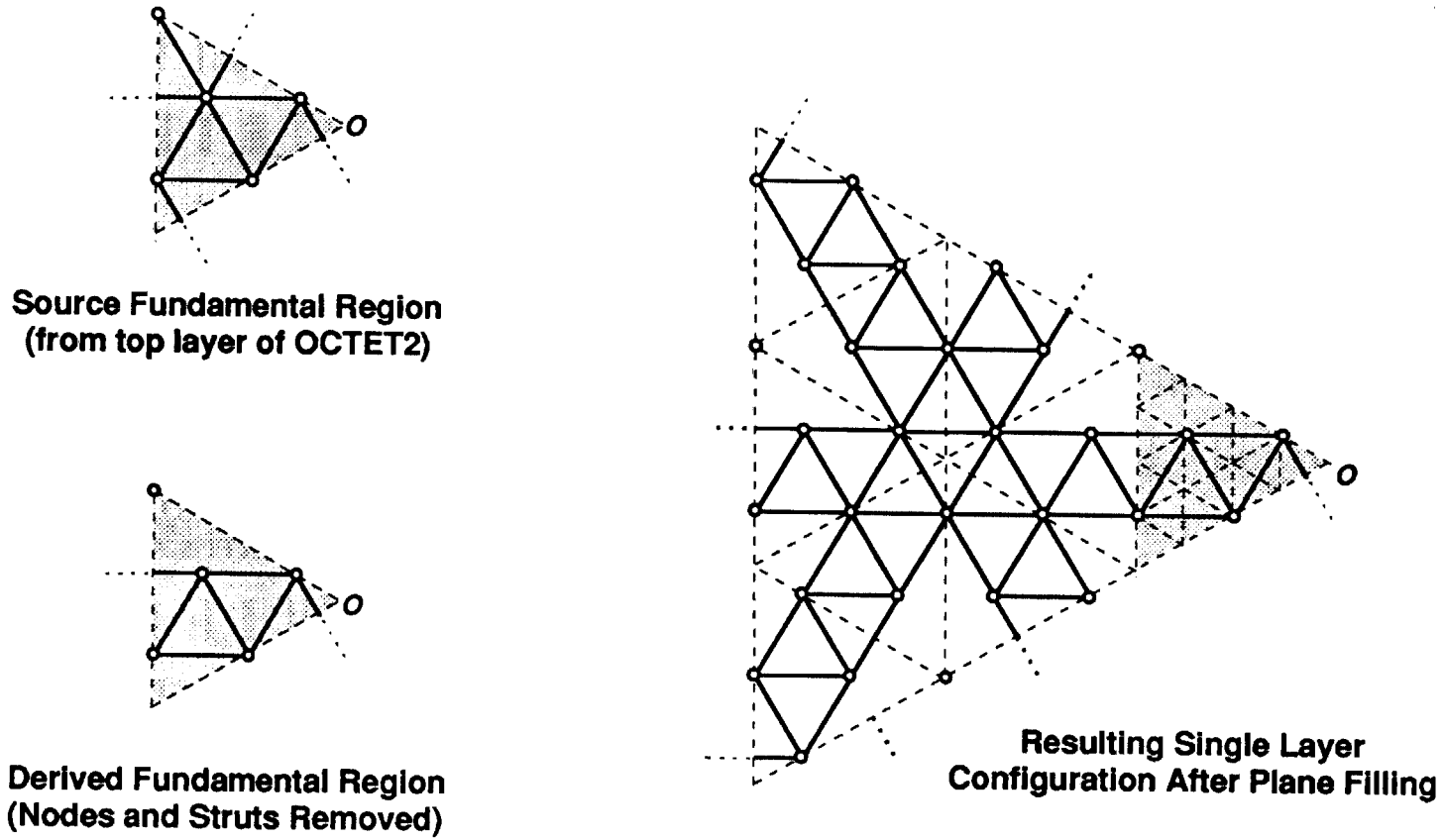

Figure 31a. The Top Layer of **TOROID4** Derived from the Top Layer of OCTET2.

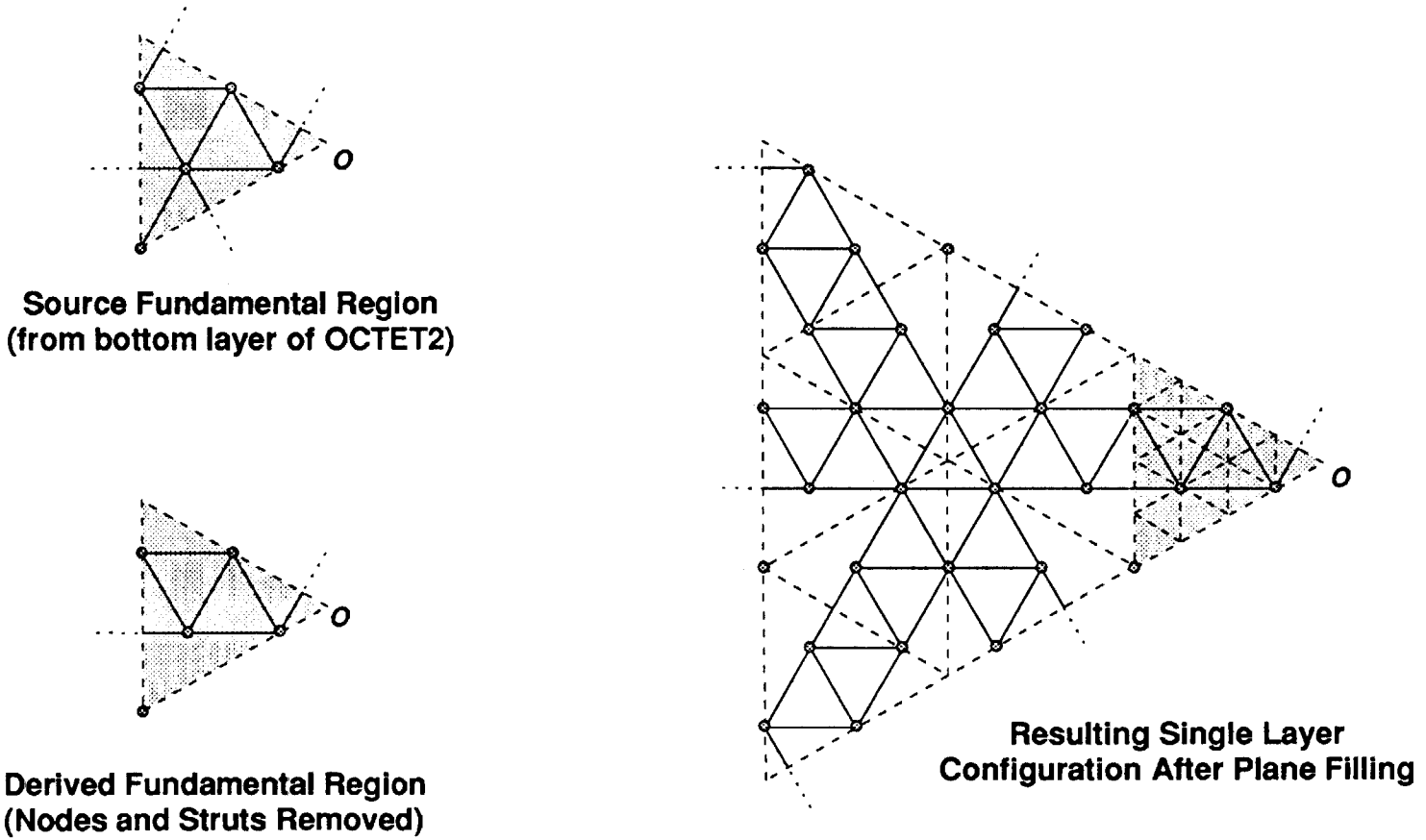

Figure 31b. The Bottom Layer of **TOROID4** Derived from the Bottom Layer of OCTET2.

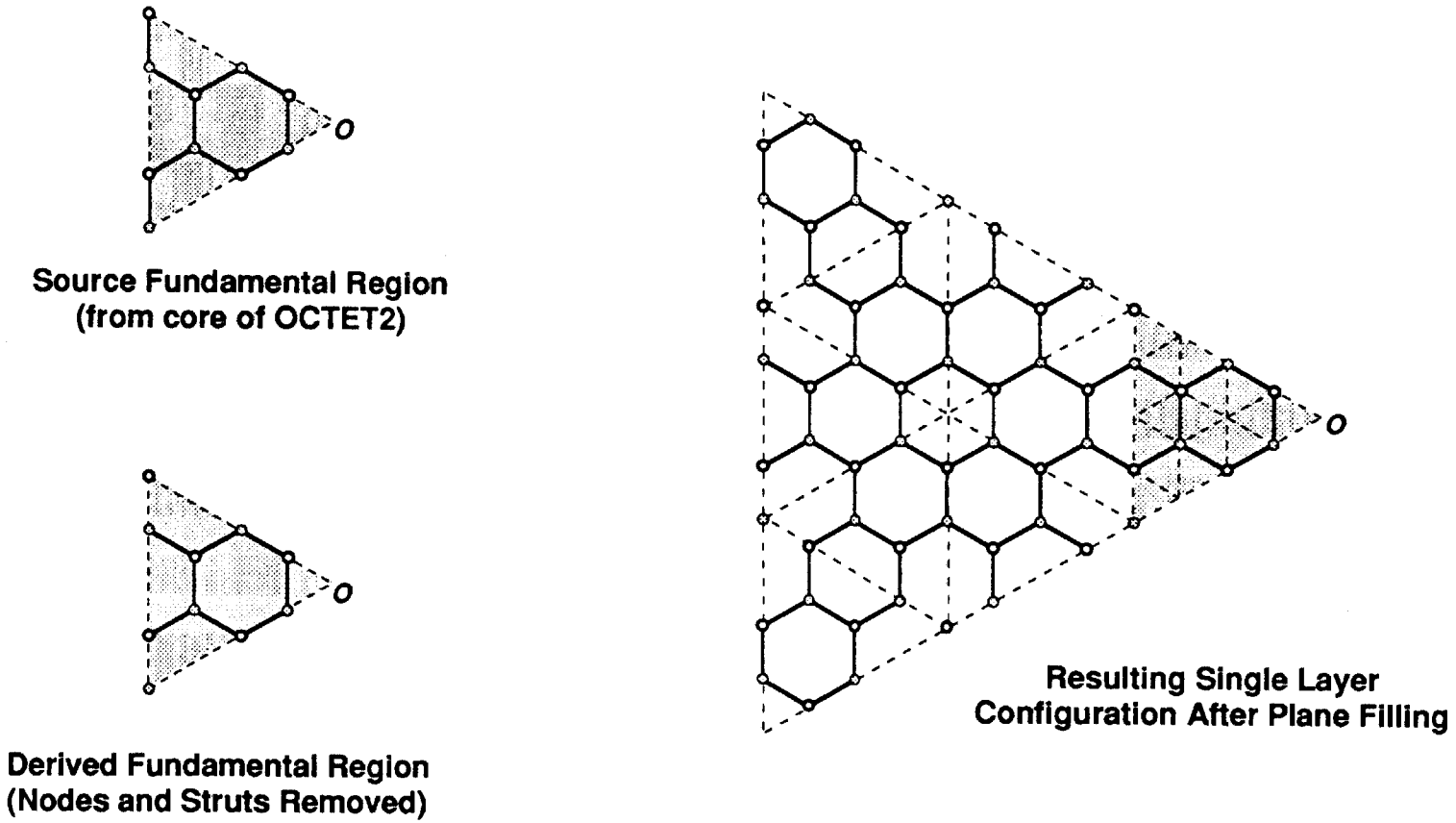

Figure 31c. The Core of **TOROID4** Derived from the Core of OCTET2.

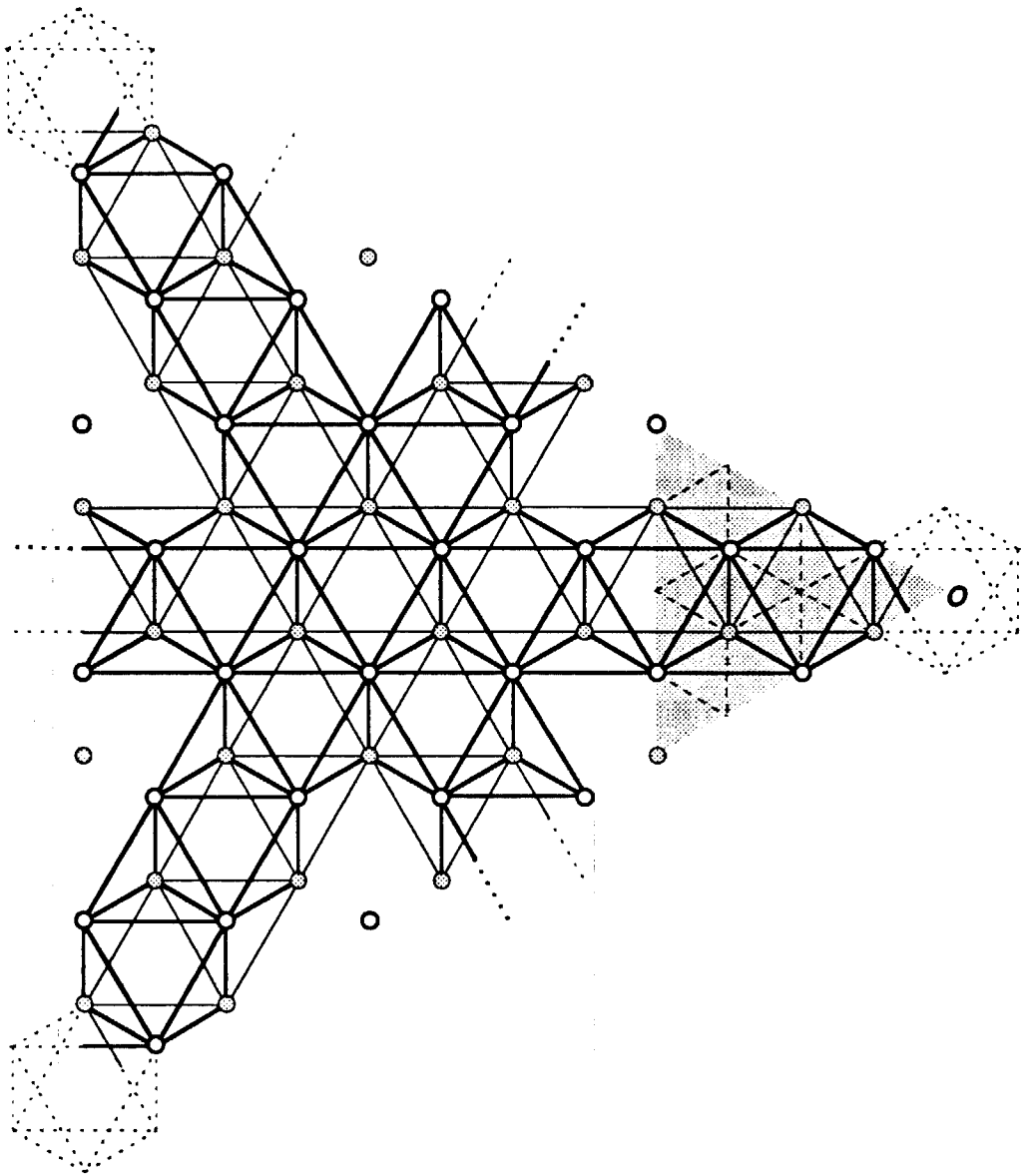

Figure 31d. The Double-Layered Configuration **TOROID4** Derived from the Octet Configuration OCTET2 by Removing Nodes and Struts.

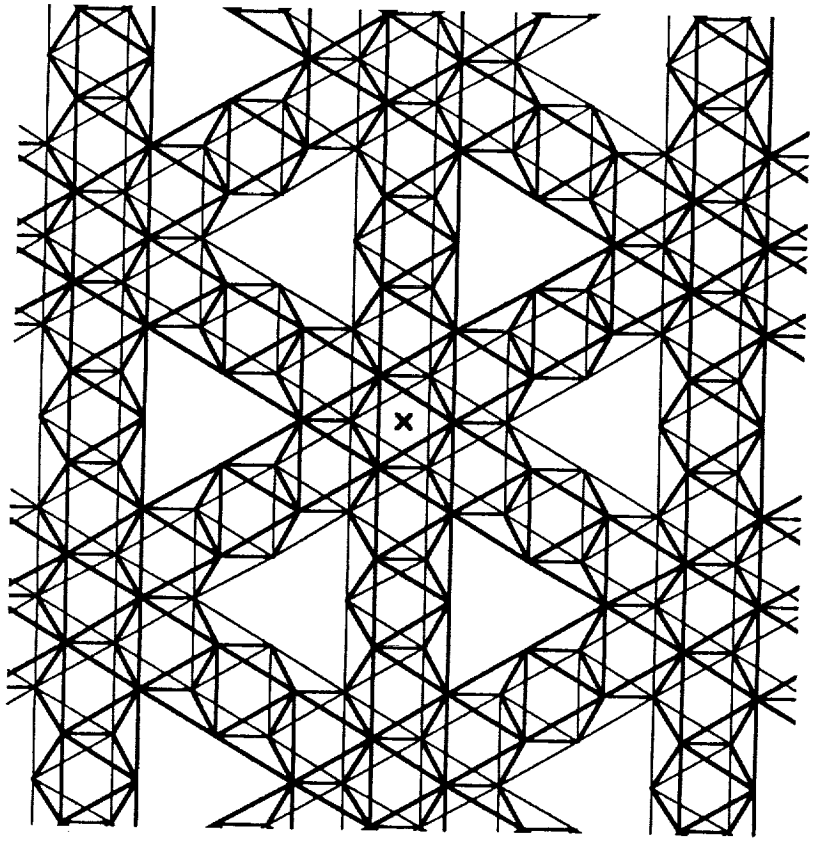

Figure 31e. A Portion of the Infinite Configuration **TOROID4.**

NASA National Aeronautics and Space Administration

Report Documentation Page

1. Report No.	2. Government Accession No.	3. Recipient's Catalog No.
NASA TM-102768		

4. Title and Subtitle	5. Report Date
Comparative Morphology of Configurations with Reduced Part Count Derived From The Octahedral-Tetrahedral Truss	February 1991
	6. Performing Organization Code

7. Author(s)	8. Performing Organization Report No.
Haresh Lalvani and Timothy J. Collins	
	10. Work Unit No.
	506-43-41-02

9. Performing Organization Name and Address	11. Contract or Grant No.
Langley Research Center Hampton, VA 23665-5225	
	13. Type of Report and Period Covered
12. Sponsoring Agency Name and Address	Technical Memorandum
National Aeronautics and Space Administration Washington, DC 20546-0001	14. Sponsoring Agency Code

15. Supplementary Notes

Haresh Lalvani: Joint Institute for Advancement of Flight Sciences, George Washington University, NASA Langley Research Center, Hampton, Virginia (on sabatical from Pratt Institute, Brooklyn, New York, at the time of this work).
Timothy J. Collins: Langley Research Center, Hampton, Virginia.

16. Abstract

The morphology (the study of structure and form) of the octahedral-tetrahedral (octet) truss is described. Both the geometry and symmetry of the octet truss are considered. Morphological techniques based on symmetry operations are presented which enable the derivation of reduced-part-count truss configurations from the octet truss by removing struts and nodes. These techniques are unique because of their Morphological origination and because they allow for the systematic generation and analysis of a large variety of structures. Methods for easily determining the part count and redundancy of infinite truss configurations are presented. Nine examples of truss configurations obtained by applying the derivation techniques are considered. These configurations are structurally stable while at the same time exhibiting significant reductions in part count. Some practical and analytical considerations, such as structural performance, regarding the example reduced-part-count truss geometries are briefly discussed.

17. Key Words (Suggested by Author(s))	18. Distribution Statement
Morphology, Part Count, Truss Design, Truss Structure, Tetrahedral Truss, Truss Redundancy	Unclassified - Unlimited Subject Category - 18

19. Security Classif. (of this report)	20. Security Classif. (of this page)	21. No. of pages	22. Price
Unclassified	Unclassified	137	A07